

DETERMINING THE BEHAVIOUR OF SAND UNDER CYCLIC LOADING  
IN THE DIRECT SIMPLE SHEAR APPARATUS

FOR REFERENCE

NOT TO BE TAKEN FROM THIS ROOM

Thesis by  
ALI SÜHA KIN

Submitted to the Institute for Graduate Studies in  
Science and Engineering in partial fulfillment of  
the requirements for the degree of

Master of science

in

Civil Engineering

Bogazici University Library



39001100314643

14

Boğaziçi University

Bebek - Istanbul

March- 1985

DETERMINING THE BEHAVIOUR OF SAND UNDER CYCLIC LOADING  
IN THE DIRECT SIMPLE SHEAR APPARATUS

This Thesis has been approved by

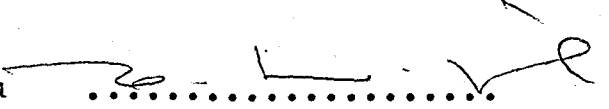
Doç. Dr. Erol Güler  
(Thesis Supervisor)

.....

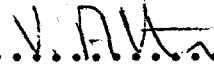
Prof. Dr. Ergün Toğrol

.....

Prof. Dr. Turan Durgunoğlu

.....

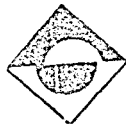
Doç. Dr. Vural Altın

.....

Boğaziçi University

Bebek - Istanbul

March- 1985



ACKNOWLEDGEMENTS

I would like to express my sincere gratitude to Doç. Dr. Erol Güler for his very kind advice and helps supplied all throughout the study.

I also would like to thank Mr. Isa Kul for photographic works, and all the members of Soil Laboratory of Boğaziçi University for their helps.

Ali Süha Kın

## A B S T R A C T

DETERMINING THE BEHAVIOUR OF SAND UNDER CYCLIC LOADING  
IN THE DIRECT SIMPLE SHEAR APPARATUS

In the past years, significant advances have been made in the analysis of the dynamic behaviour of soils and many analytical models, in-situ and laboratory techniques, and apparatus have been developed. In order to be able to predict the behaviour of a certain soil under cyclic loads, the damping ratio and the shear modulus of that soil have to be determined.

The objective of this thesis is to study the factors such as shear strain amplitude, vertical pressure, number of loading cycle and relative density which affect the shear modulus and damping ratio of clean dry sand subjected to cyclic simple shear tests. For this purpose several samples of sand with relative densities of 50% and 65% were subjected to strain-controlled dynamic loading using Direct Simple Shear Apparatus developed by Norwegian Geotechnical Institute. In this study, five different vertical pressures namely 0.5, 1.0, 2.0, 4.0 and 8.0 kg/cm<sup>2</sup> and the strain levels of about 0.25%, 0.50%, and 0.75% were applied to the specimens. Prescribed deformations were applied to each sample and shear stress-strain hysteresis loops

were obtained in order to determine shear modulus and damping ratio at the corresponding strain levels. Shear modulus and damping ratio values obtained from each test were plotted versus shear strain amplitudes under various testing conditions in order to observe the factors affecting shear modulus and damping ratio.

The test results have shown that, shear modulus decreases and damping ratio increases with increasing shear strain. Increasing vertical pressure, number of loading cycles, or relative density causes an increase in shear modulus. On the other hand, damping ratio increases with decreasing relative density, vertical pressure or number of loading cycles.

## Ö Z E T

DİREKT BASİT KESME ALETİNDE KUMUN TEKRARLI YÜKLER  
ALTINDAKİ DAVRANIŞININ BELİRLENMESİ

Geçmiş yıllarda, zeminlerin dinamik davranışının analizinde önemli ilerlemeler kaydedilmiş, ve birçok analitik modeller, arazi ve labaratuvar teknik ve aletleri geliştirilmiştir. Belirli bir zeminin tekrarlı yükler altındaki davranışının önceden tahmin edilebilmesi için o zemine ait kayma modülü ve sönüm oranı belirlenmelidir.

Bu tezin konusu, dinamik basit kesme deneyine tabi tutulmuş temiz kuru kumun kayma modülü ve sönüm oranına etki eden birim kayma deformasyonu, düşey basınç, titreşim devir sayısı ve relatif sıklık gibi faktörleri incelemektir. Bu amaçla relatif sıklıkları 50 % ve 65 % olan kum numuneleri, Norveç Geoteknik Enstitüsü tarafından geliştirilmiş Direkt Basit Kesme Aleti kullanılarak deformasyon kontrollü dinamik yüke maruz bırakılmışlardır. Bu çalışmada, 0.5 , 1.0 , 2.0 , 4.0 ve 8.0 kg/cm<sup>2</sup>lik beş değişik düşey basınç ve yaklaşık 0.25 % , 0.50 % ve 0.75 % lik birim deformasyon seviyeleri numunelere uygulanmıştır. Önceden belirlenmiş olan deformasyonlar herbir numuneye uygulanmış ve bu deformasyon seviyelerine tekabül eden kayma modülü ve

sönüm oranını belirlemek için, kayma gerilme-deformasyon histerizis ilmiği elde edilmiştir. Kayma modülü ve sönüm oranına etki eden faktörleri incelemek için, herbir testten elde edilen kayma modülü ve sönüm oranı değerleri değişik deney durumlarında, birim kayma deformasyonlarına karşı çizilmiştir.

Deney sonuçları göstermiştir ki; artan birim kayma deformasyonu ile kayma modülü azalır ve sönüm oranı artar. Düşey basınç, titreşim devir sayısı veya relatif sıkılıktaki artma, kayma modülünde bir artmaya neden olur. Diğer taraftan, sönüm oranı azalan relatif sıkılık, düşey basınç veya titreşim devir sayısı ile birlikte artar.

## TABLE OF CONTENTS

	Page
ACKNOWLEDGEMENTS.....	iii
ABSTRACT.....	iv
ÖZET .....	vi
LIST OF FIGURES .....	x
LIST OF TABLES .....	xiv
LIST OF SYMBOLS .....	xv
CHAPTER	
1. INTRODUCTION .....	1
2. PREVIOUS RESEARCH .....	3
2.1. INTRODUCTION .....	3
2.2. DYNAMIC STRESS-STRAIN BEHAVIOUR OF SANDS .....	3
2.3. LABORATORY METHODS FOR EVALUATING DYNAMIC SOIL PROPERTIES .....	11
2.3.1. RESONANT COLUMN TESTS .....	13
2.3.2. ULTRASONIC PULSE TESTS .....	14
2.3.3. CYCLIC TRIAXIAL TESTS .....	15
2.3.4. CYCLIC TORSIONAL SIMPLE SHEAR TESTS .....	16
2.3.5. CYCLIC SIMPLE SHEAR TESTS .....	17
2.4. PARAMETERS AFFECTING DYNAMIC SOIL PROPERTIES ...	20
2.5. THE EQUIVALENT LINEAR IDEALIZATION .....	26
2.5.1. SEED-IDRISS MODEL .....	26



	Page
2.5.2 HARDIN-DRNEVICH MODEL .....	29
2.5.3. THE USE OF EQUIVALENT LINEAR IDEALIZATION: EQUIVALENT LINEAR METHOD .....	37
2.6. NONLINEAR MODELS .....	38
2.6.1. MASING CRITERION .....	38
2.6.2. RELATIONSHIP BETWEEN NONLINEAR AND EQUIVALENT LINEAR MODELS .....	41
3. EXPERIMENTAL STUDY .....	45
3.1. APPARATUS .....	45
3.1.1. INTRODUCTION .....	45
3.1.2. APPARATUS REQUIREMENTS .....	47
3.1.3. DESCRIPTION OF APPARATUS .....	47
3.1.3.1. THE SAMPLE ASSEMBLY .....	49
3.1.3.2. THE VERTICAL AND HORIZONTAL LOAD UNITS .....	49
3.2. SAMPLE PREPARATION AND MATERIAL TESTED .....	52
3.3. MOUNTING OF THE SAMPLE ASSEMBLY IN THE SHEAR APPARATUS AND TESTING .....	55
3.4. ANALYSIS OF DATA .....	57
3.5. SCHEDULE OF THE TESTS .....	59
4. TEST RESULTS AND DISCUSSION .....	61
4.1. HYSTERESIS LOOPS .....	61
4.2. SHEAR MODULUS VALUES .....	61
4.3. DAMPING RATIO VALUES .....	65
5. CONCLUSIONS .....	106
REFERENCES .....	109

## LIST OF FIGURES

FIGURE	<u>Page</u>
2.1 Strain-Softening Type of Hysteresis Loop	4
2.2 Definition of Modulus and Damping Ratio	5
2.A Mass-Spring-Dashpot System	7
2.B Free Vibration of a Viscously Damped System	7
2.C Shearing Stress-Strain Ellipse for Viscoelastic Material	9
2.3 Shearing Strain Amplitude Capabilities of Laboratory Apparatus	19
2.4 Effects of Strain Amplitude, Effective Confining Stress and Number of Cycles of Loading on Shear Modulus of Sand.	22
2.5 Effects of Strain Amplitude, Effective Confining Stress and Number of Cycles of Loading on Damping Ratio of Sands.	24
2.6.A Shear Moduli of Sands at Different Relative Densities	27
2.6.B Damping Ratio for Sands.	28
2.7 Hyperbolic Stress-Strain Relation	31
2.8 Hyperbolic Strain versus Normalized Shear Strain for Shear Modulus.	36
2.9 Typical Stress-Strain Relationship	39

FIGURE	Page
2.10 Definition of Equivalent-Linear Shear Modulus and Damping.	42
2.11 Derivation of Equivalent Damping.	42
3.1 General View of the Apparatus	48
3.2 General Principle of Direct Simple Shear Apparatus	51
3.3 Grain Size Distribution Curve for the Sand Tested	54
3.4 Typical Record of Deformation and Load During Simple Shear Test.	57
4.1 Hysteresis Loop of Test A1	70
4.2 Hysteresis Loop of Test A2	71
4.3 Hysteresis Loop of Test A3	72
4.4 Hysteresis Loop of Test A4	73
4.5 Hysteresis Loop of Test A5	74
4.6 Hysteresis Loop of Test A6	75
4.7 Hysteresis Loop of Test B1	76
4.8 Hysteresis Loop of Test B2	77
4.9 Hysteresis Loop of Test B3	78
4.10 Hysteresis Loop of Test B4	79
4.11 Hysteresis Loop of Test B5	80
4.12 Hysteresis Loop of Test B6	81
4.13 Hysteresis Loop of Test C1	82
4.14 Hysteresis Loop of Test C2	83

FIGURE	<u>Page</u>
4.15 Hysteresis Loop of Test C3	84
4.16 Hysteresis Loop of Test C4	85
4.17 Hysteresis Loop of Test C5	86
4.18 Hysteresis Loop of Test C6	87
4.19 Hysteresis Loop of Test D1	88
4.20 Hysteresis Loop of Test D2	89
4.21 Hysteresis Loop of Test D3	90
4.22 Hysteresis Loop of Test D4	91
4.23 Hysteresis Loop of Test D5	92
4.24 Hysteresis Loop of Test D6	93
4.25 Hysteresis Loop of Test E1	94
4.26 Hysteresis Loop of Test E2	95
4.27 Hysteresis Loop of Test E3	96
4.28 Hysteresis Loop of Test E4	97
4.29 Hysteresis Loop of Test E5	98
4.30 Hysteresis Loop of Test E6	99
4.31 Effects of Shear Strain Amplitude and Vertical Stress on Shear Modulus in Fifth Loading Cycle.	100
4.32 Effects of Vertical Pressure and Relative Density on Shear Modulus in Fifth Loading Cycle.	101
4.33 Effect of Number of Loading Cycles on Shear Modulus.	102

FIGURE	<u>Page</u>
4.34 Effects of Shear Strain Amplitude and Vertical Pressure on Damping Ratio in Fifth Loading Cycle.	103
4.35 Effects of Vertical Pressure and Relative Density on Damping Ratio in Fifth Loading Cycle.	104
4.36 Effect of Number of Loading Cycles on Damping Ratio.	105

## LIST OF TABLES

TABLE	<u>Page</u>
2.1 Laboratory Techniques for Measuring Dynamic Soil Properties.	18
2.2 Relative Importance of Parameters Affecting Shear Modulus and Damping Ratio.	20
3.1 Test Program.	60
4.1 Shear Modulus Values Obtained from the Tests.	62
4.2 Comparison of Shear modulus Values Obtained by Seed-Idriss Model and Hardin-Drnevich Model with the Results of Tests A1, B1, C1, D1 and E1.	64
4.3 Damping Ratio Values Obtained from the Tests.	66
4.4 Comparison of Damping Ratio Values Obtained by Using Seed-Idriss Model and Hardin-Drnevich Model with the Average of the Results Obtained in this Study.	68

## LIST OF SYMBOLS

## SYMBOL

$A_L$	= the area within a full hysteresis loop in Fig.2.10
$A_T$	= triangular area in Fig.2.10
$A_s$	= area of the sample
$a, b$	= empirical soil constants
$c$	= viscous damping constant
$c_{cr}$	= critical viscous damping coefficient defined by Eq.2.b
$D$	= damping ratio
$D_e$	= equivalent linear damping ratio
$D_{max}$	= maximum damping ratio
$D_r$	= relative density defined by Equation 3.1
$E$	= Young's modulus
$e$	= void ratio, also base of natural logarithms
$f$	= frequency of vibration
$G$	= dynamic shear modulus
$G_e$	= equivalent linear shear modulus
$G_{max}$	= maximum dynamic shear modulus (initial tangent shear modulus)
$G_s$	= specific gravity
$K_0$	= coefficient of lateral earth pressure at rest
$K_2$	= shear modulus parameter defined by Eq.2.3

$k$	= spring constant
$L_s$	= sample length
$\Delta L$	= cyclic horizontal displacement
$m$	= mass of specimen
$N$	= number of cycles
$P_h$	= cyclic horizontal load
$Q_0$	= amplitude of external force acting on elastic system
$Q(t)$	= time-dependent external force acting on elastic system
$t$	= time
$W$	= input energy
$\Delta W$	= energy lost
$x$	= horizontal displacement
$z$	= displacement in the vertical direction
$\delta$	= amplitude of shear strain
$\delta_1$	= shear strain at the instant immediately after the last load reversal
$\delta_d$	= unit dry weight of sand
$\delta_h$	= hyperbolic strain defined by Eqn.2.8
$\delta_r$	= reference strain defined by Eqn.2.6
$\delta/\delta_r$	= normalized strain
$\delta_y$	= shear strain at yield
$\delta$	= logarithmic decrement defined by Eqn.2.c
$\epsilon$	= linear strain
$\nu$	= Poisson's ratio



$\pi$	= 3.14159...
$p$	= normal stress
$p_a$	= cell pressure in triaxial test
$p_{dc}$	= axial stress in triaxial test
$\sigma_o$	= effective mean principal stress
$\sigma_1, \sigma_2, \sigma_3$	= principal stresses
$\sigma_v$	= vertical effective stress
$\tau$	= shear stress
$\tau_1$	= shear stress at the instant immediately after the last load reversal
$\tau_{max}$	= shear stress at failure
$\phi$	= phase angle
$w$	= frequency

## CHAPTER 1

## INTRODUCTION

Dynamic analyses to evaluate the response of earth structures to dynamic stress applications such as those produced by earthquakes, blasting and wind loading are finding increased application in civil engineering practise. Therefore various analytical techniques and idealized models are being developed to predict the soil-structure interaction and the dynamic behaviour of soil deposits and soil structures. In most cases, each method requires an evaluation of the stress-strain properties of the soil, represented as a dynamic modulus, and a measure of the energy absorbing properties of the materials in the deposit, represented by material damping values.

The shear modulus and damping values in soils are important factors for the analysis of all soil vibration and structural design problems. In order to develop an improved understanding of the behaviour of cohesionless soils under dynamic loading conditions, the dynamic stress-strain properties of sand represented by values of modulus and damping should be investigated.

Dynamic stress-strain behaviour of soils are affected by various factors such as strain amplitude, void ratio, vertical stress, number of cycles of loading etc., and dynamic stress-strain relationships are very complex in nature. The purpose of this study is to show how some of these factors influence the dynamic stress-strain behaviour of dry sand.

Several different field and laboratory methods can be used to determine dynamic moduli and damping ratio of soils, and to examine the factors which affect them. In this investigation, the dynamic properties of sand are determined by cyclic loading simple shear tests which provide a good representation of the shear conditions imposed on a soil element during many seismic events, and these tests are very convenient for examining the factors affecting shear modulus and damping ratio.

In Chapter 2, a literature survey on dynamic stress-strain behaviour of sandy soils, laboratory methods to measure dynamic soil parameters and important factors affecting dynamic behaviour are outlined.

Chapter 3 includes the laboratory work done. In this chapter a description of testing apparatus, the characteristics of soil tested, method of sample preparation and some details of testing procedure are also given.

In Chapter 4, evaluation of dynamic soil parameters, and discussion of results are presented.

Finally Chapter 5 covers the conclusions derived from this study.

## CHAPTER 2

## PREVIOUS RESEARCH

## 2.1- INTRODUCTION

In this Chapter, an outline of some important results obtained from previous studies on dynamic soil parameters (i.e. shear modulus and damping ratio) are presented. Dynamic stress-strain behaviour of soils, definitions of dynamic soil parameters laboratory methods to measure dynamic soil parameters, and important factors affecting dynamic behaviour are briefly summarized in this chapter. Then based upon these parameters, the equivalent linear and true nonlinear formulations of hysteretic stress-strain relations are reviewed in the sections (2.5) and (2.6). The soil selected for this study is cohesionless therefore mainly researches conducted on sands are taken into consideration in the following sections.

## 2.2- DYNAMIC STRESS-STRAIN BEHAVIOUR OF SANDS

Dynamic loading develops stress-strain relationships in soils which may be different from those developed under static loadings. The shape of the stress-strain curve provides information on the dynamic moduli and damping, which are the principal soil properties required for evaluation of wave propagation in soils and for dynamic soil-structure interaction studies.

The shape of the stress-strain relationships for any particular soil depends upon the type of loading and boundary restraining conditions.

In the case of dynamic loading, strain-softening type stress-strain hysteresis loops are developed for each load cycle as shown in Fig. 2.1. The first complete load cycle begins after the sample has been subjected to a quarter cycle of loading. In other words, loading begins from zero stress and strain, reaches the first maximum stress. On the stress-strain plane, this curve is called as "backbone curve". Each sample has a backbone curve and the first load cycle begins from that curve, and forms a hysteresis loop.

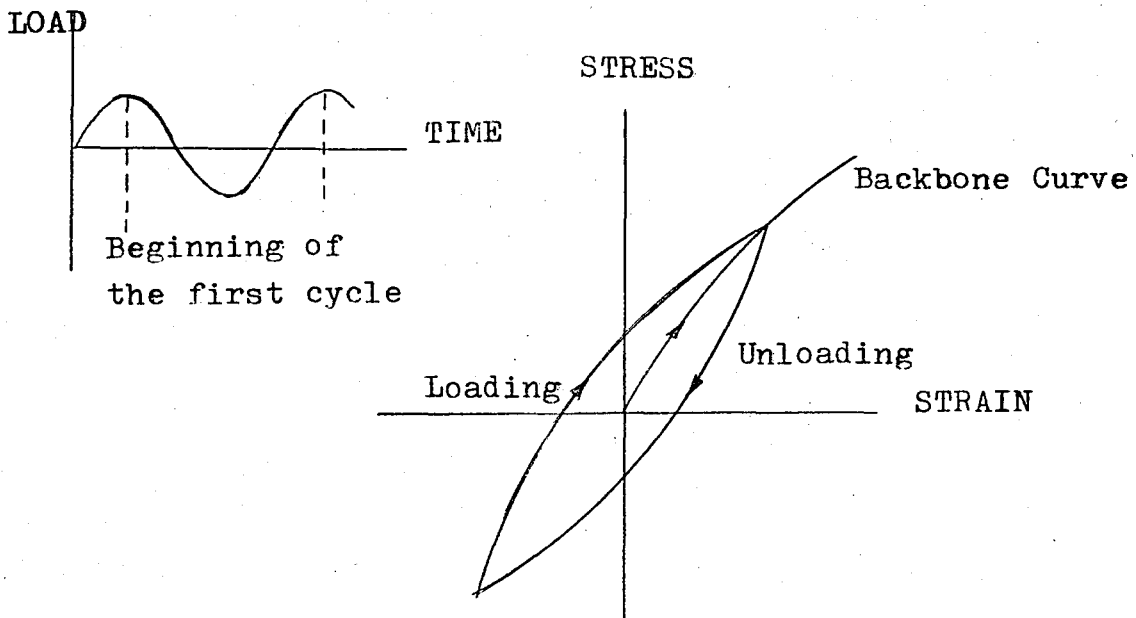
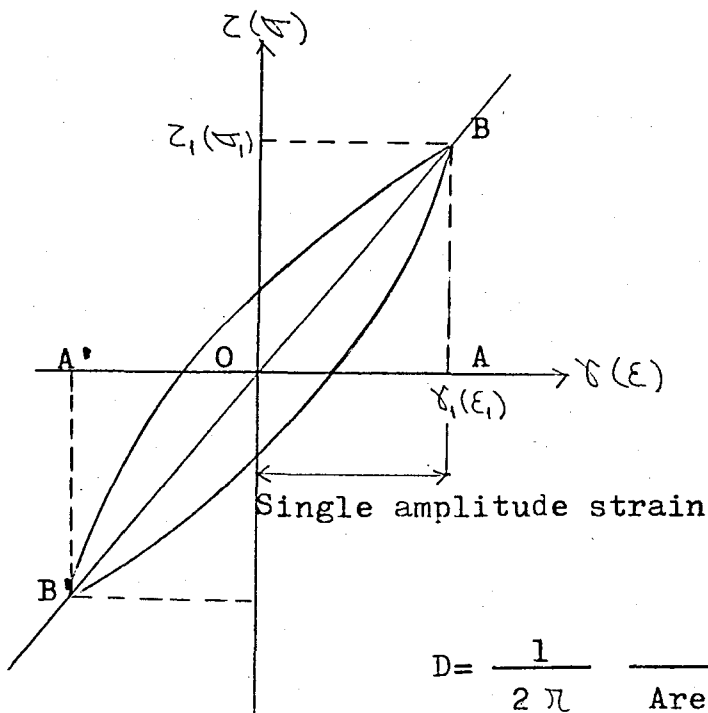


Figure 2.1- Strain-Softening Type of Hysteresis Loop

The response of the sample is calculated from such hysteresis loops. This response is mainly determined by shear modulus,  $G$ , and hysteretic damping ratio,  $D$ . Since the soils have curvilinear stress-strain relationships as mentioned before, shear modulus is expressed as the secant modulus determined by the slope of the line connecting the two extreme points of the hysteresis loop as shown in Fig. 2.2. In the case of normal stress-strain hysteresis loop, this modulus corresponds to Young's modulus,  $E$ . The area within the hysteresis loop is a measure of energy dissipated per cycle and it is proportional to damping ratio.



$$G = \frac{\tau_1}{\gamma_1}$$

$$E = \frac{\tau_1}{\epsilon_1}$$

$$D = \frac{1}{2\pi} \frac{\text{Loop area}}{\text{Area of triangles OAB and OAB'}}$$

Figure 2.2- Definition of Modulus and Damping Ratio

(After Silver and Park, 1975)

Material damping describes the energy losses within loaded soil masses caused by interparticle slip and friction of particle contacts. The energy losses in soils during cyclic or reversed loadings can be significant during vibratory or transient loadings which involve large strain amplitudes, as may be developed during earthquakes. Field methods for evaluating damping in soils have not yet been developed for practical use, consequently the following discussion will treat only laboratory methods.

#### Fundamental Relationships :

Although interparticle friction develops hysteretic damping in sands, Hall and Richart (1963), and Hardin (1965) demonstrated that the results could be readily interpreted in terms of damping of a viscoelastic system.

Figure(2.A) shows a simple mass-spring-dashpot which is set into motion in the vertical direction ,  $z$  , by a dynamic force  $Q(t)$ . The equation of motion for this one-degree-of-freedom system is

$$m\ddot{z} + c\dot{z} + kz = Q(t) \quad (2.a)$$

The damping constant,  $c$  , is often combined with the mass,  $m$  , and spring constant,  $k$  , to form a " damping ratio "

$$D = \frac{c}{2\sqrt{km}} = \frac{c}{c_{cr}} \quad (2.b)$$

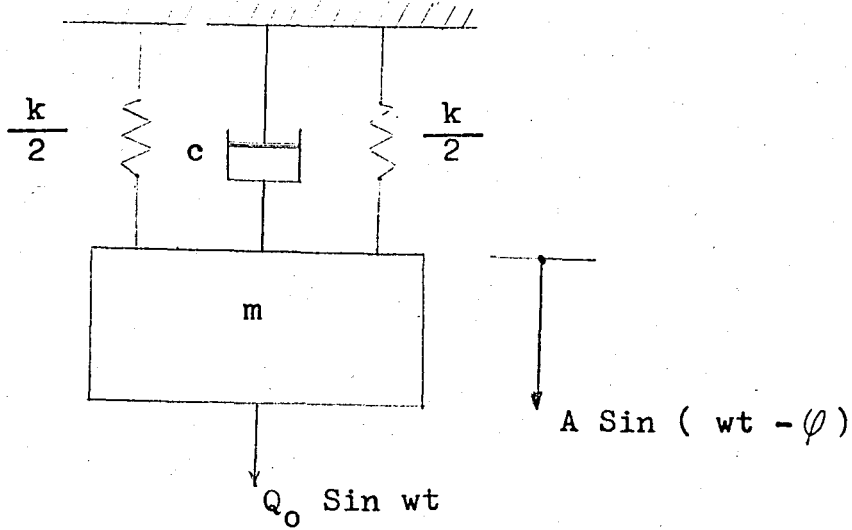


Figure 2.A- Mass-Spring-Dashpot System

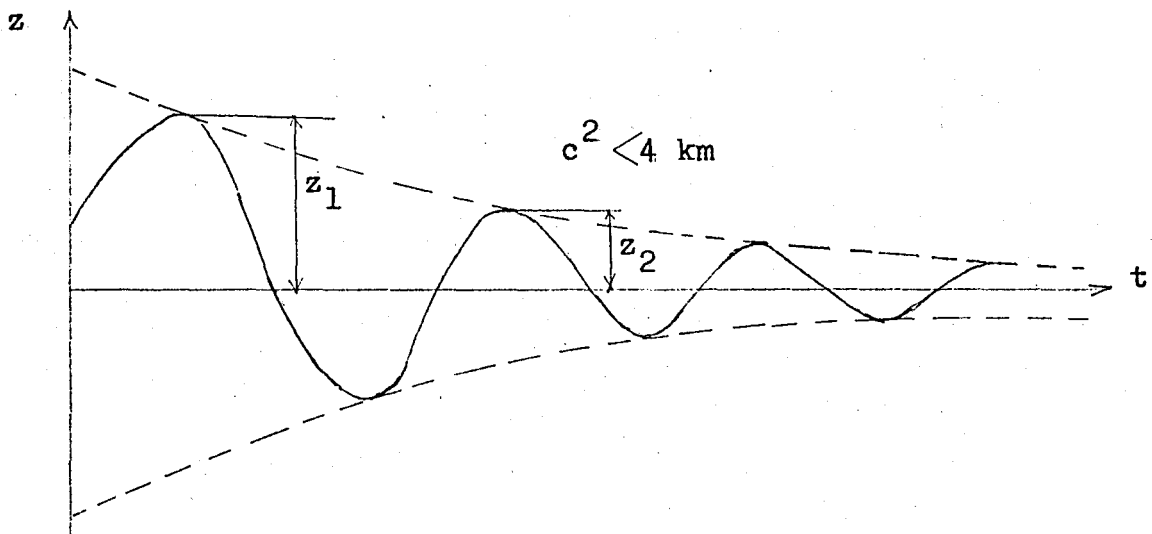


Figure 2.B- Free Vibration of a Viscously Damped System



when the system shown in Fig.(2.A) is set into steady state vibration and the exciting force  $Q(t)$  is removed, the vibration amplitude will decay with time, as shown in Fig.(2.B), because of the damping. The amplitude ratio of decaying vibration is also a measure of damping and is designated as the "logarithmic decrement"

$$\delta = \ln \frac{z_1}{z_2} \approx \frac{2\pi D}{\sqrt{1-D^2}} \approx 2\pi D \quad (2.c)$$

The loss of energy in viscoelastic systems may also be described by the strain energy lost during oscillations. The stress strain curves from reversed loading ( $\tau - \gamma$  curves in Fig.(2.C)) form an ellipse which has its major axis along a line at the slope of  $G$ . The slope of this major axis along a line stant regardless of the magnitude of the shearing stress developed. The ratio of energy lost in one cycle of oscillation,  $\Delta W$ , to the input energy,  $W$ , is often called the "specific damping capacity", and it is related to other damping terms by

$$\frac{\Delta W}{W} \approx 2\delta \approx 4\pi D \quad (2.d)$$

for values of  $\delta$  smaller than about 0.25. The relation between  $\delta$  and

$\Delta W/W$  is

$$\frac{\Delta W}{W} = 1 - e^{-2\delta} \quad (2.e)$$

for a system having a modulus independent of strain amplitude.

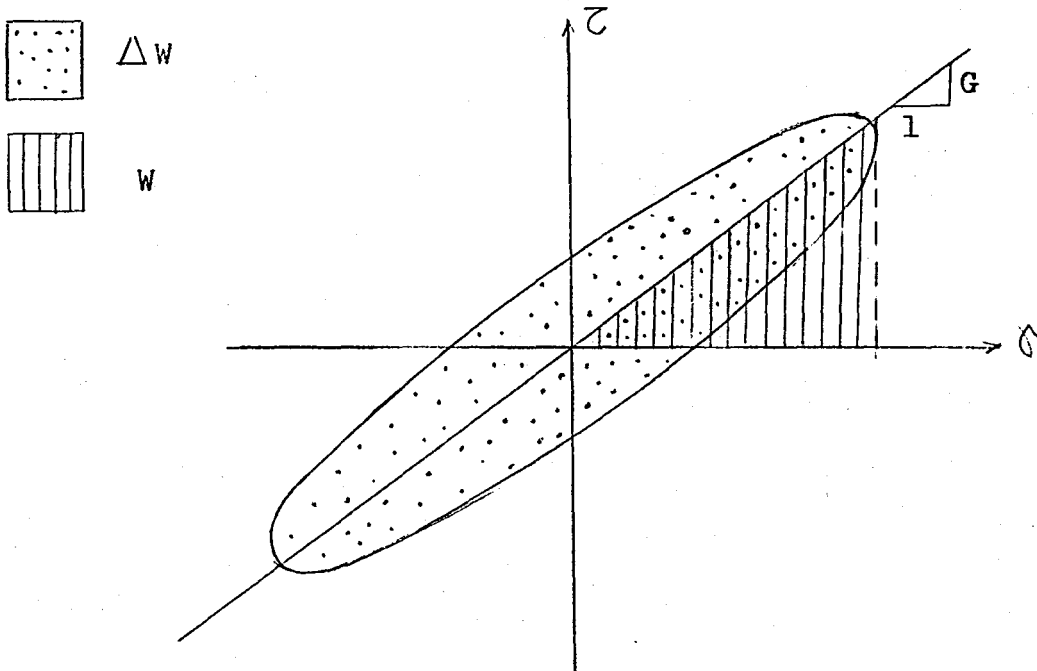


Figure 2.C- Shearing Stress-Strain Ellipse For Viscoelastic Material

Thus, damping ratio,  $D$ , is a function of energy ratio which can be defined as the energy dissipated per cycle to the maximum energy applied. Since the energy dissipated per cycle is proportional to the area inside the loop, and the maximum energy applied is proportional to the area of triangles under the peak to peak line, damping ratio can be calculated from the equation given in Fig.(2.2) as :

$$D = \frac{1}{2\pi} \frac{\text{Loop Area}}{\text{Area of Triangles OAB and OAB}} \quad (2.f)$$

It should be noted that  $G$  and  $D$  depend on the magnitude of the strain for which the hysteresis loop is obtained. Thus,  $G$  and  $D$  are determined as functions of strain level as well as other factors among which the most important ones will be briefly discussed in Section 2.4.

## 2.3- LABORATORY METHODS FOR EVALUATING DYNAMIC SOIL PROPERTIES

Numerous problems in engineering require a knowledge of dynamic soil properties for satisfactory solutions. These problems span a range of situations involving at one end of the scale very small amplitudes of motion, e.g., foundations for electron microscopes, and at the other end, attempts to mitigate effects of strong motion earthquakes or nuclear explosions. The need to solve this range of problems stimulated the development of a variety of laboratory and field techniques for evaluating dynamic soil properties and dynamic soil behaviour.

The major soil properties and characteristics which are needed in soil dynamics and earthquake engineering are

Dynamic moduli -- Young's Modulus, shear modulus, bulk modulus and constrained modulus

Damping and attenuation

Poisson's ratio

Liquefaction parameters -- Cyclic shearing stress ratio, cyclic deformation and pore pressure response.

Most analytical techniques currently used in assessing response of soils or soil-structure systems to

Earthquakes

Wave forces

Explosions

Construction vibrations

Machine vibrations

We can measure the dynamic soil properties in situ, only for low strain amplitudes. So it is necessary to determine the behaviour at higher strain amplitudes or soil behaviour under loading conditions not initially prevalent in situ; therefore laboratory techniques are required. Consequently, both laboratory and field techniques are necessary for satisfactory solution of many dynamic soil problems.

Field seismic methods are used to measure the velocity of propagation of compression waves, shear waves, and Rayleigh waves from which values of shear modulus can be determined for low strain conditions.

Since this study deals with the determination of dynamic properties of soils in the laboratory methods will be discussed in a general manner. Some laboratory tests are designed to measure specific basic soil properties like shearing strength or shear modulus, while others are designed to determine soil behaviour in a simulated dynamic environment like a saturated sand subject to earthquake excitation. Attempts to measure dynamic shearing strength of soils have been reported since about 1948, but in the past two decades the emphasis in dynamic laboratory testing has been directed to ward measuring dynamic moduli ( Young's modulus and shearing modulus ), damping and to some extent Poisson's ratio. Also, considerable effort has been directed at determining cyclic loading behaviour of soils in shear and

compression in efforts to model earthquake loadings.

There are several kinds of laboratory tests which can be used to determine the modulus and damping characteristics of soils. Frequently used laboratory tests are resonant column tests, ultrasonic pulse test, cyclic triaxial compression test, cyclic torsional simple shear test and cyclic simple shear test.

### 2.3.1- RESONANT COLUMN TESTS

The resonant column test for determining modulus and damping characteristics of soils is based on the theory of wave propagation in prismatic rods ( Richart, Hall and Woods, 1970 ). Either compression waves or shear waves can be propagated through the soil specimen from which either Young's modulus or shear modulus can be determined. In a resonant column apparatus the exciting frequency is adjusted until the specimen experiences resonance. The modulus is computed from the resonant frequency and the geometric properties of the specimen and driving apparatus. Damping is determined by turning off the driving power at resonance and recording the decaying vibrations from which a logarithmic decrement is calculated. Alternative methods of damping measurement include determining damping from the shape of the resonance curve or determining a " resonant factor " from driving-coil current measurements as described by Hardin and Music (1965) or Drnevich Hardin and Shippy (1977).

In the resonant column device, a cylindrical column of soil

is replaced with in a rubber membrane, placed in a triaxial cell, and set into motion either in the longitudinal or torsional mode of vibration in order to obtain Young's modulus,  $E$ , and shear modulus,  $G$ , respectively. The frequency of the input vibration is changed until the first mode resonant condition is determined. The resonant frequency, the geometry of the sample, and end restraint conditions provide necessary information to calculate the velocity of wave propagation in the soil sample. Various types of resonant column device have been used in many researches to examine the factors effecting shear modulus and damping.

### 2.3.2- ULTRASONIC PULSE TESTS

Using piezoelectric crystals, it is possible to generate and receive ultrasonic waves in soils. Crystals can be obtained which generate either compression or shear waves. By timing the travel of these waves over a fixed distance, the wave velocities can be obtained and from the velocities, moduli can be computed. Lawrence (1963) described the basic apparatus required to measure propagation velocities through sand and Nacci and Taylor (1967) describe an application with clays in a common triaxial cell.

The pulse test is not adaptable for studies of the effects of stress (or strain) amplitudes, or frequency on the wave propagation velocities in soils. It provides no information on internal damping with in the soil sample. Furthermore, the techniques involved in

generating and interpreting the electrical signals are sufficiently complicated that the pulse method as used in the laboratory is restricted primarily to research investigations.

### 2.3.3- CYCLIC TRIAXIAL TESTS

Cyclic triaxial tests have been used since the mid- 1960's (Seed and Lee, 1966 ) and are currently the most widely used laboratory method of evaluating liquefaction characteristics of cohesionless soils.

In this test cylindrical triaxial samples are initially consolidated under a cell pressure ( $\sigma_a$ ). In principle the sample is then subject to an increase in axial stress  $\sqrt{\sigma_{dc}/2}$  and a simultaneous reduction in the cell pressure by an equal amount. For convenience the test is normally performed by maintaining the cell pressure at a constant value and cycling the axial stress by  $+\_ \sigma_{dc}$ . This technique results in essentially the same stress conditions as long as the sample is saturated and tested undrained. ( Seed and Lee , 1966 ) If samples are partially saturated or tested with drainage, it is necessary to utilize axial and lateral stress control to simulate earthquake loading.

In the many variations of the cyclic triaxial test, the configuration of the specimen is standard but the loading and control equipment are variable. Most currently used apparatus are stress controlled devices in which a cyclic axial load is applied to an undrained specimen. Pore pressure, vertical load and vertical deformation are recorded as a function of the number of cycles of load.

In addition to liquefaction characteristics of soils, Young's



modulus,  $E$ , and damping ratio,  $D$ , are often measured in the cyclic triaxial test by performing strain-controlled tests. These tests are performed in essentially the same manner as the stress-controlled test, however, a servo system is used to apply cycles of controlled deformation. Young's modulus is determined from the ratio of the applied axial stress to axial strain. For strain-controlled tests, shear modulus is computed from

$$G = E / 2 ( 1 + \nu )$$

in which  $\nu$  is Poisson's ratio.

Like all laboratory attempts to duplicate dynamic field conditions, the cyclic triaxial test has some limitations.

#### 2.3.4- CYCLIC TORSIONAL SIMPLE SHEAR TESTS

Dynamic torsion test makes accurate measurements of shear modulus and damping values for single amplitude shear strain as small as 0.0025 % at a frequency range of 0.2 Hz to 5 Hz. ( Hardin and Drnevich , 1972 ; Richart 1975 ). For this test two types of samples can be used. One is solid cylinder sample; other is hollow-cylinder sample. However, the difference between the behaviour of solid and hollow samples is not significant in most the cases. ( Hardin and Drnevich , 1972 ) Hollow-cylinder samples are mostly used to make accurate measurements, and higher values of shear strain can be applied

to the hollow-cylinder samples than those of the solid samples. Hardin has developed a dynamic torsion test device which tests the hollow-cylinder samples having 13 cm. outer diameter, 10 cm. inner diameter, and 23 cm. height. In this device a dead weight loading system applies a pure torque to the top of the sample through a system of strings and levers. Later, this device has been modified by Hardin in order to use electromagnetic loading system. This device gives shear stress-shear strain hysteresis loops for calculating shear modulus and damping.

### 2.3.5- CYCLIC SIMPLE SHEAR TESTS

The simple shear principle appeared to many investigators to be an appropriate way of reproducing in the laboratory the stresses experienced by an element of soil subject to the ideal earthquake loading. Dynamic simple shear test is very convenient for evaluating the dynamic stress-strain characteristics of soils. Many researches have been carried out using this test ( Matsui, Ohara, Ito , 1980 ; Seed and Idriss, 1970 ; Silver and Seed 1971 ). Since this is the test used here, the relevant characteristics will be discussed in detail in Chapter 3 :

The laboratory techniques presented in this section are tabulated in Table 1 where the specific properties or characteristics measured by each are indicated. The ranges of shearing strain amplitudes over which each technique is applicable are shown in Fig. 2.3.

	<u>Shear Modulus</u>	<u>Young's Modulus</u>	<u>Material Damping</u>	<u>Cyclic Stress Behaviour</u>
Resonant Column	X	X	X	
Ultrasonic Pulse	X	X		
Cyclic Triaxial		X	X	X
Cyclic Torsional Shear	X		X	X
Cyclic Simple Shear	X		X	X

Table-2.1 Laboratory Techniques for Measuring Dynamic Soil Properties  
( From Woods, R.D., (1978))

## Shearing Strain Amplitude (%)

$10^{-4}$	$10^{-3}$	$10^{-2}$	$10^{-1}$	1
PULSE METHODS			CYCLIC TRIAXIAL TEST	
RESONANT COLUMN (Solid samples)				
	RESONANT COLUMN (Hollow samples)			
	TORSIONAL SHEAR (Hollow samples)			
			CYCLIC SIMPLE SHEAR	
PROPERLY DESIGNED MACHINE FOUNDATION	Typical Motion Characteristics	STRONG GROUND SHAKING FROM EARTQUAKE	CLOSE-IN NUCLEAR EXPLOSION	
$10^{-4}$	$10^{-3}$	$10^{-2}$	$10^{-1}$	1

Figure 2.3- Shearing Strain Amplitude Capabilities of Laboratory Apparatus  
( From Woods, R.D., 1978 )

## 2.4- PARAMETERS AFFECTING DYNAMIC SOIL PROPERTIES

The dynamic stress-strain relations of soils are quite complex because of the large number of parameters involved in their definitions. The relative importance of these parameters on the dynamic properties of soils have already been examined by Hardin and Drnevich (1972, a ) in detail. These parameters and their relative importance on shear modulus and damping can be observed in Table 2.2.

PARAMETER	Shear Modulus		Damping Ratio	
	Sands	Clays	Sands	Clays
Shear strain amplitude	++	++	++	++
Effective confining pressure	++	++	++	++
Relative density (or void ratio )	++	++	++	++
Number of loading cycles	-	-	++	++
Degree of saturation	-	++	+	?
Frequency of loading ( above 0.1 Hz. )	-	-	-	+
Grain size, shape, gradation, minerology	-	-	-	-
Soil structure	-	-	-	-
Volume change due to shear strain	?	-	?	-

(++) very important, (+) less important, (-) relatively unimportant except as it may affect another parameter

(?) relative importance is not clearly known yet

Table-2.2 Relative Importance of Parameters Affecting Shear Modulus And Damping Ratio ( After Hardin and Drnevich, 1972, a )

Among them, it is observed that, there are three or four factors such as shear strain amplitude, effective mean principal stress, void ratio and number of cycles of loading, which govern the behaviour while the remaining are relatively less important and can be considered as parameters of secondary importance.

Fig. 2.4. shows the variation of shear modulus of a clean dry sand with respect to shear strain amplitude, effective mean principal stress, and number of cycles of loading. With increasing shear strain amplitude shear modulus decreases very rapidly. The rate at which the shear modulus decreases differs from different soil types and it depends primarily on the values of maximum shear modulus,  $G_{max}$ , and the shear strength of soils. The curves shown in Fig. 2.4 may be extrapolated to zero strain to obtain a value of  $G_{max}$  and these values are found in good agreement with the measurements taken during the resonant column test for strains as low as about  $10^{-6}$  percent of shear strain amplitude. The same figure shows the influence of effective mean principal stress,  $\sigma_0 = (\sigma_1 + \sigma_2 + \sigma_3) / 3$  on the shear modulus. Many investigators have shown that  $G_{max}$  varies with square root of  $\sigma_0$ , ( Drnevich and Richart, 1965 ; Hardin, 1965 ; Hardin and Black, 1968 ; Lawrence, 1965 )

However, at large shear strain amplitudes shear modulus mainly depends on the strength of soil which is a function of effective mean principal stress to the first power.

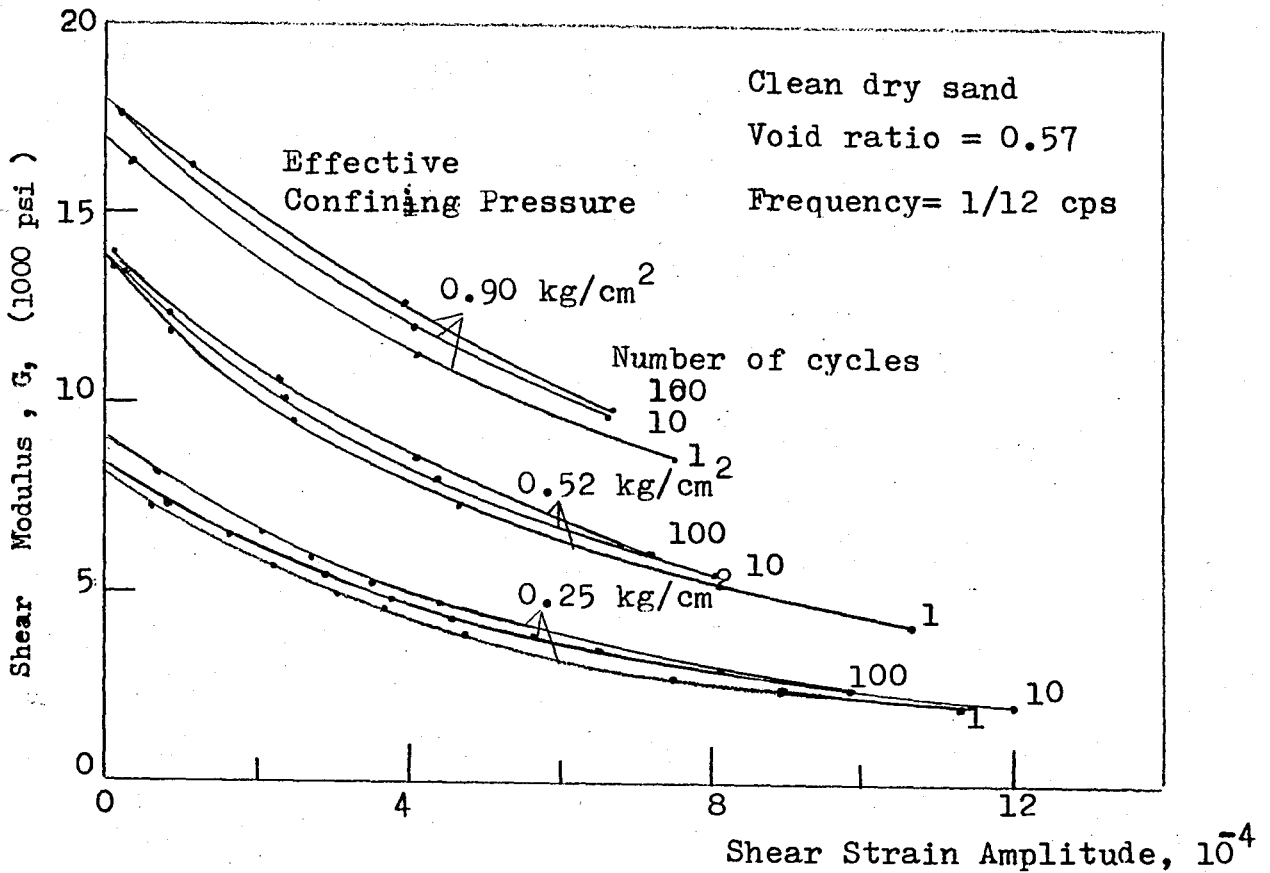


Figure 2.4- Effects of Strain Amplitude, Effective Confining Stress, and Number of Cycles of Loading on Shear Modulus of Sand. (After Hardin and Drnevich, 1972)

The effect number of cycles of loading,  $N$ , on the shear modulus of cohesionless soils is also shown in Fig. 2.4. The shear modulus increases slightly with the number of cycles. It is worth noting that, although the data in Fig. 2.4 are for clean dry sands, the general shape of the shear modulus shear strain amplitude curves is the same for cohesive soils and for other sands. It has been

also demonstrated by Hardin and Drnevich (1972,a) that a six fold difference in  $G_{max}$  (11.7 kN/m<sup>2</sup> to 75.9 kN/m<sup>2</sup> ) can be observed which is primarily due to the difference in void ratio (1.9 to 0.61) and this effect has been reviewed in several references,(Hardin, 1965; Hardin and Black, 1968 ; Hardin and Richart, 1963 ; Lambe and Whitman, 1969 ; Richart, Hall and Woods, 1970 ).

The effect of void ratio can be taken into account by a function,

$$F(e) = \frac{(2.973 - e)^2}{1 + e} \quad ( 2.1 )$$

which has been proposed by Hardin, 1965 ; and Hardin and Black,1968. When  $G_{max}$  is divided by  $F(e)$  to remove the effect of void ratio, the range for  $G_{max}/F(e)$  becomes 21.4 bars to 29.4 bars(1 bar=1 kg/cm<sup>2</sup>)

Edil and Luh, (1978), using resonant column test, have shown that grain shape, characterized by roundness, has a significant effect on shear modulus, namely, increasing roundness causes a decrease in shear modulus, on the other hand grain size distribution is found to be ineffective.

The effects of above mentioned parameters on the damping ratio,  $D$  , of soils can be reviewed in Fig. 2.5. Starting from a zero shear strain amplitude, damping ratio increases with increasing strain amplitude.



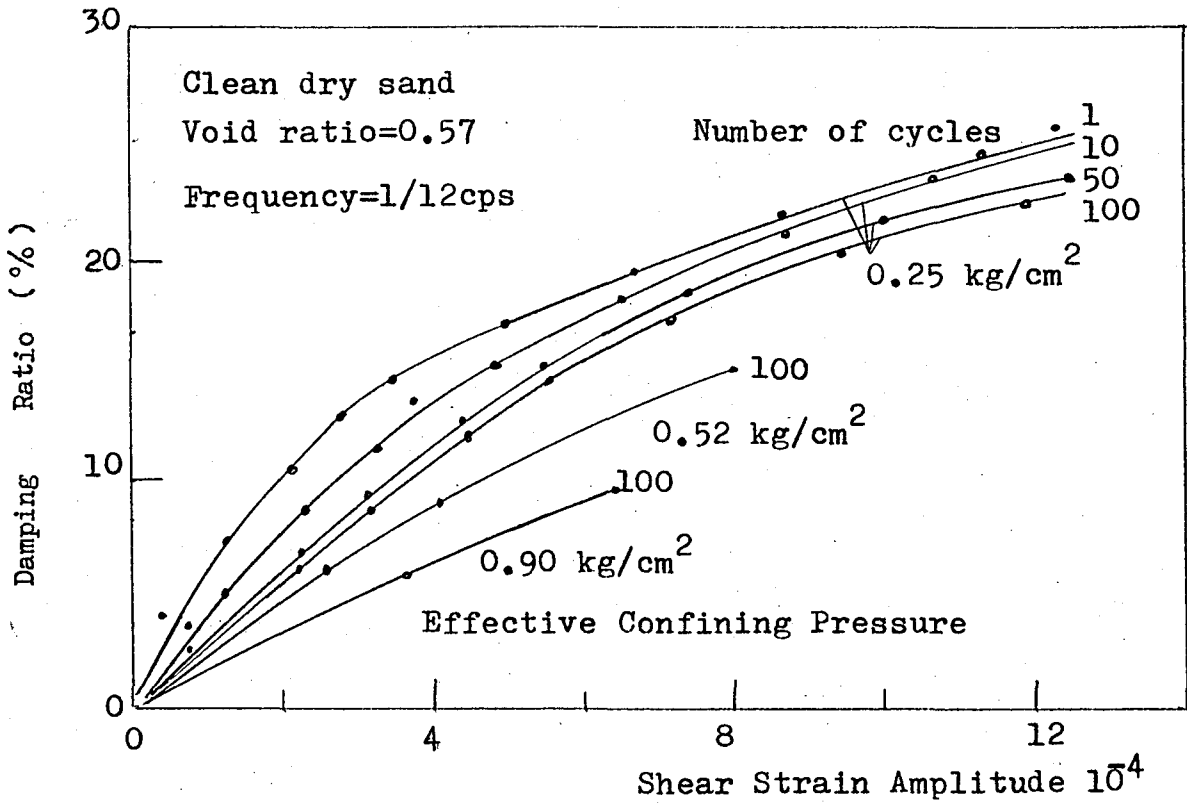


Figure 2.5- Effects of Strain Amplitude, Effective Confining Stress, and Number of Cycles of Loading on Damping Ratio of Sands.(After Hardin and Drnevich, 1972)

The general trend of damping curves is to approach a maximum value,  $D_{max}$ , asymptotically and this concept of  $D_{max}$  has been successfully used by Hardin and Drnevich (1972,b), to define the damping curves over the range of shear strain amplitudes tested by using modified hyperbolic relationship. It may be observed from Fig.2.5 that, a decrease in damping ratio occurs due to

increases both in effective mean principal stress and number of cycles of loading. The rate at which damping ratio decreases is proportional with the logarithm of number of cycles of loading,  $N$ , both in cohesive and cohesionless soils. This can be represented by the empirical equation ( Seed and Idriss, 1970 )

$$D_{max} = 30 - 1.5 \log N \quad (2.2)$$

where  $D_{max}$  is the maximum damping ratio.

It has also established that the general shape of the damping ratio-shear strain amplitude curves for clean dry sands also applies to cohesive soils and other type of sands.

The effect of relative density on damping ratio is not shown in Fig. 2.5. But the tests on undisturbed natural soils clearly show the trend of decreasing damping ratio with decreasing relative density (Hardin and Drnevich, 1972,a)

The effects of grain shape and grain size distribution on damping ratio have been examined by Edil and Luh (1978) and they have concluded that these effects are unimportant.

The effects of other parameters such as initial shear stress, degree of saturation and thixotropic effects on shear modulus and damping ratio are assumed to be of secondary importance and are still under investigation.

## 2.5- THE EQUIVALENT LINEAR IDEALIZATION

Based on the discussion made in section 2.2, the equivalent linear idealization of cyclic shear stress-strain relations of soils gives fairly good approximations in practical ranges. In this idealization, the soil is represented as a linear visco-elastic material whose stiffness and energy dissipation characteristics are introduced by using equivalent shear modulus and equivalent viscous damping. To day, there exists two different equivalent linear models widely used in soil dynamics problems. One of these models was proposed by Seed and Idriss (1970), and the other was proposed by Hardin and Drnevich (1972).

### 2.5.1- SEED-IDRISS MODEL

Seed and Idriss (1969-1970) have proposed approximate design curves for shear modulus and damping ratio for two different soil types, namely for cohesionless and cohesive soils.

In their model for sands, the shear modulus shows a variation depending on two parameters, so called effective mean confining pressure,  $\sigma_0$ , and shear modulus parameter  $K$ . The authors constructed an expression for  $G$  in which shear modulus varies with the square root of the effective mean confining pressure.

$$G = K \sqrt{\sigma_0} \text{ kg/cm}^2 \quad ( 2.3 )$$

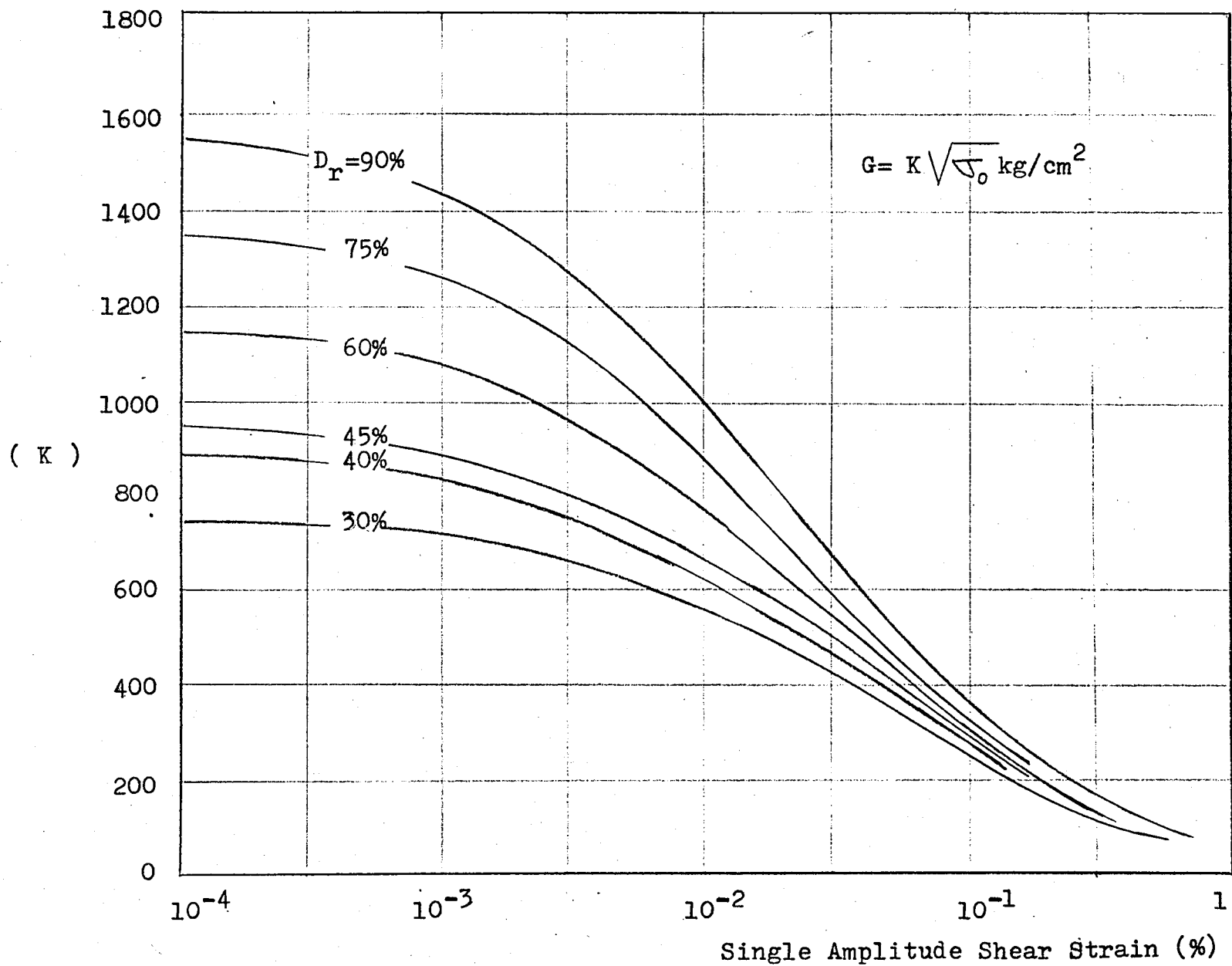


Figure 2.6.A- Shear Moduli of Sands at Different Relative Densities (After

Seed and Idriss, 1970 )

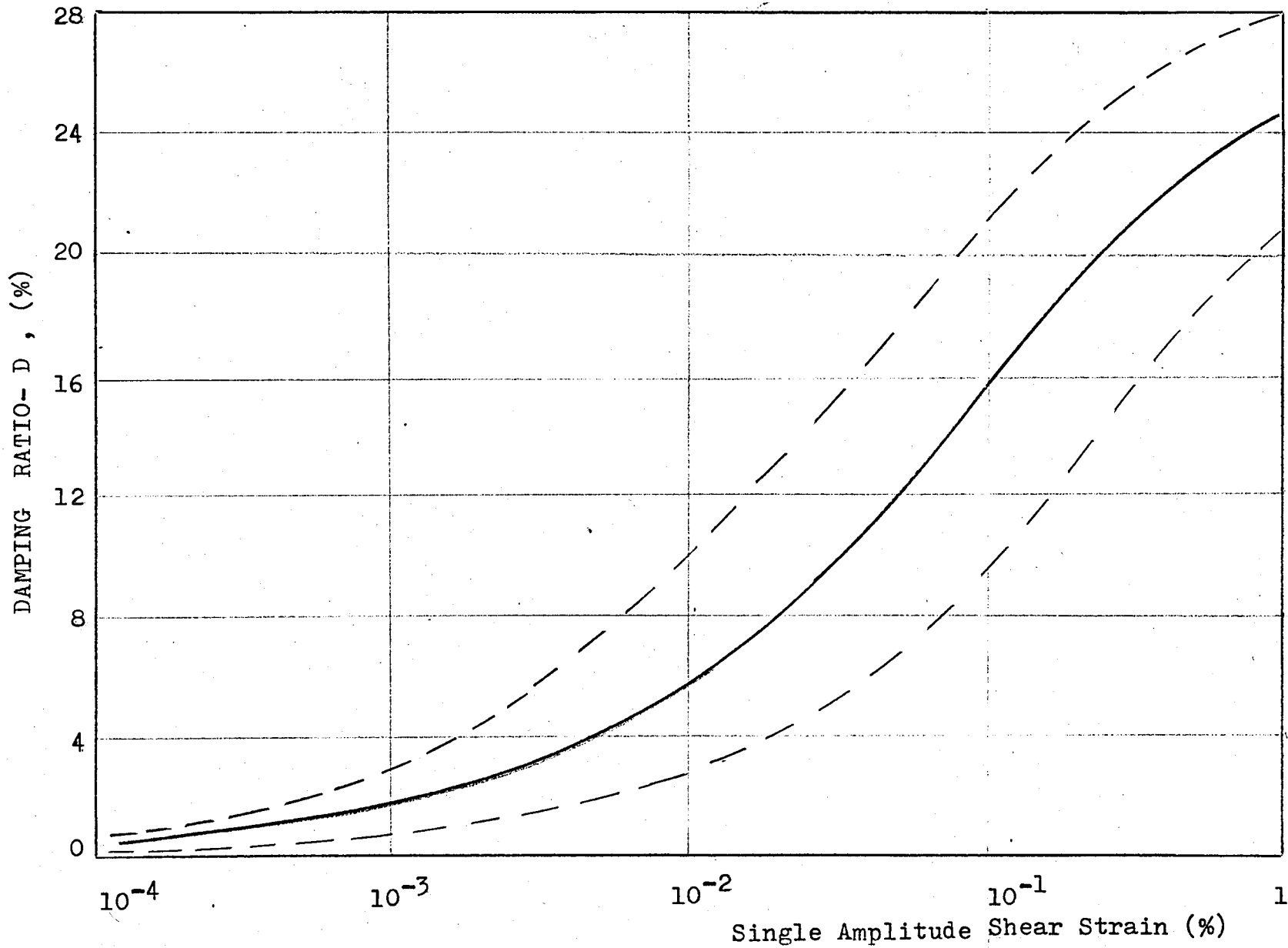


Figure 2.6.B- Damping Ratio for Sands (After Seed and Idriss, 1970)

They have shown that K parameter depends on relative density, and shear strain amplitude that the sand deposit experience. A decrease is observed in K parameter both with an increase in shear strain amplitude and with a decrease in relative density, Fig. 2.6.A. In the same figure, it can be seen that at very low strains ( $10^{-3}\%$ ), K depends only on the relative density, and at very high strains ( $10^{-1}\%$ ), the values of K are almost independent of relative density.

In this model, the damping ratio for sands increases uniquely with increasing strain amplitude, Fig. 2.6.B. In this figure, approximate upper and lower bounds for damping ratio of various soils are shown by the dashed lines, and representative average values are indicated by the solid line. This solid line is likely to provide values of damping ratio with sufficient accuracy for many practical purposes.

#### 2.5.2- HARDIN-DRNEVICH MODEL

Hardin and Drnevich (1972,b) have stated that a given shear strain does not have the same effect on all soils, nor on the same soil under different pressures. The critical soil properties i.e. shear modulus and damping ratio, are dependent on many different parameters. For a given problem these properties may vary by a factor 10 in a soil deposit that appear to be relatively homogenous due to their dependence on such parameters ( Among

these parameters the relatively more important ones discussed in section 2.4 ).

Plotting the end points of cyclic stress-strain curves, for a constant number of cycles of loading but for varying shear strain amplitudes, Hardin and Drnevich obtained a curve which is similar to ordinary stress-strain curves, Fig. 2.7 a. A hyperbola approximation to this curve may be written as

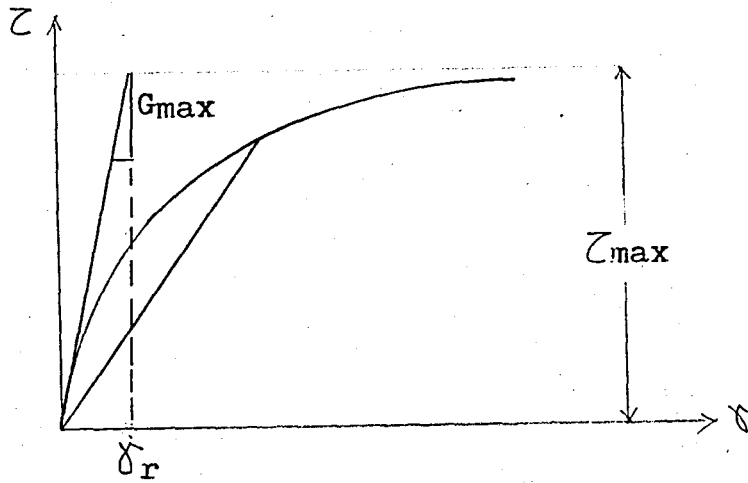
$$\tau = \frac{\delta}{\frac{1}{G_{\max}} + \frac{\delta}{\tau_{\max}}} \quad (2.4)$$

in which  $\delta$  = shear strain,  $G_{\max}$  is initial tangent modulus, and  $\tau_{\max}$  is the shear stress at failure. The secant modulus of any point on this hypothetical, stress-strain curve gives the cyclic loading modulus for the loop with its end at the same point. Hence, the variation of shear modulus with shear strain amplitude can be defined by this hypothetical, hyperbolic stress-strain curve. Dividing both sides of Eq.(2.4) by  $\delta$ , the secant modulus,  $G = \tau / \delta$ , is obtained

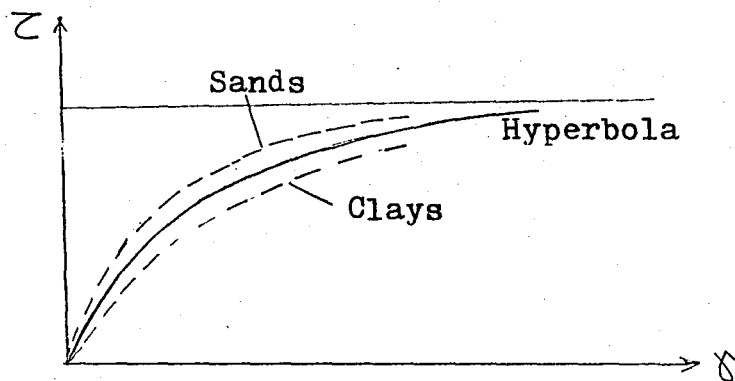
$$G = G_{\max} \left( \frac{1}{1 + \delta / \delta_r} \right) \quad (2.5)$$

in which  $\delta_r$  is named as reference strain, and defined by

$$\delta_r = \frac{\tau_{max}}{G_{max}} \quad (2.6)$$



(a) Hyperbolic : 
$$= \frac{\tau}{\frac{1}{G_{max}} + \frac{\delta}{\tau_{max}}}$$



(b) Modified Hyperbolas

Figure 2.7- Hyperbolic Stress-Strain Relation



The same authors have found that when the critical soil properties,  $G$  and  $D$ , are plotted against normalized strain  $\delta/\delta_r$ , a single curve may be used for the variation of these properties for a given soil, even under different ambient stresses.

The hyperbolic curve, defined by Eq. (2.4), now can be written in terms of normalized strain as

$$\tau = \tau_{\max} \left( \frac{\delta/\delta_r}{1 + \delta/\delta_r} \right) \quad (2.7)$$

Hardin and Drnevich have proposed a modification on this curve in order to diminish the variations from the true stress-strain relations, because the exact stress-strain relations for soils are not truly hyperbolic. Their proposal is as follows:

By distorting the strain scale, the real stress-strain curve can be forced to have a real hyperbolic shape. To achieve this goal, they have defined a hyperbolic strain as

$$\delta_h = \frac{\delta}{\delta_r} \left[ 1 + a e^{-b (\delta/\delta_r)} \right] \quad (2.8)$$

in this equation  $a$  and  $b$  are considered to be empirical soil

constants, and  $e$  denotes the exponential function. In the definition of hyperbolic strain  $a$  and  $b$  determine the deviation of the stress-strain relation of a particular soil from the hyperbolic shape. Now, in terms of hyperbolic strain a modified hyperbolic relation may be written as, Fig.(2.7 b) :

$$\tau = \tau_{\max} \left( \frac{\gamma_h}{1 + \gamma_h} \right) \quad (2.9)$$

Using the definition of hyperbolic strain Eq. (2.5) can be rewritten as

$$G = G_{\max} \left( \frac{1}{1 + \gamma_h} \right) \quad (2.10)$$

In their study Hardin and Drnevich have proposed an approximate relation which express damping ratio,  $D$  , in terms of shear modulus,  $G$  , that is

$$D = D_{\max} \left( 1 - \frac{G}{G_{\max}} \right) \quad (2.11)$$

in which  $D_{\max}$  is the maximum value of damping ratio,  $D$  , and is about 20 to 30 % for different soils, (the original curve

fitting expressions for  $D_{max}$  may be found in Hardin and Drnevich 1972,b). When equation (2.11) is used together with Eq. (2.10), an expression for damping ratio in terms of hyperbolic strain is obtained, that is

$$D = D_{max} \left( \frac{\gamma_h}{1 + \gamma_h} \right) \quad (2.12)$$

The empirical coefficients  $a$  and  $b$  in Eq.(2.8) for the definition of damping relationship, Eq.(2.12), differ somewhat from those defining modulus, Eq.(2.10). This is because Eq.(2.11) is not exact but an approximation. In the original paper the values of these coefficients are given for a fairly wide range of soils that the authors have tested. Using the equations along with Eq.(2.8), the curves in Fig.(2.8) were computed to give the value of hyperbolic strain,  $\gamma_h$ , corresponding to a given value of normalized strain.

The values of  $G_{max}$  and  $D_{max}$  are needed to calculate  $G$  and  $D$ . For practical purposes a value of shear modulus measured accurately for a strain amplitude of about  $0.25 \text{ in/in} \times 10^{-4} \text{ in/in}$ . or less can be taken to equal  $G_{max}$ . This can not be done with conventional static testing equipment, but  $G_{max}$  can be measured directly in the laboratory using the resonant column vibration

test or in the field using seismic techniques to measure shear or Rayleigh wave velocities. Also, Hardin and Black(1969), have shown that for many undisturbed cohesive soils, as well as sands,  $G_{max}$  can be calculated from

$$G_{max} = 1230 \frac{(2.973 - e)^2}{(1 + e)} (OCR)^K \bar{\sigma}_o^{1/2}$$

in which  $e$  = void ratio;  $OCR$  = over consolidation ratio;  $\bar{\sigma}_o$  = mean principal effective stress; and both  $\bar{\sigma}_o$  and  $G_{max}$  are in pounds per square inch. The value of  $K$  depends on the plasticity index,  $PI$ , of the soil.

Values of  $D_{max}$  for dry clean sand can be calculated from

$$D_{max} = 33 - 1.5 (\log N)$$

in which  $N$  = number of loading cycles.  $D_{max}$  for clean sands depends only on number of cycles of loading; but, for cohesive soils it depends also on ambient mean principal effective stress, and frequency.

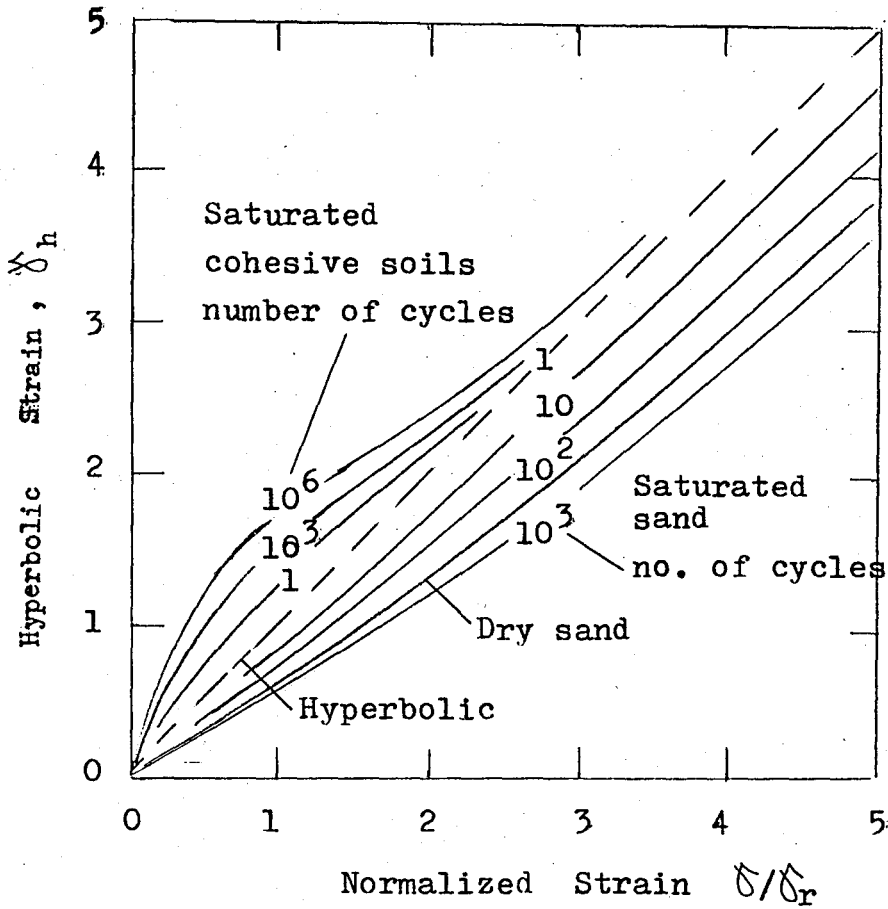


Figure 2.8- Hyperbolic Strain versus Normalized Shear Strain for Shear Modulus.  
(Hardin and Drnevich, 1972)

2.5.3- THE USE OF EQUIVALENT LINEAR IDEALIZATION :  
EQUIVALENT LINEAR METHOD.

Equivalent linear method is an iterative soil-response analysis technique which implements equivalent linear idealization. The procedure of this method is as follows:

- (1) Shear moduli and damping values are estimated for each layer in the soil profile based on initial estimates of shear strains.
- (2) The system is analyzed using these properties, acceleration and strain time histories are computed through the soil deposit.
- (3) From these time histories average shear strain amplitudes are estimated for each soil layer, and equivalent linear models, such as those discussed in sections 2.5.1 and 2.5.2, are consulted to see whether the shear moduli and damping values used in the response evaluation are compatible with the strains developed.
- (4) If the computed properties are compatible with the ones used in the previous iteration, the solution is completed. Otherwise,
- (5) Steps (2) through (4) are repeated until the difference between estimated and computed strains, moduli and damping

are sufficiently small.

In any soil amplification problem, analysis is done as if the material were linear, therefore formulation and solution of the problem become easier while nonlinearity of the stress-strain relation is taken into account approximately. This is the main advantage of the method. However, this advantage give rise to following limitation. To linearize a nonlinear problem, constant values of shear modulus,  $G$ , and damping ratio,  $D$ , are used throught cyclic loading. This may be an oversimplification with an unknown degree of approximation. The error involved can only be assessed by comparing the results of analyses by those of a truly nonlinear analysis.

## 2.6- NONLINEAR MODELS

### 2.6.1- MASING CRITERION

Under cyclic excitations the stress-strain behaviour of soils is nonlinear and hysteretic Fig.(2.9) shows a typical idealization of this behaviour. The stress-strain loop, i.e. loop ABCDA, is associated with a given maximum values of shearing stress,  $\tau_1$ , and shear strain,  $\delta_1$ , and the coordinates of the tip points of the loop, points A and C, are defined in terms of these values.

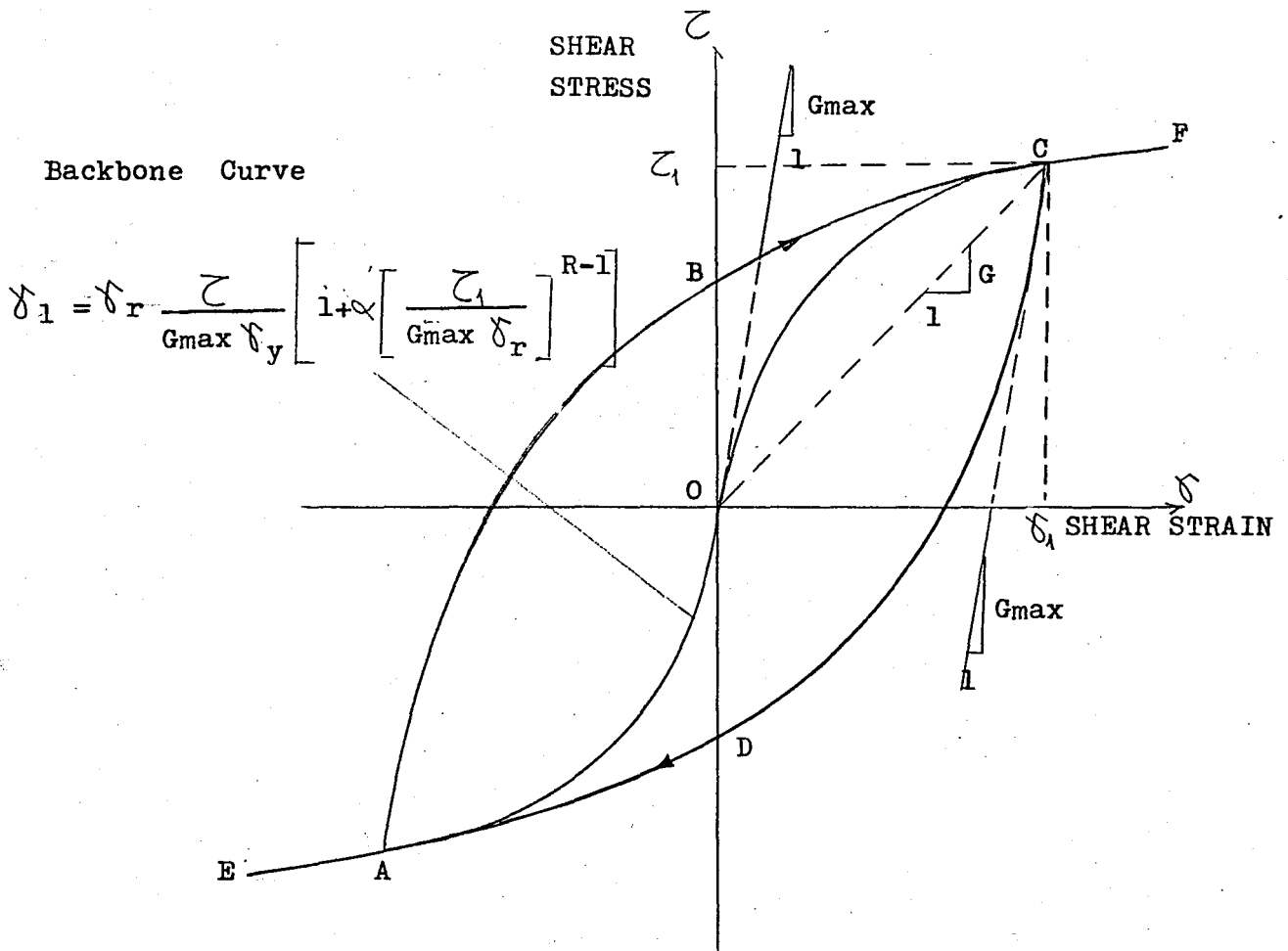


Figure 2.9- Typical Stress-Strain Relationship



The path (EAOCF) followed by the tip points of all hysteresis loops, associated with different values of  $\delta_1$ , is defined as backbone or skeleton curve for this soil specimen. This curve constitutes the basis for characterizing the stress-strain behaviour of soils. The slope of backbone curve at the origine gives the maximum shear modulus,  $G_{max}$ , while secant slope corresponding to strain level  $\delta_i$  gives the secant shear modulus at that strain level. The backbone curve do not give any idea about the damping characteristics of the soils solely. For this reason the shape of the hysteresis loop is also required. The most widely accepted rule for generating hysteresis loops from a backbone curve is to assume that the soil behaviour satisfies Masing criterion.

This criterion states that: The stress-strain curve associated with one-dimensional symmetrical closed hysteresis loops should be of the same form as those of stabilized initial loading curve (or backbone curve), except for an enlargement by a factor of two, Masing, (1926). Or in other words, according to this criterion the unloading and reloading branches of the hysteresis loop can be obtained from backbone curve by enlarging it twice and shifting its origin. One consequence of this criterion is that, the tangent modulus at the tips of the loop immediately after the load reversal is equal to  $G_{max}$  which agrees with

experimental evidence of wide variety of soils, Hardin and Drnevich (1972). The hysteresis loops satisfying the Masing criterion causes systems to behave as if they had an equivalent damping ratio independent of the frequency of vibration, which is observed behaviour of soils and rock over a wide range of frequency Hardin and Drnevich (1972) ; Rosenblueth and Herrera (1964).

#### 2.6.2- RELATIONSHIP BETWEEN NONLINEAR AND EQUIVALENT LINEAR MODELS

As explained in previous section the cyclic stress-strain relationship determined by a laboratory test is usually characterized by two parameters, shear modulus and damping ratio. Due to nonlinearity, both of these parameters are strain dependent. At any shear strain amplitude,  $\delta_1$ , these " equivalent linear " shear modulus,  $G_e$ , and damping ratio,  $D_e$ , defined as follows

$$G_e = \tau_1 / \delta_1 \quad (2.13)$$

$$D_e = 1/4\pi \frac{A_L}{A_T} \quad (2.14)$$

in which  $A_L$  and  $A_T$  denote, the area within a full hysteresis loop, and the equivalent linear strain energy, respectively, Fig.(2.1

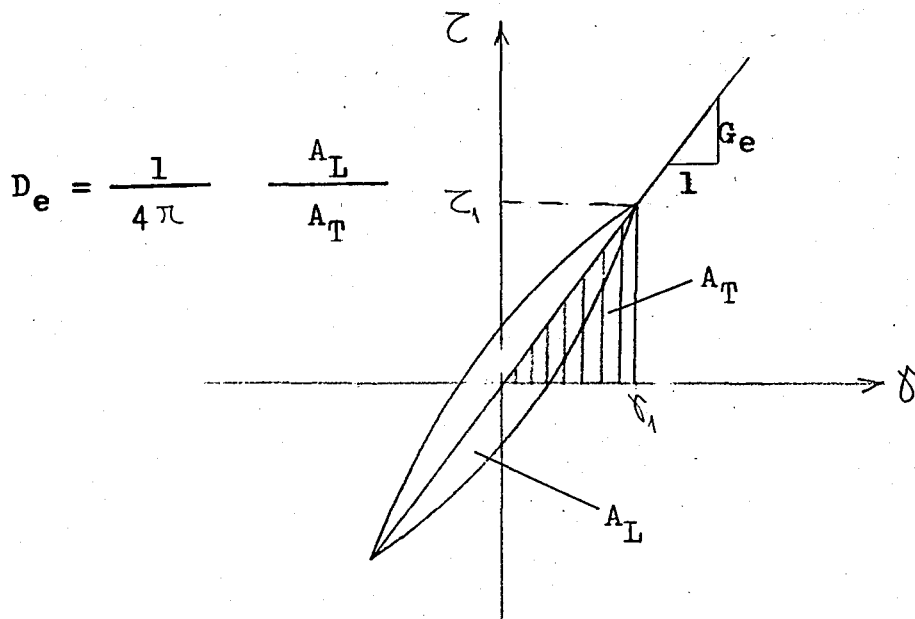


Figure 2.10- Definition of Equivalent-Linear Shear Modulus and Damping.

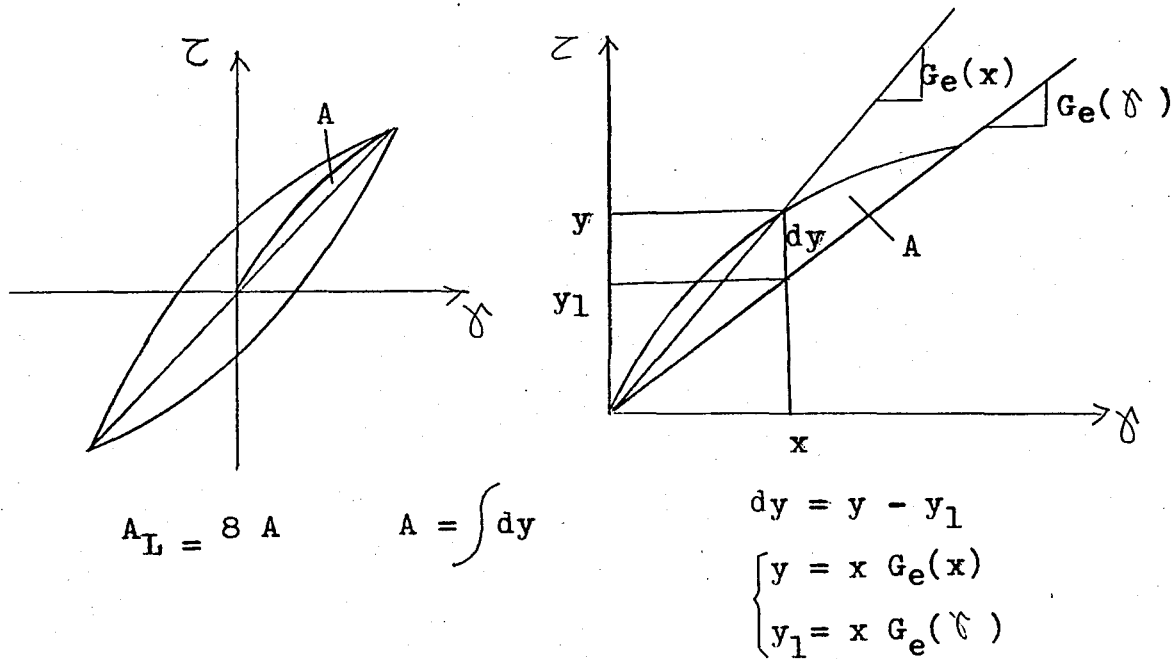


Figure 2.11- Derivation of Equivalent Damping

In order to test a proposed nonlinear soil model, or to determine its unknown parameters, one may make use of Eqs.(2.13) and (2.14). Since the determination of the shear modulus from a nonlinear model is fairly straight forward, this section is devoted to the definition of the equivalent damping inherent in a model.

Before defining the equivalent damping inherent in a model it is useful to develop the expression for damping in a general nonlinear model.

It is assumed that the equivalent linear shear modulus corresponding to a nonlinear model is known. The triangular area,  $A_T$ , in Eq.(2.14), may be expressed as

$$A_T = \frac{1}{2} \tau_1 \delta_1 \quad (2.15)$$

or, by making use of the expression for modulus,  $\tau_1 = \delta_1 G_e$ , as

$$A_T = \frac{1}{2} G_e \delta_1^2 \quad (2.16)$$

For any nonlinear model where the unloading curve is assumed to be geometrically similar to the initial loading curve, i.e. Masing criterion, it may be shown that the loop area,  $A_L$ , can be expressed as

$$A_L = 8 \int_0^{\delta_1} [G_e(x) - G_e(\delta)] x dx \quad (2.17)$$

where  $x$  denotes a dummy variable replacing shear strain for integration. In Eq.(2.17), integration is actually taken for a strain range from zero to desired strain amplitude,  $\delta_1$ . As it can easily be verified, this integration gives the area  $A$  shown in Fig.(2.11). The factor 8 in Eq.(2.17) comes from similarity considerations.

By substituting Eqs.(2.16) and (2.17) in Eq.(2.14) one obtains the general expression for equivalent damping inherent in a nonlinear model as:

$$D_e = \frac{4}{\pi} \cdot \frac{\int_0^{\delta} [G_e(x) - G_e(\delta)] x dx}{G_e(\delta) \delta^2} \quad (2.18)$$

The equivalent damping corresponding to the nonlinear model may be calculated by performing the integration in Eq.(2.18) once the appropriate  $G_e$  function for the same model has been defined.

## CHAPTER 3

## EXPERIMENTAL STUDY

## 3.1- APPARATUS

## 3.1.1- INTRODUCTION

The purpose of this section is to describe the design and operation of the H-12 Direct Simple Shear Apparatus. The apparatus was developed by Norwegian Geotechnical Institute for testing undisturbed and disturbed soils for conditions of simple shear and plane strain (that is, uniform strain through the soil sample and no change of horizontal cross-sectional area): These conditions are probably similar to strain conditions in the field, and they can not be obtained in laboratory by such standard testing methods as triaxial compression and shear-box tests.

The apparatus differs in a major respect from the conventional direct shear box apparatus. In a shear box, the top and bottom halves of which are moved with respect to each other, strains are non-uniform and failure occurs in an indeterminate zone. In the h-12 direct simple shear apparatus, the sample is placed between loading caps in a rubber membrane of circular cross section, reinforced by a spiral wire winding. This provides lateral restraint against horizontal linear strains, but possesses a very small resistance to horizontal shear strains. When the loading caps are displaced relative to each other, horizontal cross sections remain horizontal and undergo no horizontal

linear strains. Vertical cross sections normal to the direction of shear remain plane but tilt through an angle equal to the shearing strain. An element of the soil will therefore undergo deformations corresponding to a condition of simple shear in the direction of the shear force, and plane strain in the transverse direction. All elements undergo the same strain, excluding boundary effects near the rubber membrane, which are minimized by making the sample height small in relation to the sample diameter.

The apparatus thus offers the possibility of loading a sample to failure in a manner which differs from the usual direct shear test, and also differs the triaxial tests. It offers an advantage over the former test in that the whole sample is strained uniformly, and the maximum shear resistance is less influenced by any tendency to progressive failure than it would be with a less homogeneous condition of stress and deformation. A further advantage is found in undrained tests. In these tests drainage leads are kept open and hence pore water pressures are zero, but volume change is prevented by adjusting the external stresses. These tests can be carried out with greater precision since, because of the type of deformation, the requirements of no volume change can be met simply by controlling the sample height. This is done using the manual worm gear to adjust the vertical pressure. An advantage which the h-12 shear apparatus offers over the triaxial

test is that the conditions of uniform simple shear and plane strain simulate more closely the conditions on the failure plane in certain types of field problems.

### 3.1.2- APPARATUS REQUIREMENTS

The design is based on the following requirements :

- (1) Simple shear and plane strain, drained and constant volume tests.
- (2) Upper and lower part of sample are kept parallel during test.
- (3) Controlled strain or stress.
- (4) Maximum vertical load, 800 kilos, horizontal load, 400 kilos, accuracy estimated to  $\pm 1$  % of maximum load of load gauges.
- (5) Designed for  $50 \text{ cm}^2 \times 1.4 \text{ cm}$  samples confined in a wire-reinforced membrane. Maximum lateral stress  $1.8 \text{ kg/cm}^2$ .

Maximum height : 2 cm

Minimum height : 0 cm

- (6) Test on soft clays (quick clays) as well as stiff clays, silt and sand.

### 3.1.3- DESCRIPTION OF APPARATUS

The standard h-12 Direct Simple Shear Apparatus consists of: the sample assembly (Fig.3.1 ) and the vertical and horizontal load units (Fig.3.1 ).



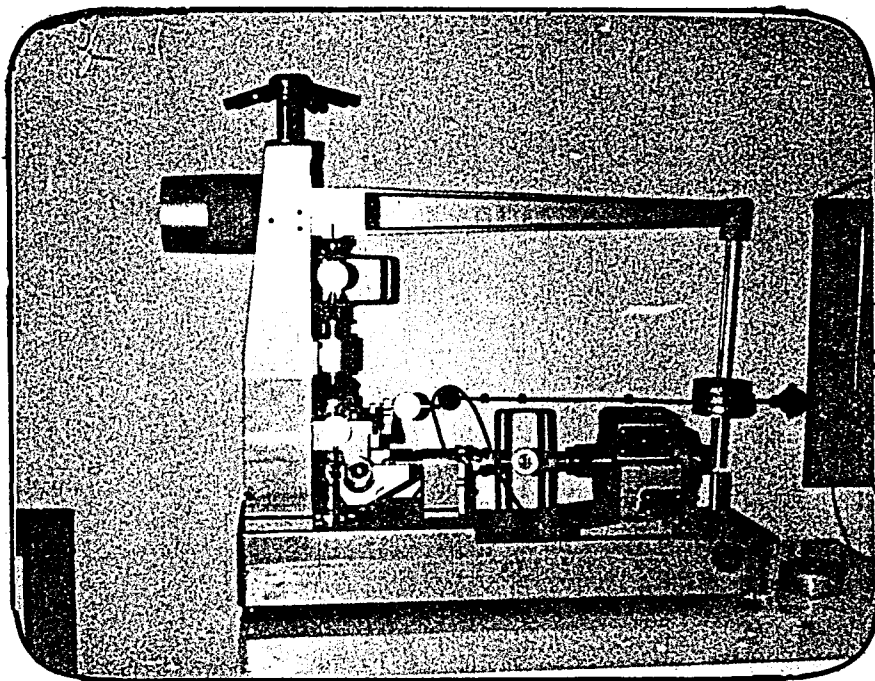


Figure 3.1- General View of the Apparatus

### 3.1.3.1- The Sample Assembly

The sample assembly consists of a pedestal, the lower and upper filter holders and a plastic container Fig.(3.2 ). The pedestal contains a mechanism for clamping and releasing the lower filter holder.

Clamping is necessary to prevent the lower filter holder from moving upwards when the rubber membrane is being mounted on the sample. The releasing mechanism facilitates the demounting of the sample when the test has been completed. The mechanism is operated by turning the screw. The lower and upper filter holders have recesses for sintered filter plates.

### 3.1.3.2- The Vertical And Horizontal Load Units

The vertical load unit consists of the apparatus base tower, leverarm with counterweight and hanger supported in a precision ball bushing, load gauge, loading piston sliding in a precision ball bushing, sliding box, vertical strain dial gauge, and lever arm adjusting mechanism. Fig.(3.2 )

The lever arm, which has a ratio of 1:10, is built into a U-shaped steel hanger supported at the top of the tower by an adjusting screw assembly. The screw allows the fulcrum of the lever arm to be adjusted vertically. To minimize friction a thrust bearing is used between the screw and the U-hanger. Loads are

applied to the hanger either by weights or by coupling the hanger to a worm gear driven by handwheel. These loads are transferred via a ball bearing, the load gauge, loading piston and sliding box to the top cap of the sample.

The horizontal unit for constant rate of strain consists of a gearbox which has three different speeds, is designed for interchangeable synchron motors with reduction gears. Motors with 117 different speeds are available giving a speed range of 0.2 to  $0.2 \times 10^{-4}$  mm/sec. The motor is removed by loosening four screws. The three different speeds of the gearbox are obtained by moving the gear shafts into the different gear positions. The horizontal movement 10 mm on both sides of the neutral position.

The horizontal unit also includes a load gauge, a piston operating through a precision ball bushing, a connecting fork and a sliding box. Fig.(3.2 ). Spherical bearings are used on both sides of the load gauges. The housing for the ball bushing has a clamp for locking the piston in any desired position. The sliding box is free to move up and down, so the horizontal force from the fork to the box is transmitted through ball bearing wheels to eliminate vertical friction.

The sliding box which ensures horizontal movement, consists of an upper and a lower part separated by steel balls in a brass housing. To keep the two parts together another series of balls

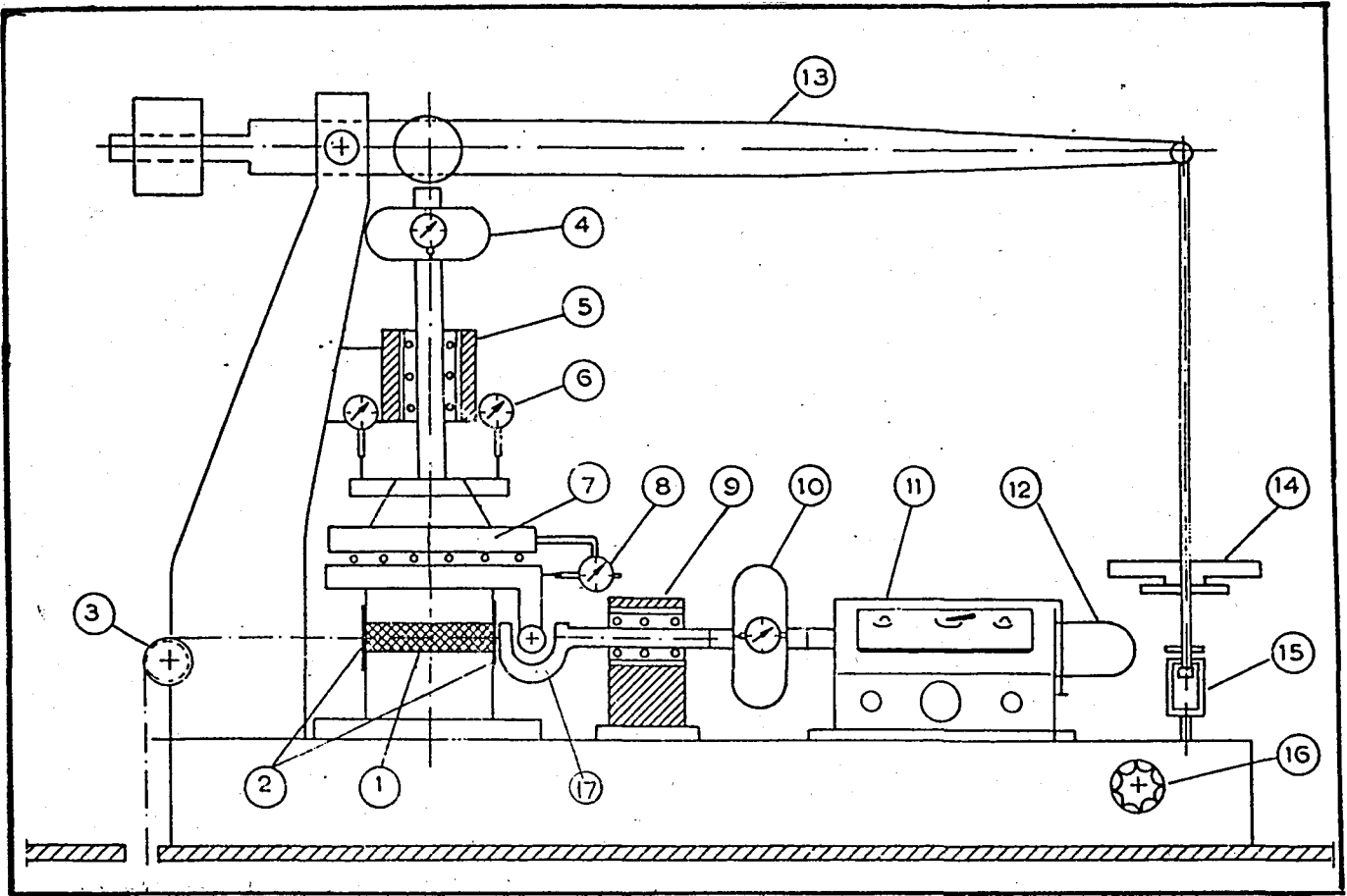


Figure 3.2 - General Principle of Direct Simple-Shear Apparatus

1-Sample 2-Reinforced rubber membrane 3-Wheels applying dead load  
 4-Load gauge for vertical load 5-Ball bushing 6-Dial gauges for  
 measurement of vertical deformation 7-Sliding box 8-Dial gauge for  
 measurement of horizontal deformation 9-Ball bushing 10-Load gauge  
 for horizontal force 11-Gear box 12-Exchangeable servogear motor  
 13-Lever arm 14-Weights 15-16-Clamping and adjusting mechanism  
 used for constant volume tests 17-Connecting fork

acts under a spring loaded plate. The whole unit is screwed on to the piston of the vertical loading frame.

The horizontal load unit for constant stress consists of an axle with 2 ball bearing mounted pulleys, 2 wires which can be fixed to the connecting fork by pins, a yoke and weight hanger for the required dead weights.

### 3.2- SAMPLE PREPARATION AND MATERIAL TESTED

In N.G.I. Simple Shear Apparatus used in this investigation, the sand sample is mounted between parallel top and bottom filter caps and confined by a wire-reinforced rubber membrane. It is assumed that, this reinforced rubber membrane will not permit the lateral expansion of sand and the cross-section of the specimen will be constant during the test. The wire used for reinforcement has a diameter of 0.15mm, an E-modulus of  $1.55 \times 10^6$  kg/cm<sup>2</sup> and a tensile strength of 5800 kg/cm<sup>2</sup>, and the reinforcement winding is 20 turns per cm. height.

During the preparation of specimen, firstly, the lower filter holder with filter is mounted on the pedestal of the sample assembly and the reinforced rubber membrane is also mounted on the lower filter holder. An O-ring is placed at the bottom of the rubber membrane. Then, the sand is uniformly filled into the membrane by means of a funnel. In this study, two different dense

sands are obtained by pouring the sand from different heights. But it is not possible to prepare a dense sand (more than the relative density of 70 %) and a loose sand (less than the relative density of 50 %), because of fairly elastic rubber membrane and a very small height of sample (approximately 1.5 cm).

After the sand is filled into the membrane, the surface of the sample is made smooth, then upper filter holder with filter is carefully lowered in to contact with the specimen and the rubber membrane mounted on the upper filter holder. An O-ring is also placed at top of the rubber membrane.

The initial heights of the samples should be measured carefully because the relative densities of sand are determined by means of the heights of the samples. After the initial height of the sample assembly, from which the initial sample height may be obtained, is measured, the sample assembly is now ready to be transferred to the shear apparatus.

The material tested in this investigation is fairly uniform subangular dry sand, having a specific gravity of solids,  $G_s$ , of 2.64. Grain size distribution curve for the sand tested is shown in Fig. 3.3. The maximum and minimum densities of the sand, as determined by American Society of Testing and Materials (A S T M) Standard (D 2049-69) Test for Relative Density of Cohesionless

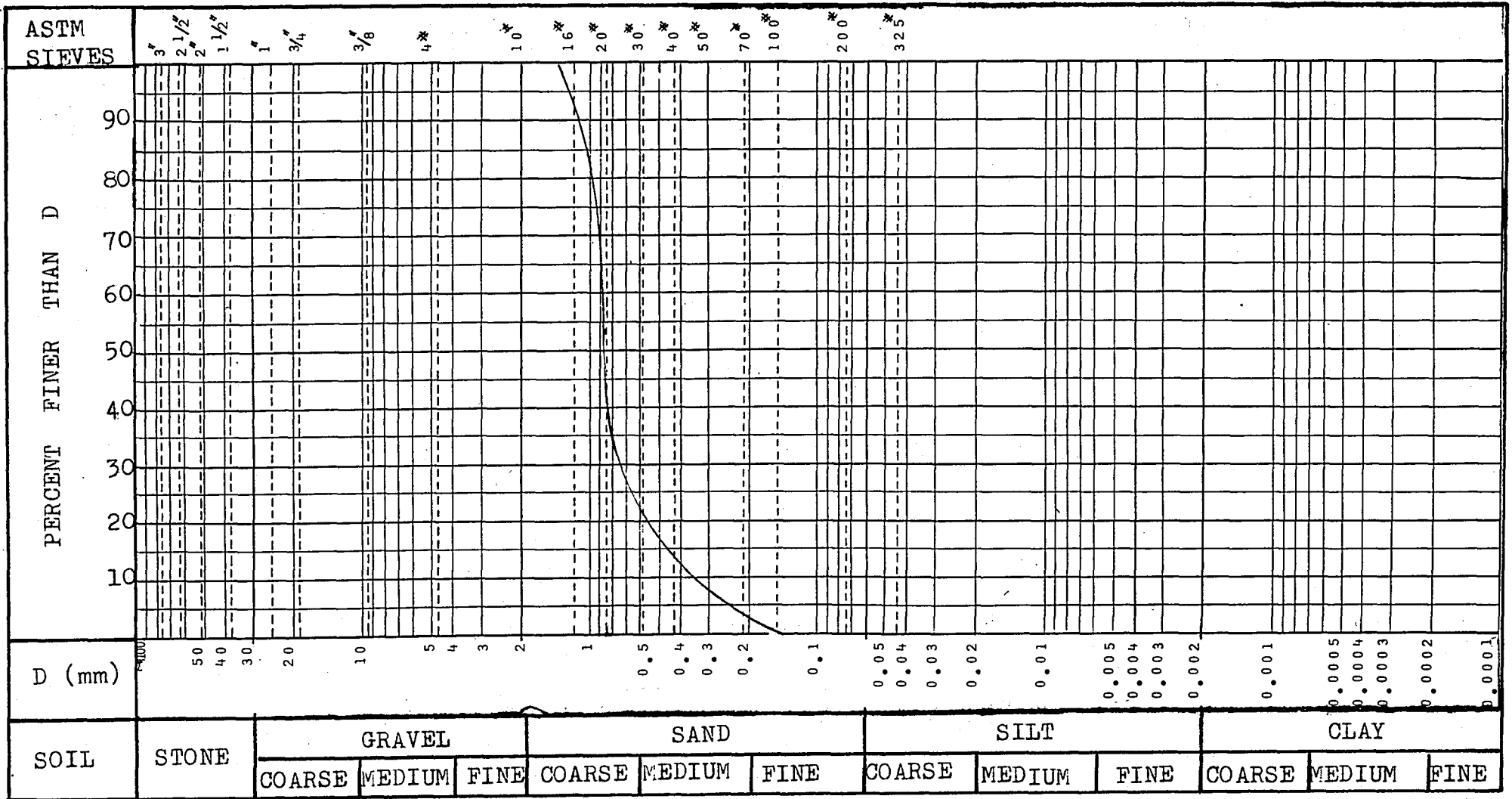


Figure 3.3 - Grain Size Distribution Curve for the Sand Tested

Soils, are  $\gamma_d \text{ max} = 1.76 \text{ gr/cm}^3$  and  $\gamma_d \text{ min} = 1.55 \text{ gr/cm}^3$ . The relative density,  $D_r$  is computed as

$$D_r = \frac{\gamma_d \text{ max}}{\gamma_d} \times \frac{(\gamma_d - \gamma_d \text{ min})}{(\gamma_d \text{ max} - \gamma_d \text{ min})} \times 100 \quad (3.1)$$

where

$\gamma_d \text{ min}$  describes the most loose state of the sand tested.

$\gamma_d \text{ max}$  describes the most dense state that the sand can be structured.

$\gamma_d$  is the density of the laboratory sample or research test specimen.

### 3.3- MOUNTING OF THE SAMPLE ASSEMBLY IN THE SHEAR APPARATUS AND TESTING.

After the sample is prepared, the sliding box is locked by means of two pins. If necessary this position can be obtained by turning the plastic knob on the gear box when it is in free gear. The lever arm which is previously balanced with the upper filter holder is placed in its upper position. Then, the sample assembly is pushed over to the base of the shear apparatus. The ring segment is fixed such that it centers the pedestal of the sample assembly. The ring segment at the opposite side is then attached to the base,



and to prevent tilting of the pedestal the two screw locks are tightened.

The lever arm is lowered carefully down and a small weight (50 gm.) is applied. The connection fork is brought in contact with the wheels. The dial gauge measuring vertical deformation is zeroed, and the weights which will apply required vertical stress are hung on the hanger. The sample is consolidated under this vertical stress. The vertical load is determined by the load gauge, and the vertical deformation is observed by means of the dial gauge during consolidation. We waited approximately an hour for consolidation of the sand in this investigation.

After the consolidation is completed the locking pins in the sliding box are removed and two clamping screws are brought into contact with the top filter holder. The dial gauge is continuously watched during this procedure, so that no horizontal deformation is applied to the sample. The fork used to transmit horizontal load to the sample is unclamped. The fork is brought in contact with the two wheels; the dial gauges for indicating the horizontal movement and the dial gauge of the proving ring are continuously watched, so that no movement occurs in the sample. The fork is moved manually by turning the plastic knob when it is in a neutral position, between the indicator grooves.

After the dial gauges are zeroed, the horizontal (shear )

loading is applied through a range of constant strain rates by a multispeed motor drive which can be operated both forwards and backwards. Horizontal load was measured both two directions since the gauge is calibrated for compression and tension forces. In this study, chosen rate of strain was 0.025 mm/min.

Strain-controlled static and cyclic simple shear test were performed at relative densities of 50 % and 65 % and vertical stresses of 0.5 , 1.0 , 2.0 , 4.0 and 8.0 kg/cm<sup>2</sup> ; strain amplitudes ranges from about 0.25 % to 6.75 % .

### 3.4- ANALYSIS OF DATA

A prescribed deformation is applied to the specimen, and the developed horizontal loads and deformations are observed by means of the dial gauges and recorded. A typical time record of the horizontal load and deformation during a simple shear test on a dry sand sample is shown in Fig. 3.4

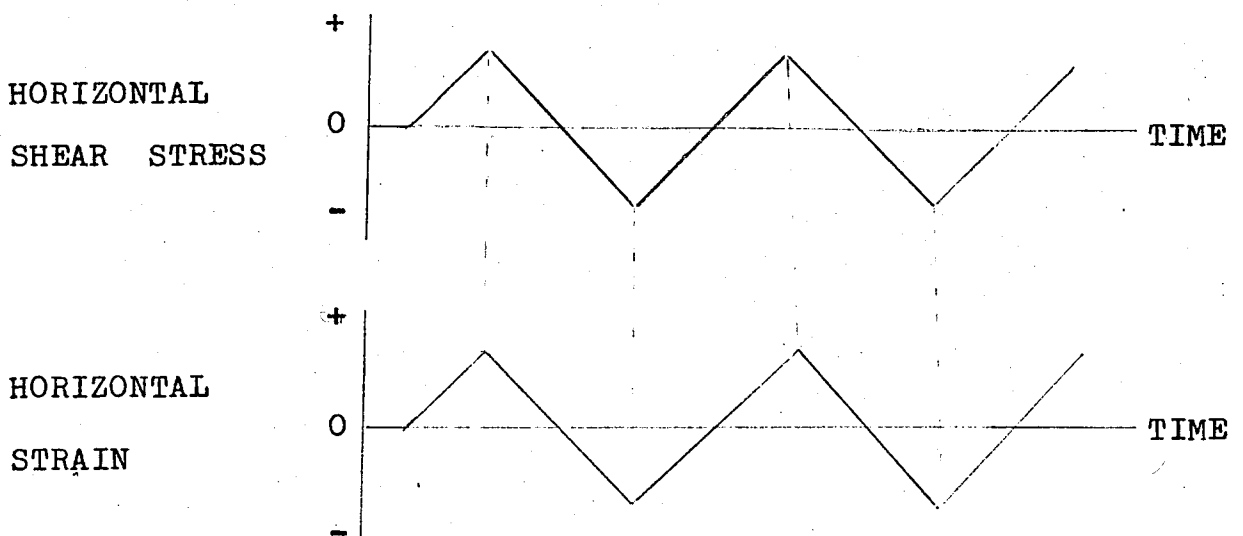


Figure 3.4 - Typical Record of Deformation and Load During Simple Shear Test.

The applied horizontal load is divided by the area of the sample,  $A_s$ , and values of cyclic shear stress are found as,

$$\tau = \frac{P_h}{A_s}$$

where  $P_h$  is the cyclic horizontal load.

Similarly, using consolidated sample length,  $L_s$ , single amplitude cyclic shear strains are calculated as,

$$\gamma = \frac{\Delta L}{L_s}$$

where  $\Delta L$  is the cyclic horizontal displacement.

Then, by plotting cyclic shear stress versus cyclic shear strain, the hysteresis loops for different cycles number are obtained. From the hysteresis loops obtained from each test, values of dynamic shear modulus,  $G$ , are determined by measuring the slope of the line connecting the extreme points of the hysteresis loops. The same loop is used to calculate the hysteretic damping,  $D$ .

Due to non-linearity, both these parameters (shear modulus and damping ratio) are strain dependent. At any shear strain amplitude  $\gamma_1$ , the equivalent shear modulus,  $G_e$ , and damping ratio,  $D_e$ , are defined as follows explained in Section 2.6.

$$G_e = \frac{\tau_1}{\gamma_1}$$

$$D_e = \frac{1}{4\pi} \frac{A_L}{A_T}$$

in which  $A_L$  and  $A_T$  denote the area within a full hysteresis loop, and the equivalent linear strain energy, respectively, Fig.(2.9).

### 3.5- SCHEDULE OF THE TESTS

The testing program performed is shown in Table 3.1. It can be seen from Table 3.1 that, vertical pressure was changed in order to investigate its effect on shear modulus and damping ratio. The initial relative densities of samples were tried to be kept constant (around 50 % and 65 %) using the sample preparation procedure explained in Section 3.2. Two different relative densities were used in order to see the effect of relative density on shear modulus and damping ratio. Data of horizontal load and displacement was drawn for the 5<sup>th</sup> cycles of loading. But five additional tests are performed applying 10 cycles of loading to evaluate the effect of number of loading cycles on shear modulus and damping ratio.

TEST	VERTICAL STRESS $\sigma_v$ (kg/cm <sup>2</sup> )	RELATIVE DENSITY (%)	NUMBER OF CYCLES (N)	STRAIN AMP. RANGES (%)
A1	0.5	63	5	0.25
A2	0.5	64	5	0.50
A3	0.5	65	5	0.75
A4	0.5	50	5	0.25
A5	0.5	51	5	0.50
A6	0.5	50	10	0.25
B1	1.0	65	5	0.25
B2	1.0	64	5	0.50
B3	1.0	65	5	0.75
B4	1.0	50	5	0.25
B5	1.0	51	5	0.50
B6	1.0	50	10	0.25
C1	2.0	67	5	0.25
C2	2.0	65	5	0.50
C3	2.0	64	5	0.75
C4	2.0	51	5	0.25
C5	2.0	52	5	0.50
C6	2.0	51	10	0.25
D1	4.0	66	5	0.25
D2	4.0	65	5	0.50
D3	4.0	64	5	0.75
D4	4.0	50	5	0.25
D5	4.0	52	5	0.50
D6	4.0	50	10	0.25
E1	8.0	67	5	0.25
E2	8.0	65	5	0.50
E3	8.0	65	5	0.75
E4	8.0	51	5	0.25
E5	8.0	50	5	0.50
E6	8.0	51	10	0.25

Table 3.1 - Test Program

## CHAPTER 4

## TEST RESULTS AND DISCUSSION

## 4.1- HYSTERESIS LOOPS

Cyclic shear stress-strain hysteresis loops obtained from tests are shown in Figs.(4.1) to (4.30). It can be seen from these figures that, all of the hysteresis loops have similar trends and the loops can be considered as fairly symmetric about the origin as in the case shown in Fig.2.2 where shear modulus and damping ratio are defined.

## 4.2- SHEAR MODULUS VALUES

Shear modulus values obtained from the tests are shown in Table 4.1. This table shows the values of shear modulus obtained under different testing conditions.

In order to discuss the effects of shear strain and vertical pressure on shear modulus, Fig.(4.31) will be referred. In this figure, shear modulus values are given for the sand tested at a relative density of 65 %. It can be observed that as the applied shear strain increases, shear modulus decreases. The same figure also shows that increasing vertical pressure causes an increase in shear modulus. One reason behind this observation may be that the strength of the soil is expected to increase with increasing vertical pressure and increase of strength of soil may result in an increase of shear modulus.

TEST	VERTICAL STRESS (kg/cm <sup>2</sup> )	RELATIVE DENSITY (%)	NUMBER OF CYCLES (N)	STRAIN AMP. RANGES (%)	SHEAR MODULUS (kg/cm <sup>2</sup> )
A1	0.5	63	5	0.25	68
A2	0.5	64	5	0.50	49
A3	0.5	65	5	0.75	40
A4	0.5	50	5	0.25	60
A5	0.5	51	5	0.50	44
A6	0.5	50	10	0.25	68
B1	1.0	65	5	0.25	112
B2	1.0	64	5	0.50	68
B3	1.0	65	5	0.75	63
B4	1.0	50	5	0.25	100
B5	1.0	51	5	0.50	56
B6	1.0	50	10	0.25	116
C1	2.0	67	5	0.25	244
C2	2.0	65	5	0.50	144
C3	2.0	64	5	0.75	120
C4	2.0	51	5	0.25	212
C5	2.0	52	5	0.50	120
C6	2.0	51	10	0.25	236
D1	4.0	66	5	0.25	404
D2	4.0	65	5	0.50	236
D3	4.0	64	5	0.75	189
D4	4.0	50	5	0.25	360
D5	4.0	52	5	0.50	203
D6	4.0	50	10	0.25	384
E1	8.0	67	5	0.25	620
E2	8.0	65	5	0.50	364
E3	8.0	65	5	0.75	313
E4	8.0	51	5	0.25	522
E5	8.0	50	5	0.50	305
E6	8.0	51	10	0.25	544

Table 4.1- Shear Modulus Values Obtained from the Tests

Another important factor affecting shear modulus is initial relative density. In order to study this effect, tests with relative densities of 50 % and 65 % were carried out. The plots of shear modulus values of these tests are shown in Fig.(4.32). As it can be seen from this figure, shear modulus increases with the increasing relative density. This behaviour might be due to increasing denseness of sand and greater interlocking of the grains caused by increasing relative density.

The effect of the number of stress cycles on the shear modulus for samples having a relative density of 50 % is shown in Fig.(4.33). It may be seen that, there is a slight increase in the shear modulus for increasing number of loading cycles, and this tendency occurs in the entire range of vertical pressures investigated.

For a comparison of the results obtained from this study and the results of previous works, Table 4.2 is to be referred. In this table, the shear modulus values obtained from tests are tabulated as well as the results obtained from Seed-Idriss model (Seed and Idriss, 1970) and Hardin-Drnevich model (Hardin and Drnevich, 1972,b) which are explained in detail in Section 2.5. Since the effect of number of loading cycle is not given in those models, only the shear modulus values obtained at 5<sup>th</sup> loading cycles of tests are considered. When the shear modulus values in Table 4.2 are compared with each other, it can be seen that, the shear modulus values obtained by using the Seed-Idriss model and the Hardin-Drnevich model give higher values than those obtained



TESTS	VERTICAL STRESS (kg/cm <sup>2</sup> )	RELATIVE DENSITY (%)	STRAIN AMP. RANGES (%)	SHEAR MODULUS (G) (kg/cm <sup>2</sup> )
A1	0.5	65	0.25	68
SEED-IDRISS MODEL	0.5	65	0.25	107
HARDIN-DRNEVICH MODEL	0.5	65	0.25	113
B1	1.0	65	0.25	112
SEED-IDRISS MODEL	1.0	65	0.25	153
HARDIN-DRNEVICH MODEL	1.0	65	0.25	168
C1	2.0	65	0.25	244
SEED-IDRISS MODEL	2.0	65	0.25	245
HARDIN-DRNEVICH MODEL	2.0	65	0.25	249
D1	4.0	65	0.25	404
SEED-IDRISS MODEL	4.0	65	0.25	348
HARDIN-DRNEVICH MODEL	4.0	65	0.25	465
E1	8.0	65	0.25	620
SEED-IDRISS MODEL	8.0	65	0.25	512
HARDIN-DRNEVICH MODEL	8.0	65	0.25	798

Table 4.2- Comparison of Shear Modulus Values Obtained by Seed-Idriss Model (Seed-Idriss, 1970) and Hardin-Drnevich Model (Hardin and Drnevich, 1972) with the Results of Tests A1, B1, C1, D1 and E1.

from the test results. But the Seed-Idriss model gives lower shear modulus values than those obtained in this study when the vertical pressures are  $4.0 \text{ kg/cm}^2$  and  $8.0 \text{ kg/cm}^2$ .

The difference is between 0.5 % and 40 %. The main sources of this difference may be due to the difference between the testing conditions, different properties of tested materials, sample preparation and testing apparatus used. Another important aspect is that both models were developed for strain levels lower than 0.1 %, but the minimum strain level used in this study is 0.25 %.

#### 4.3- DAMPING RATIO VALUES

All damping ratio values obtained from the tests performed in this study are presented in Table 4.3. This table shows the damping ratio values as functions of single amplitude shear strain, vertical pressure, relative density and number of loading cycles. In order to observe the effects of shear strain and vertical pressure on damping ratio, Fig.(4.34) are presented. It may be seen from this figure that, damping ratio increases with the increasing shear strain and decreases with the increasing vertical pressure. As shear strain increases, energy dissipated in the sample increases and also damping ratio increases.

The effect of relative density,  $D_r$ , on damping ratio is shown in Fig.(4.35). As it seen from this figure that the damping ratio decreases slightly with the increasing relative density.

TEST	VERTICAL STRESS (kg/cm <sup>2</sup> )	RELATIVE DENSITY (%)	NUMBER OF CYCLES (N)	STRAIN AMP. RANGES (%)	DAMPING RATIO (D) (%)
A1	0.5	63	5	0.25	24.84
A2	0.5	64	5	0.50	30.75
A3	0.5	65	5	0.75	34.85
A4	0.5	50	5	0.25	25.27
A5	0.5	51	5	0.50	31.43
A6	0.5	50	10	0.25	24.86
B1	1.0	65	5	0.25	22.15
B2	1.0	64	5	0.50	28.08
B3	1.0	65	5	0.75	31.69
B4	1.0	50	5	0.25	22.84
B5	1.0	51	5	0.50	28.05
B6	1.0	50	10	0.25	22.51
C1	2.0	67	5	0.25	18.35
C2	2.0	65	5	0.50	24.22
C3	2.0	64	5	0.75	28.83
C4	2.0	51	5	0.25	19.31
C5	2.0	52	5	0.50	25.08
C6	2.0	51	10	0.25	18.79
D1	4.0	66	5	0.25	12.81
D2	4.0	65	5	0.50	19.48
D3	4.0	64	5	0.75	22.67
D4	4.0	50	5	0.25	13.68
D5	4.0	52	5	0.50	19.87
D6	4.0	50	10	0.25	13.01
E1	8.0	67	5	0.25	8.68
E2	8.0	65	5	0.50	12.51
E3	8.0	65	5	0.75	17.28
E4	8.0	51	5	0.25	9.47
E5	8.0	50	5	0.50	13.03
E6	8.0	51	10	0.25	8.71

Table 4.3- Damping Ratio Values Obtained from the Tests

This figure gives the plots of damping ratio values for tests having relative densities of about 65% and 50%. These results are in agreement with the findings of Silver and Seed (1971) and Seed and Idriss (1970) who indicated that for all practical purposes the relationship between damping ratio and shear strain can be accepted independent of the relative density of sand.

Values of hysteresis damping for different strain cycles of 5 and 10 in the simple shear tests performed at relative density of 50% are plotted in Fig.(4.36). In general, damping decreases slightly with increasing number of cycles for the range of vertical pressures included in the test program. The tendency for the damping to decrease for increasing number of strain cycles may be important for analysis of ground shaking. In many cases, however, it is convenient to use an average value of damping throughout the analysis. Since in most seismic events the number of significant cycles is likely to be less than 20, values determined at 5 cycles are likely to provide reasonable values for analysis purposes.

For a comparison of the damping ratio values obtained in this study with the results obtained by using Seed-Idriss model (Seed-Idriss, 1970) and Hardin-Drnevich model (Hardin and Drnevich, 1972) Table 4.4 is presented. Because of damping ratio was given as only a function of strain amplitude (Fig.2.6 , in Section 2.5.1 )

TESTS	STRAIN AMPLITUDE RANGES (%)		
	0.25	0.50	0.75
The Average of the Damping Ratio Values Obtained in This Study.	17.68	23.25	27.06
Seed-Idriss Model	17.43	21.05	23.24
Hardin-Drnevich Model	20.12	23.08	25.56

Table 4.4- Comparison of Damping Ratio Values Obtained by Using Seed-Idriss Model and Hardin-Drnevich Model with the Average of the results Obtained in this Study.

in Seed-Idriss Model, the average of the damping ratio values obtained in this study at the same strain levels but under different vertical pressures was compared with the values obtained from the Seed-Idriss model. It may be seen from the Table 4.4 that Seed-Idriss model values of damping ratio lower than those obtained in this study. The difference is between 1.5% and 14%.

The damping ratio values in Table 4.3 have been obtained from the hysteresis loops corresponding to the 5<sup>th</sup> and 10<sup>th</sup> loading cycles. The empirical equation for dry sands given by Hardin and Drnevich (1972, b) is:

$$D_{max} = 33 - 1.5 \log N$$

In fact there would be a maximum damping ratio difference of approximately 1.41 % between the 5<sup>th</sup> and 10<sup>th</sup> cycles. Because of this small difference, the effect of number of loading cycles on damping ratio is not taken into account while calculating the values given in Table 4.4. Therefore, damping ratio can be accepted as a function of shear strain amplitude. When the damping ratio values of the Hardin-Drnevich model are compared with the average values obtained in this study, it may be seen that the difference is between 1% and 12%.

The main sources of these differences may be due to the differences between the testing conditions, different properties of tested materials, sample preparation and testing apparatus used.

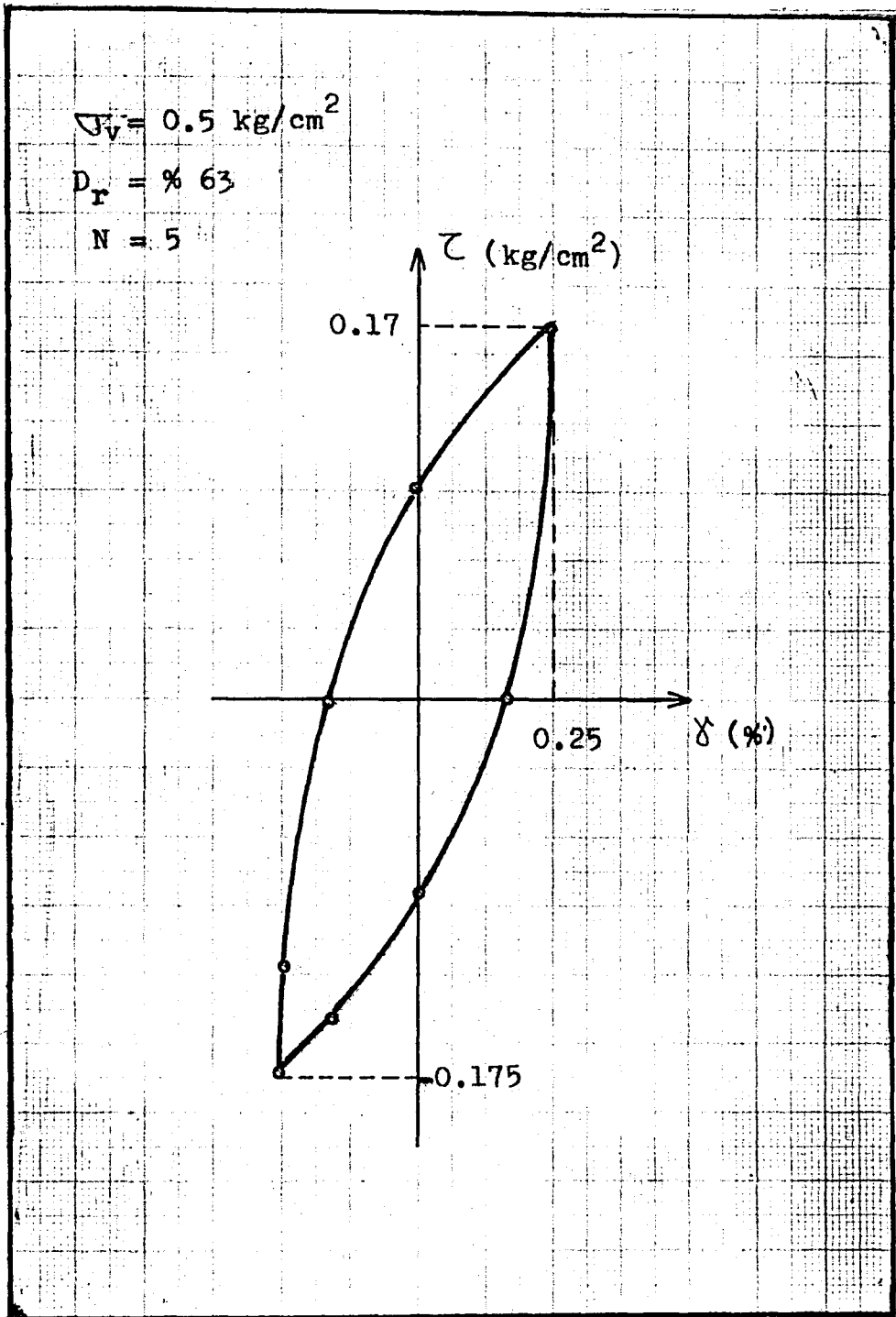


Figure 4.1- Hysteresis Loop of Test A1

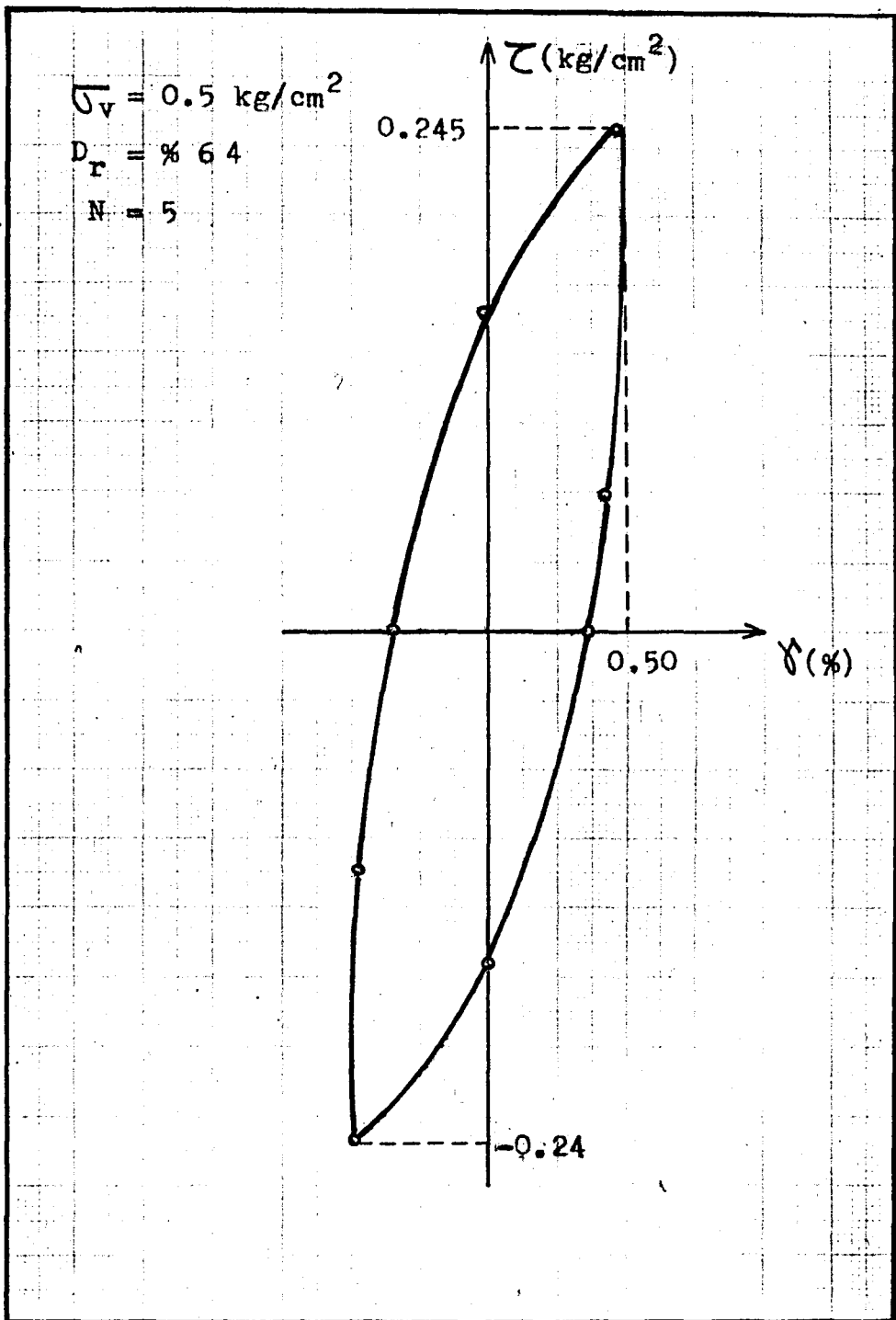


Figure 4.2 - Hysteresis Loop of Test A2



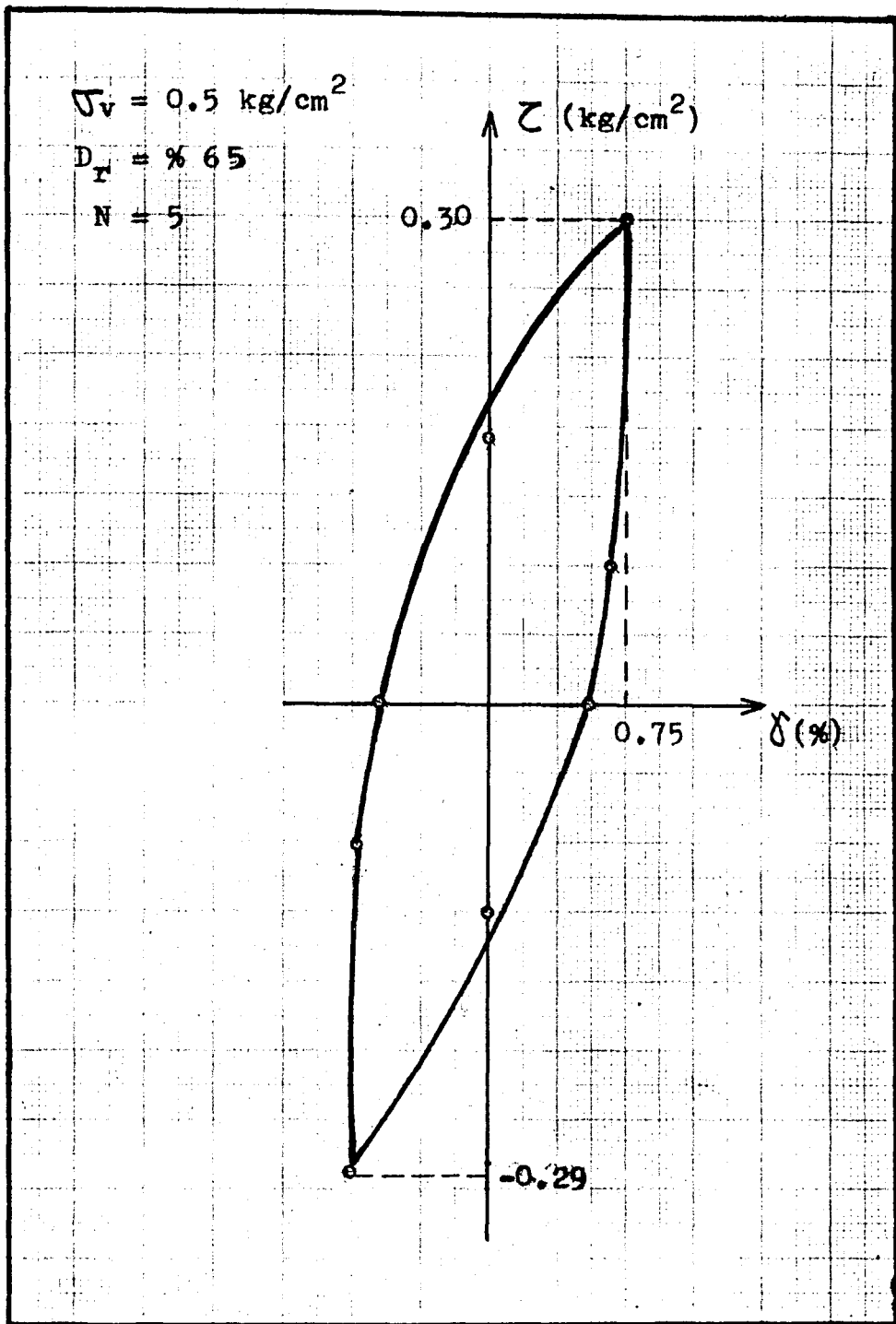


Figure 43.- Hysteresis Loop of Test A3

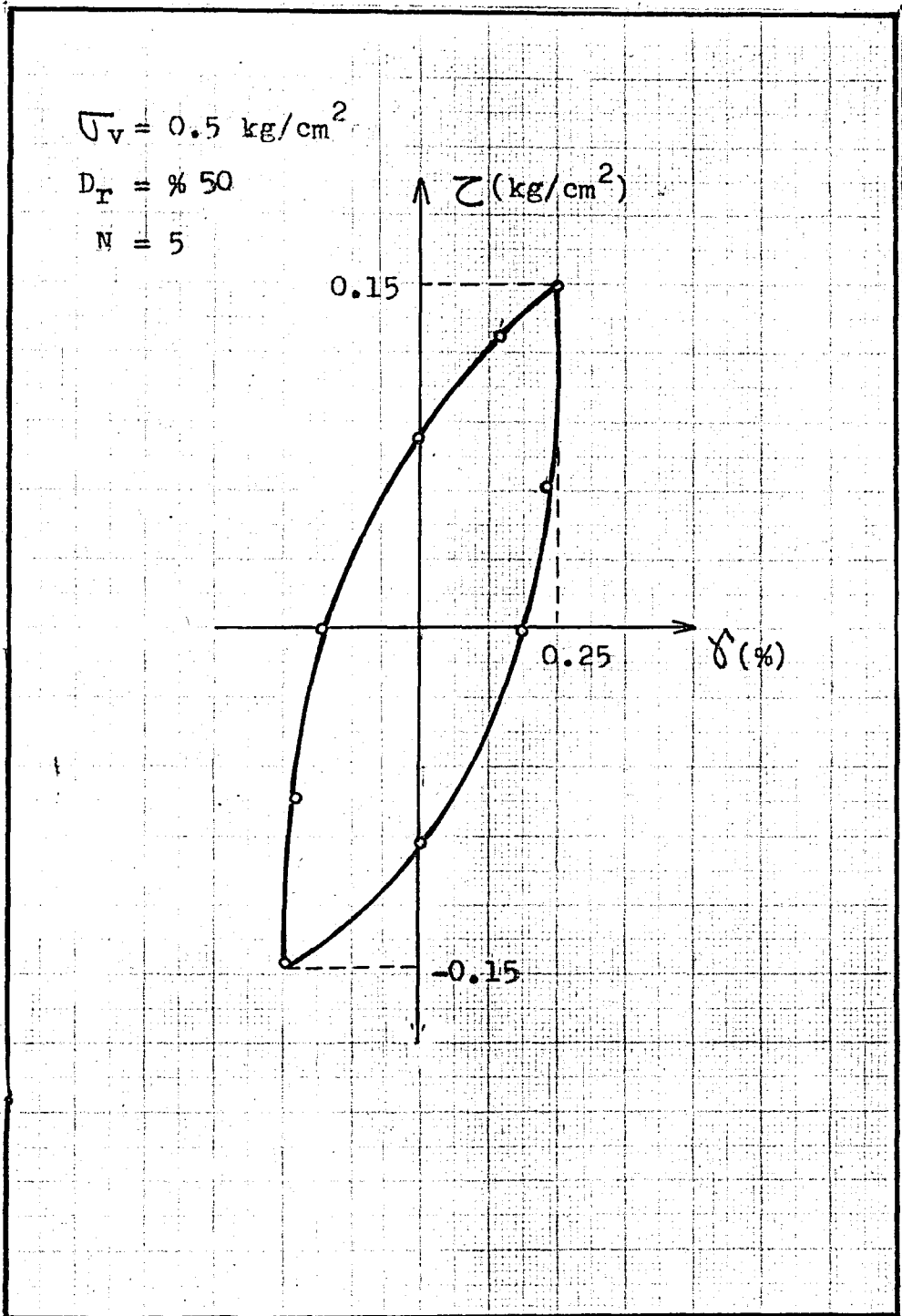


Figure 4.4-- Hysteresis Loop of Test A4

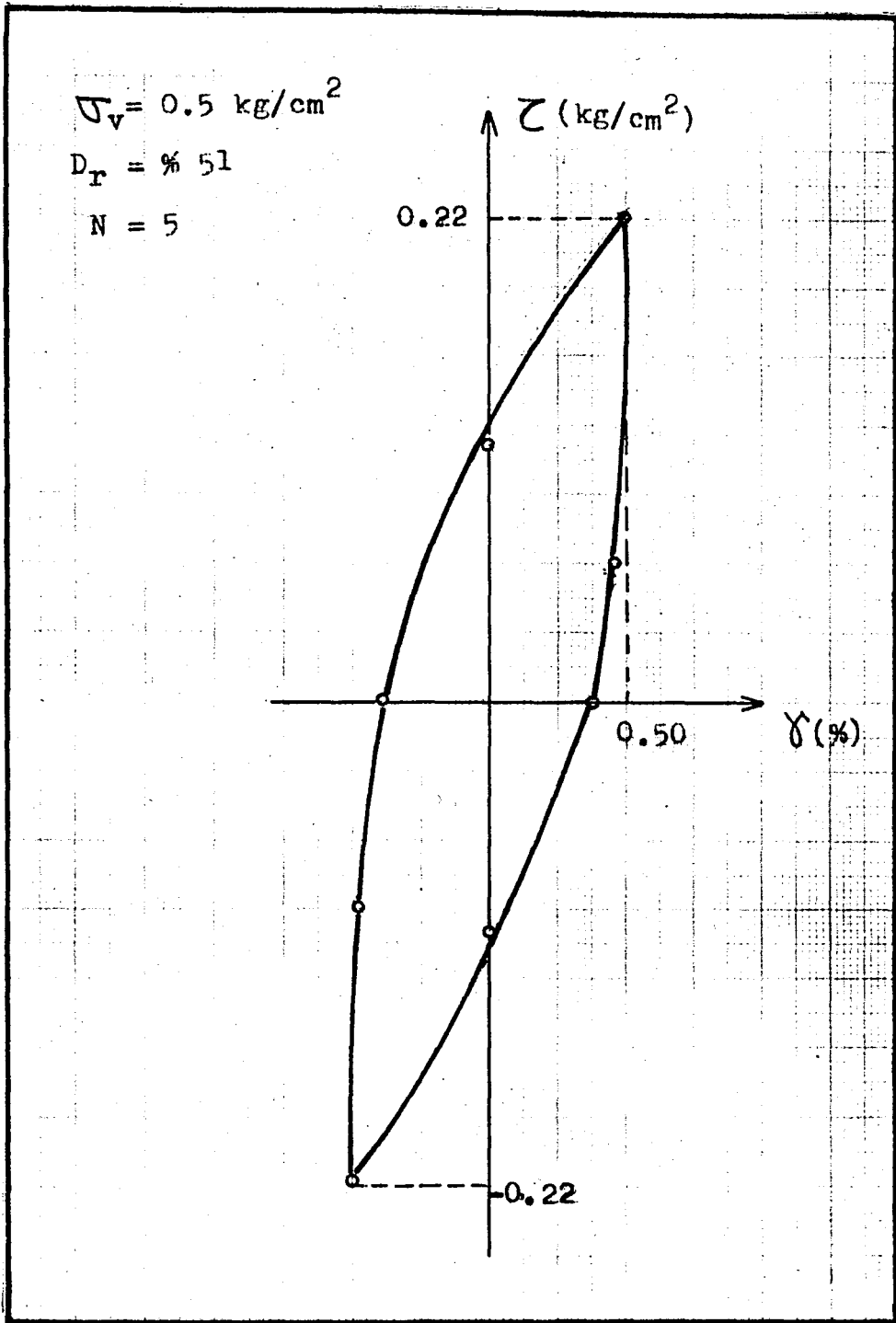


Figure 4.5 - Hysteresis Loop of Test A5

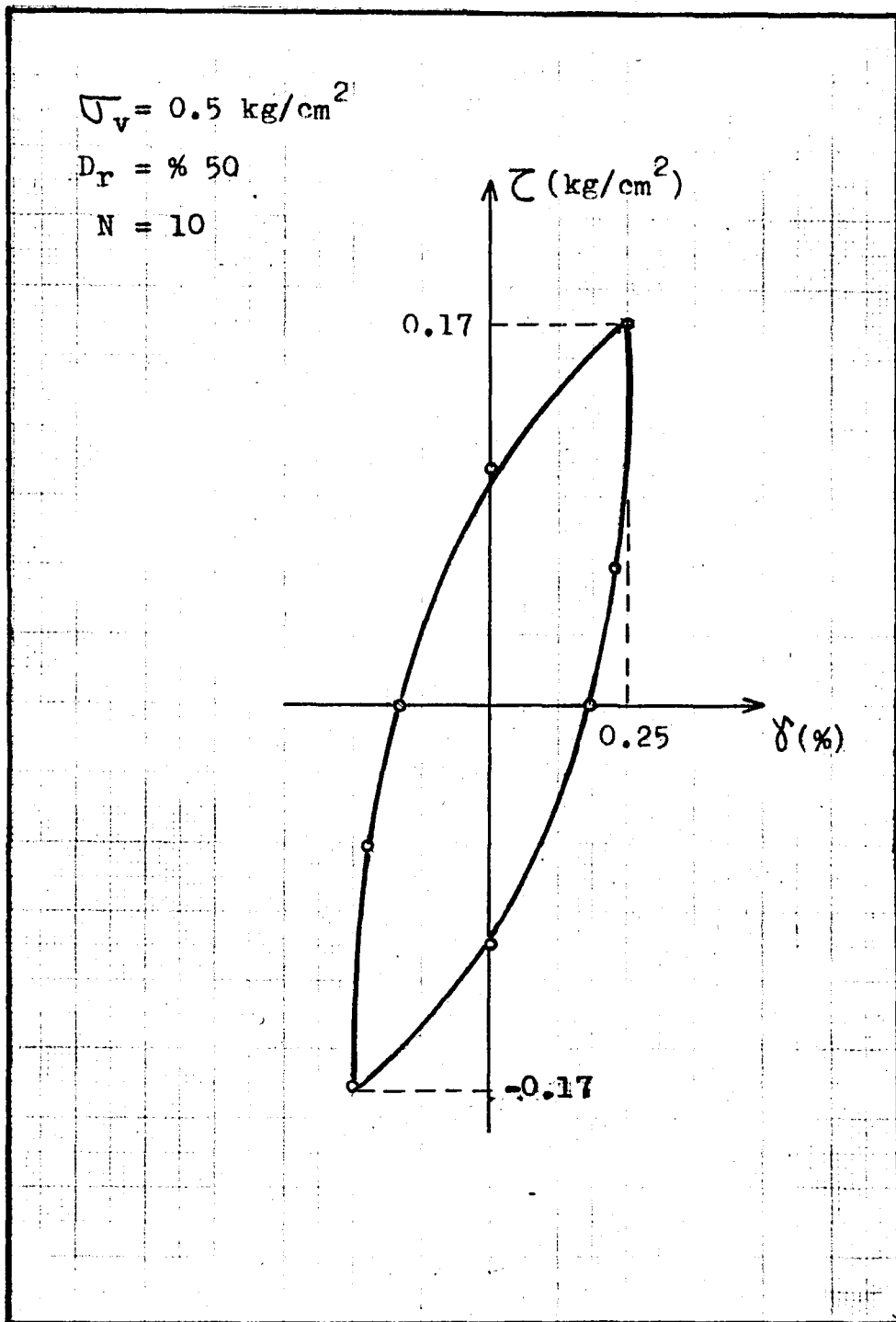


Figure 4.6 - Hysteresis Loop of Test A6

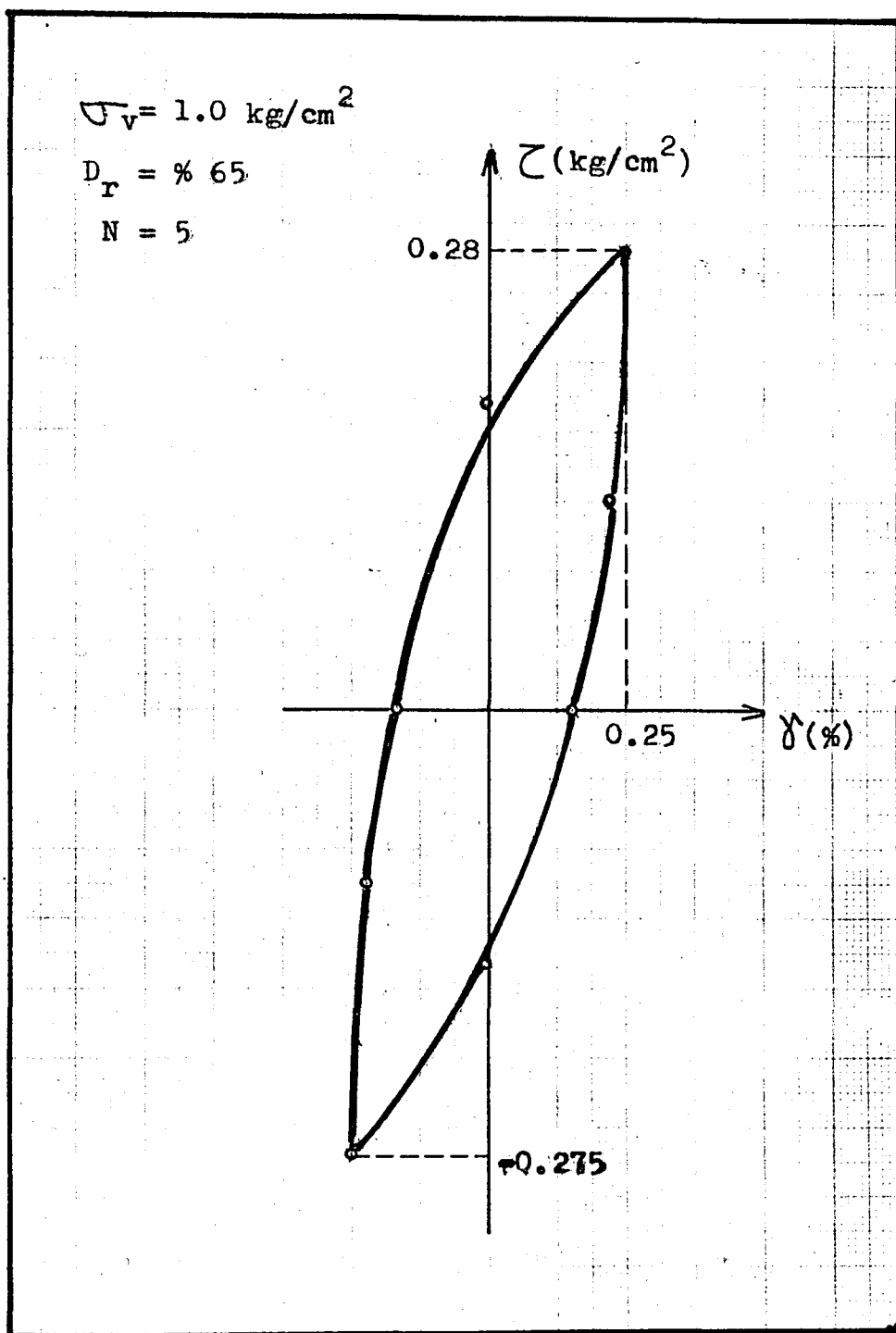


Figure 4.7.- Hysteresis Loop of Test B1

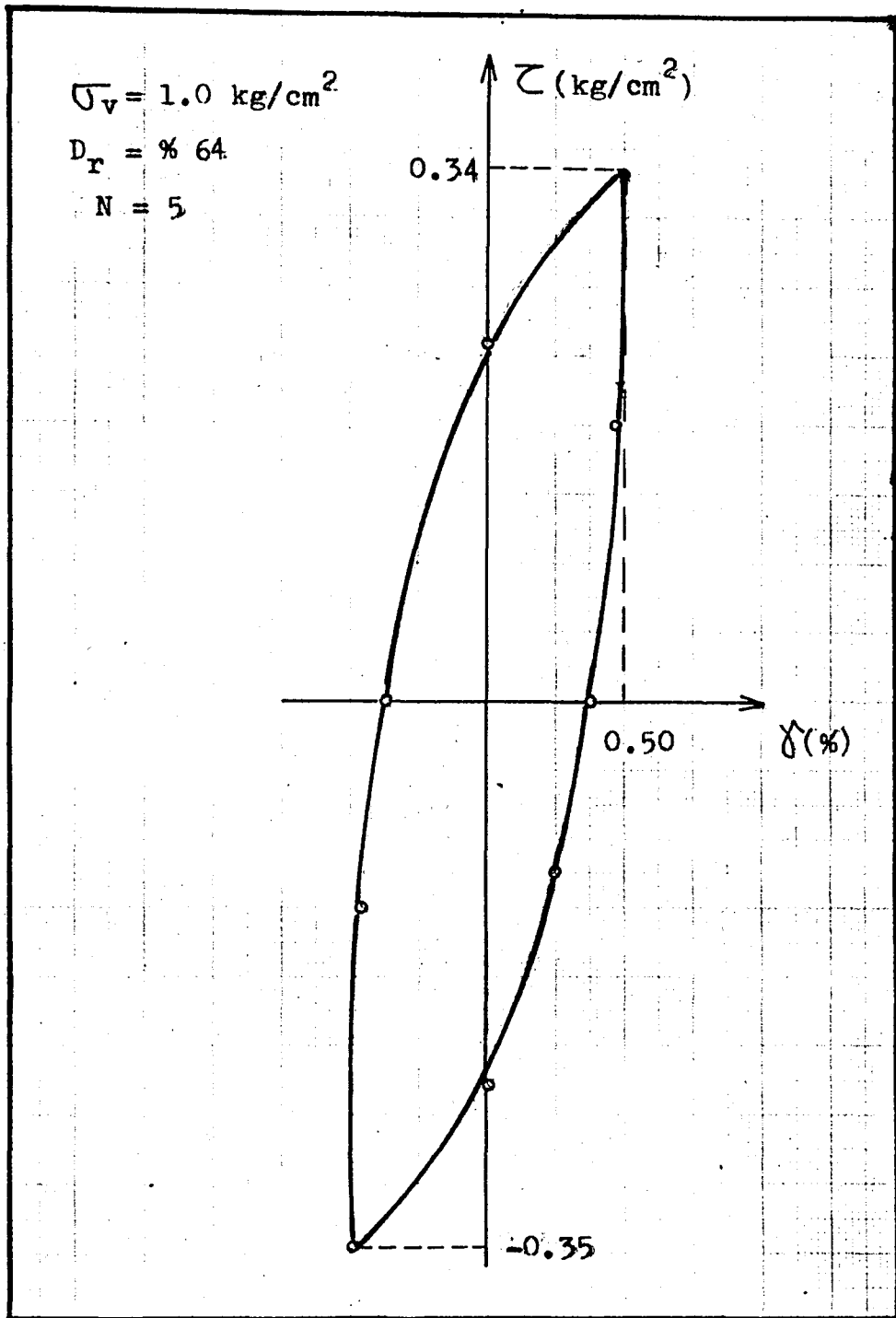


Figure 4.8 - Hysteresis Loop of Test B2

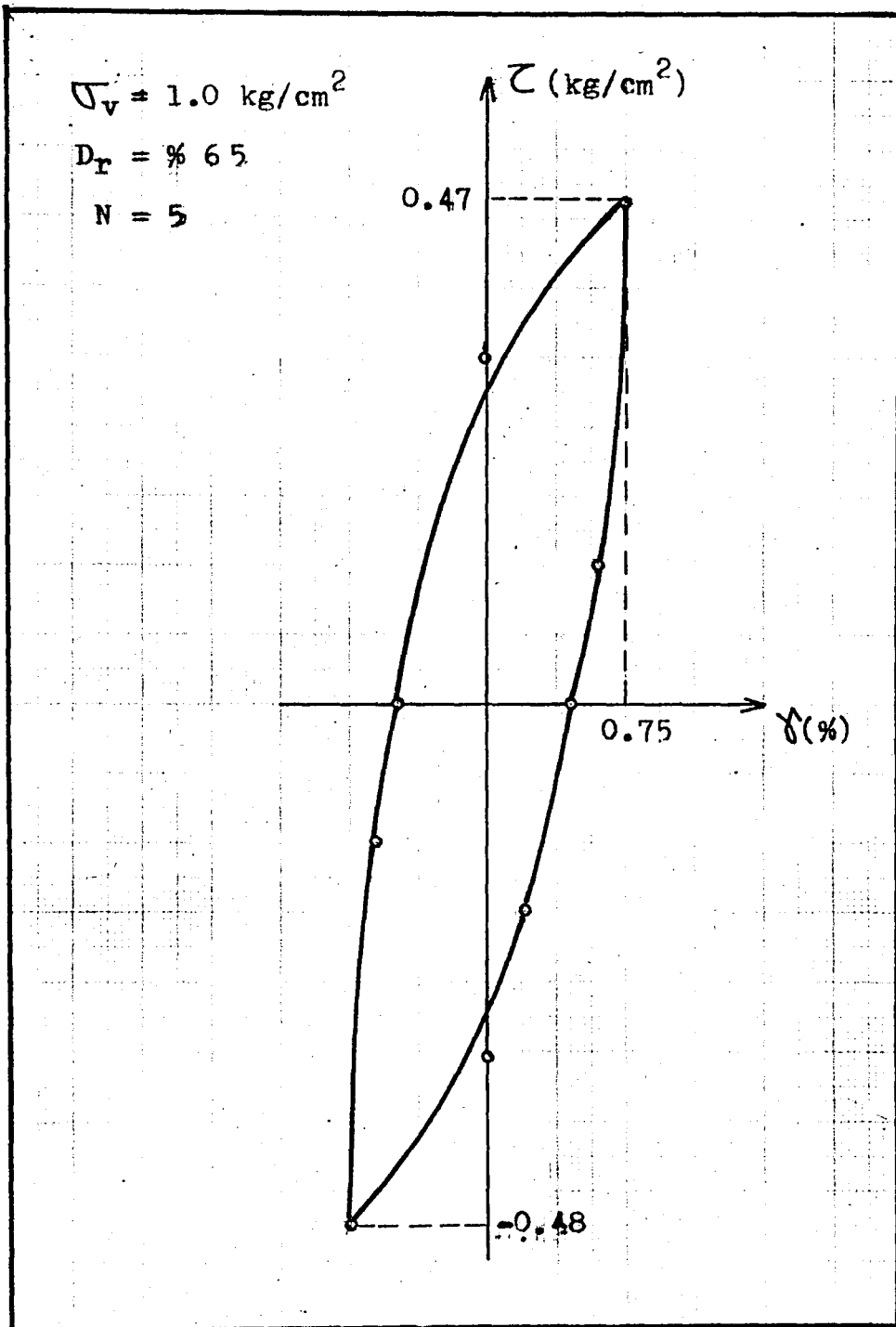


Figure 4.9- Hysteresis Loop of Test B3

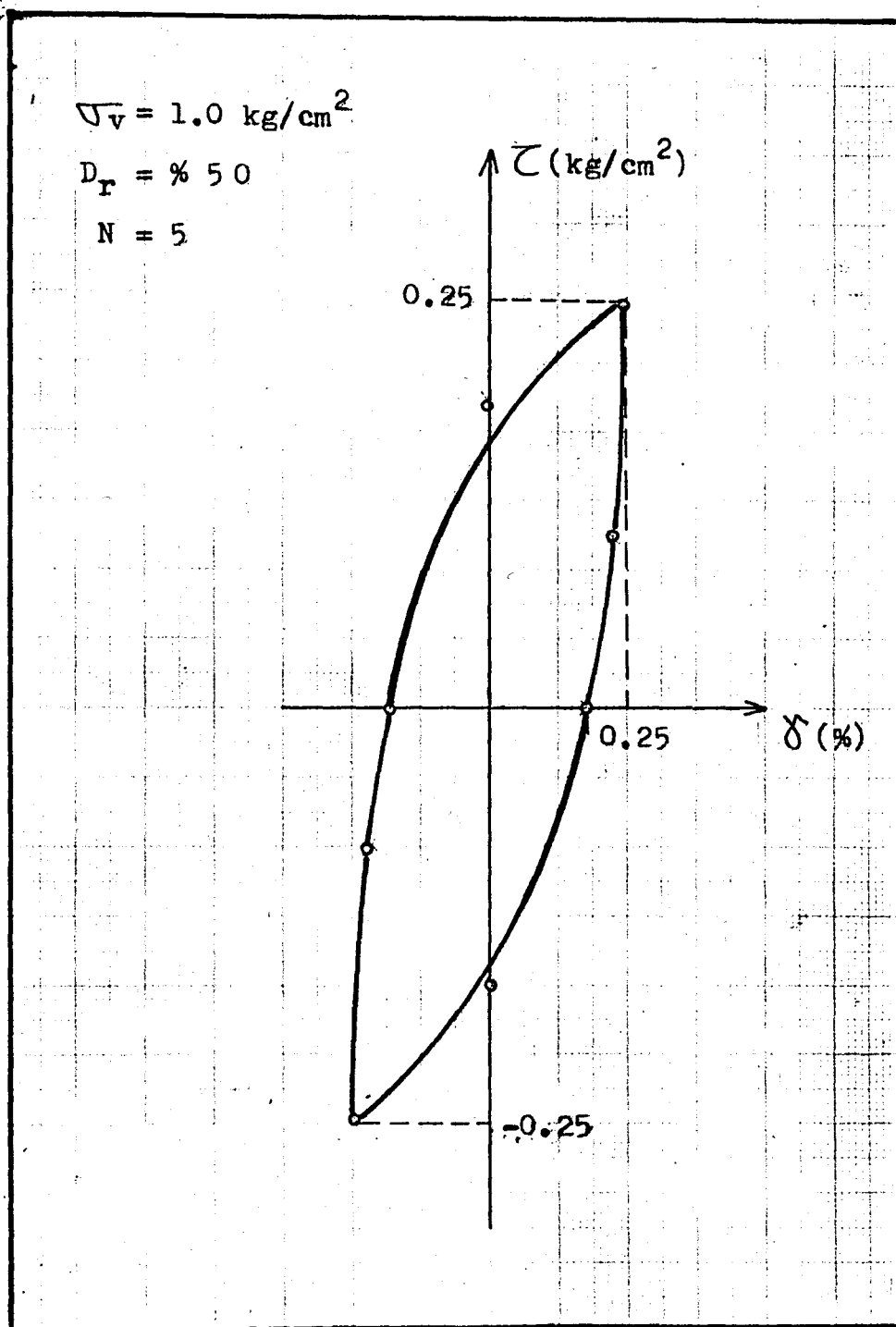


Figure 4.10-Hysteresis Loop of Test B4



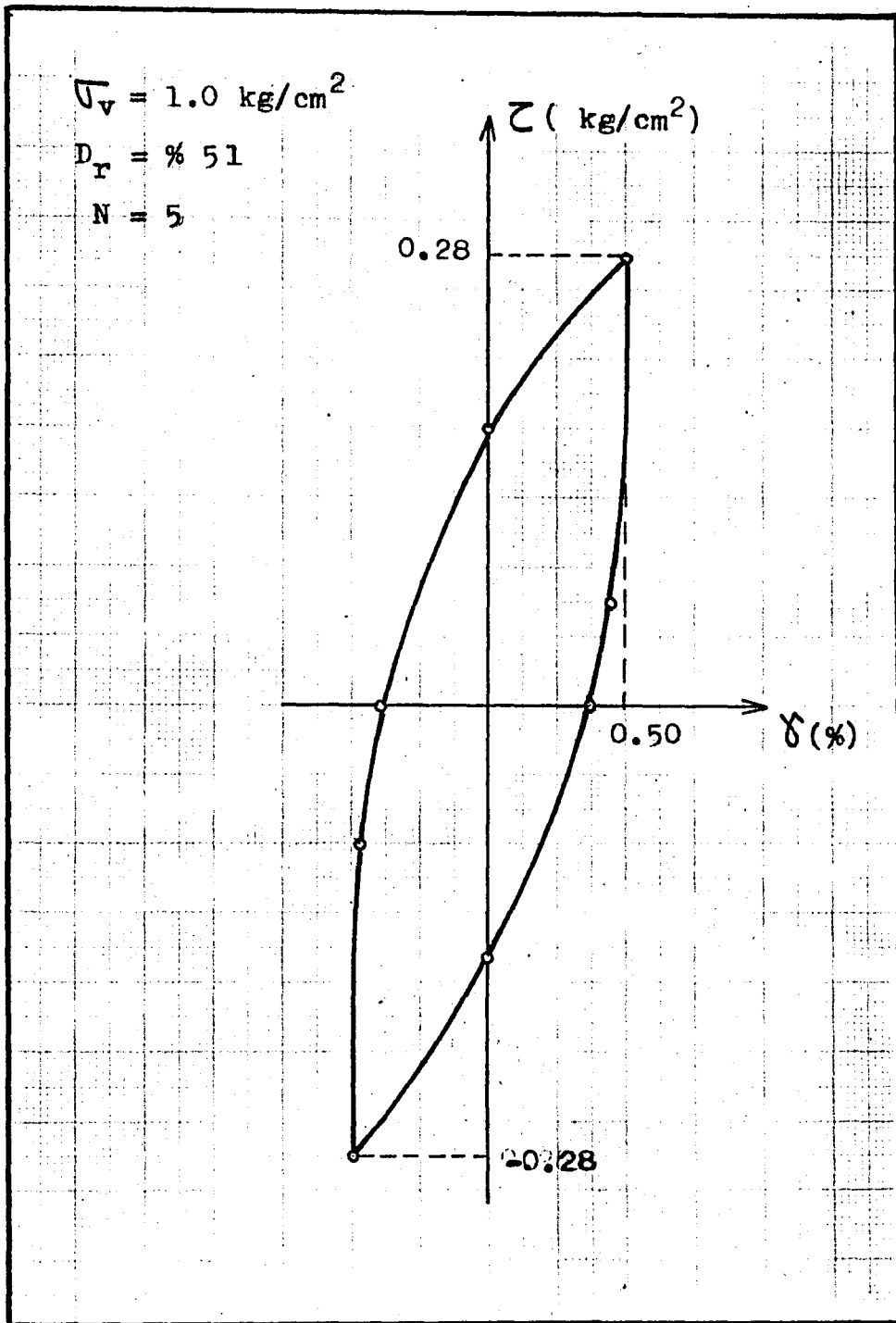


Figure 4.11- Hysteresis Loop of Test B5

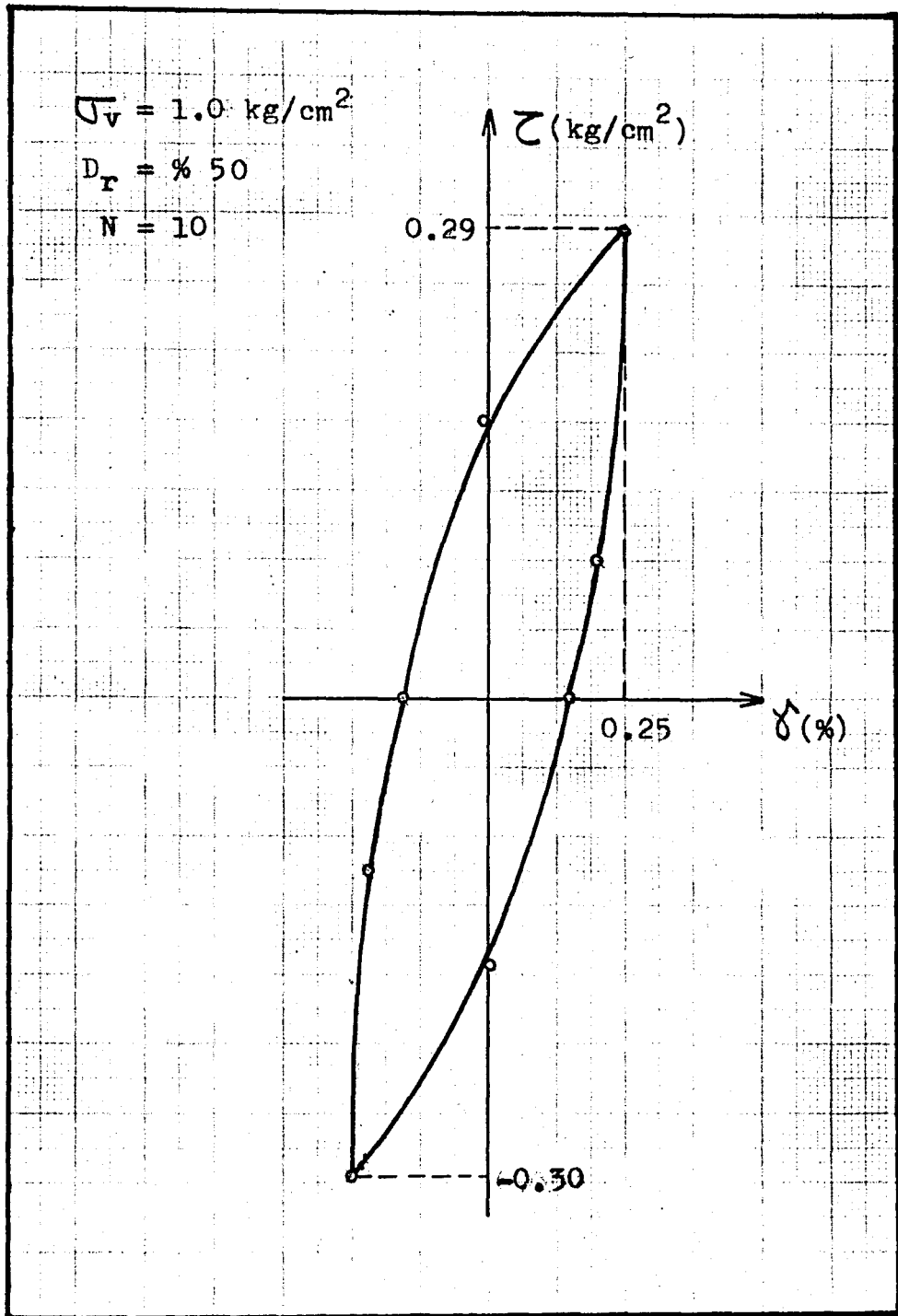


Figure 412-Hysteresis Loop of Test B6

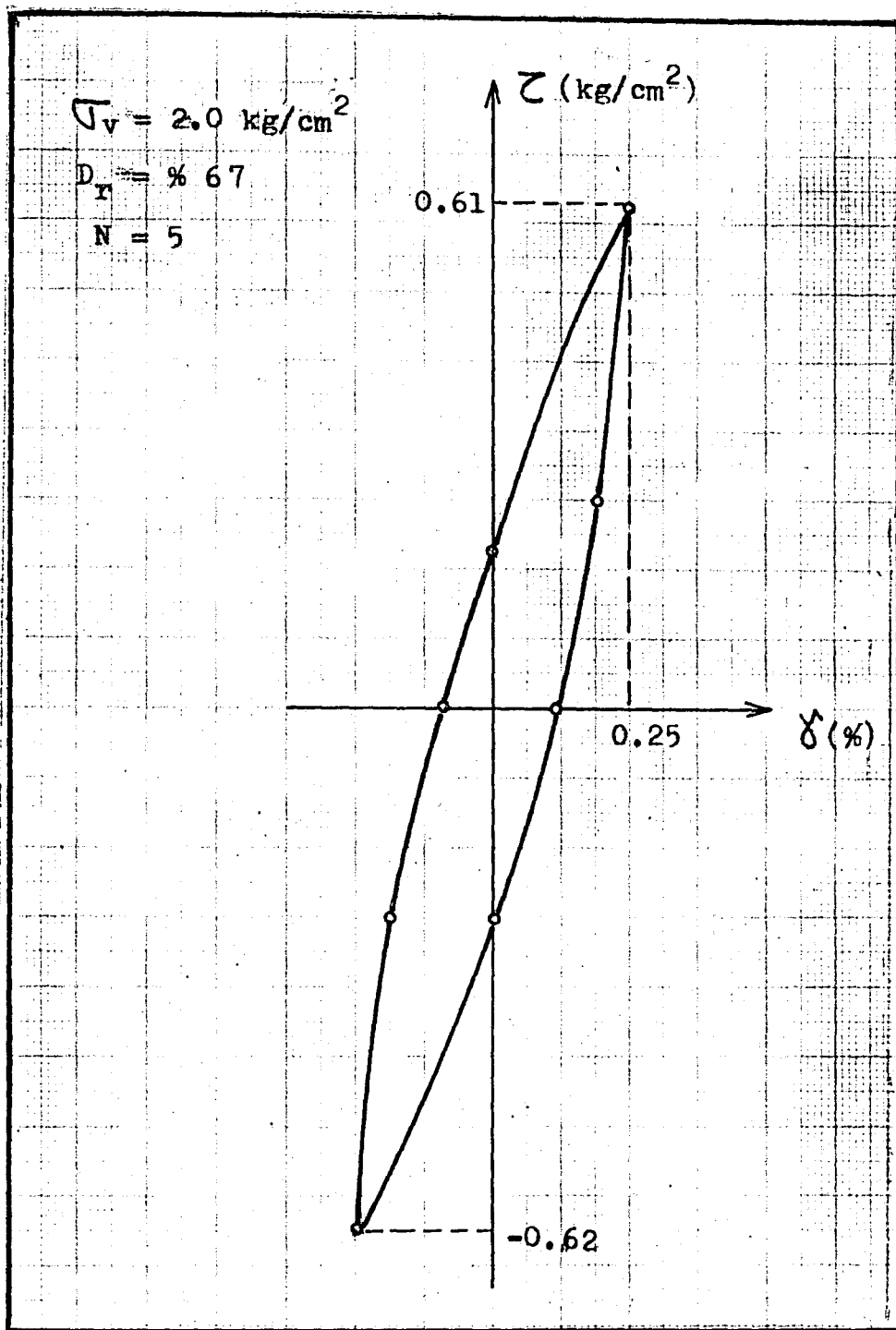


Figure 4.13-Hysteresis Loop of Test C1

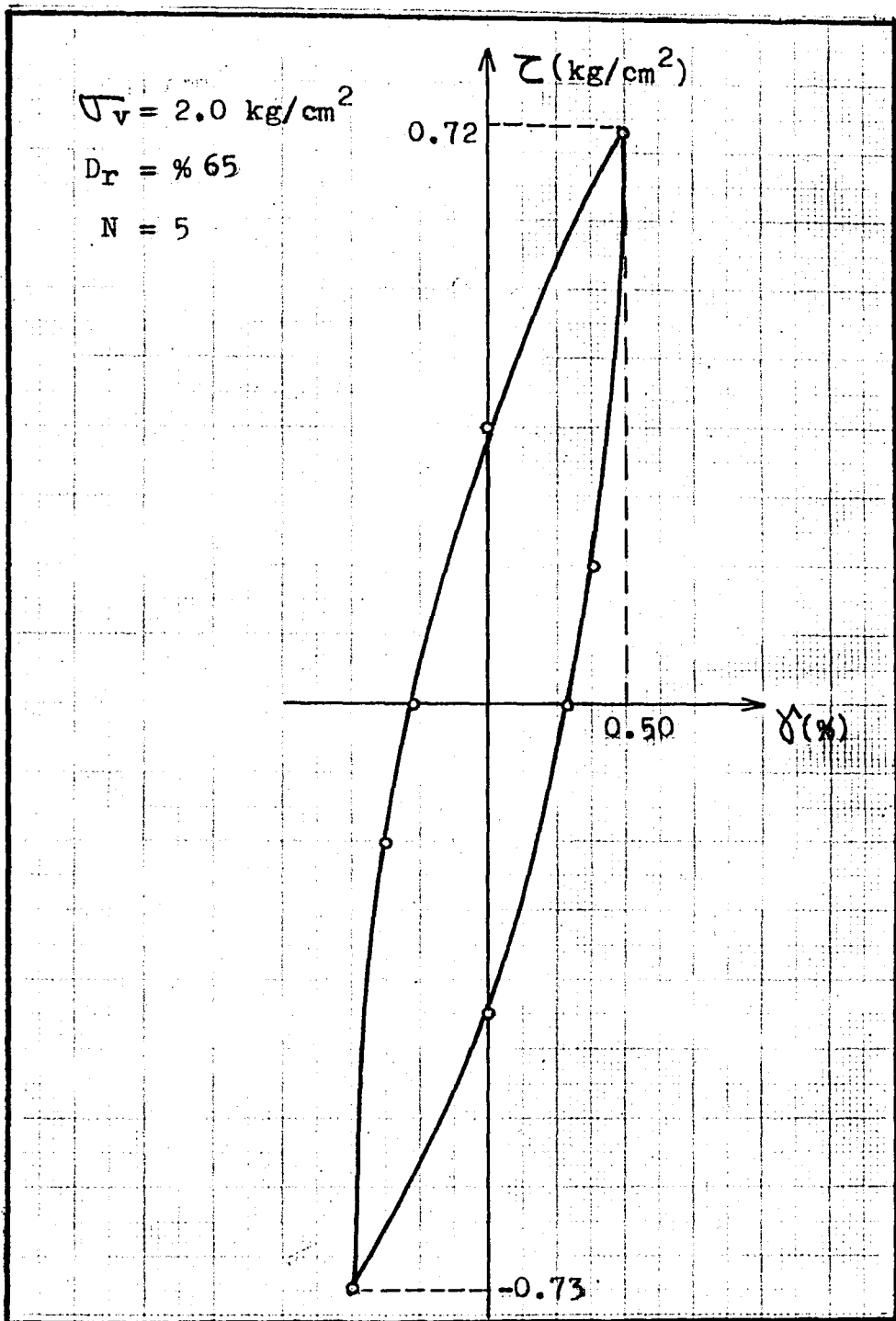


Figure 4.14-Hysteresis Loop of Test C2

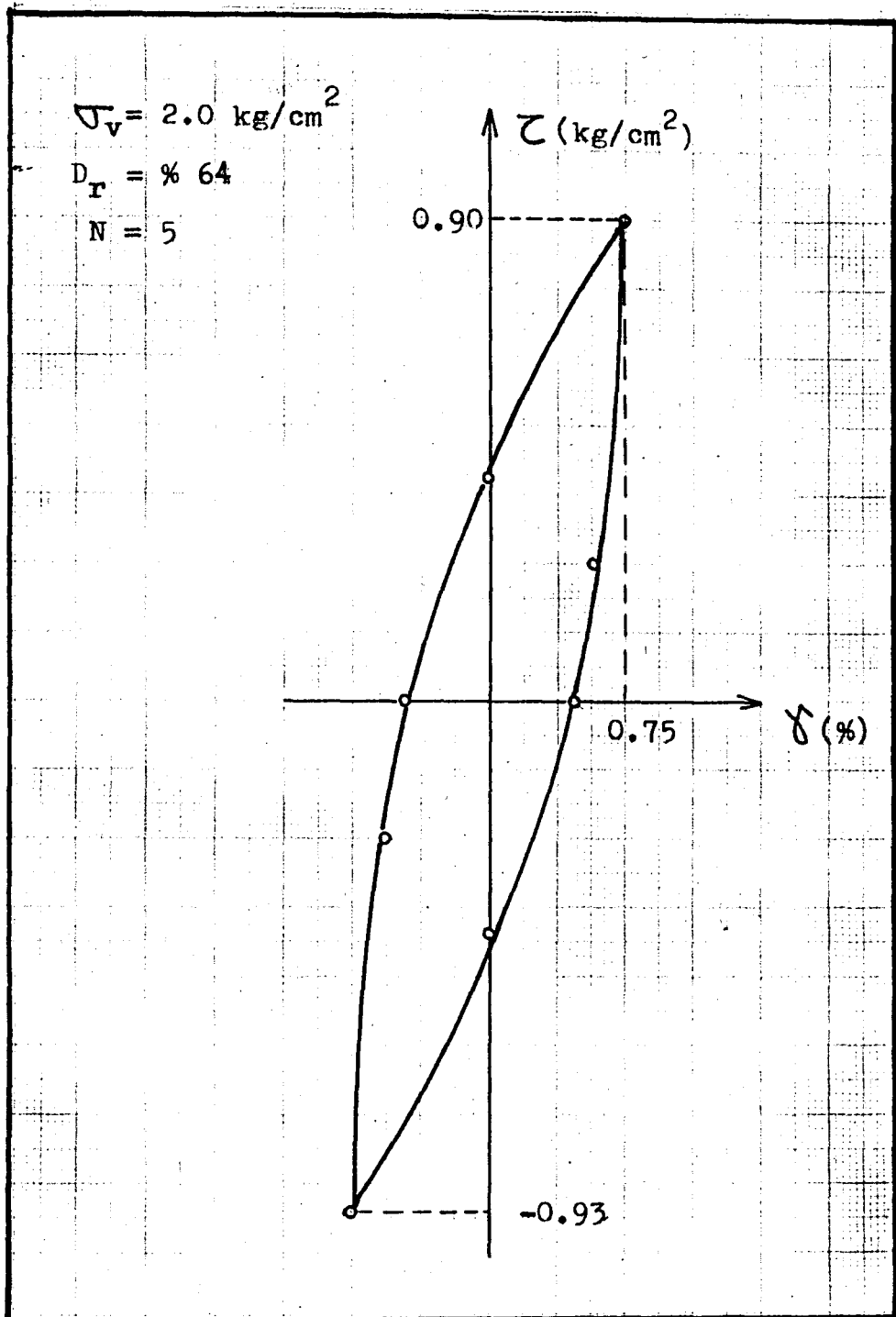


Figure 4.15-Hysteresis Loop of Test C3

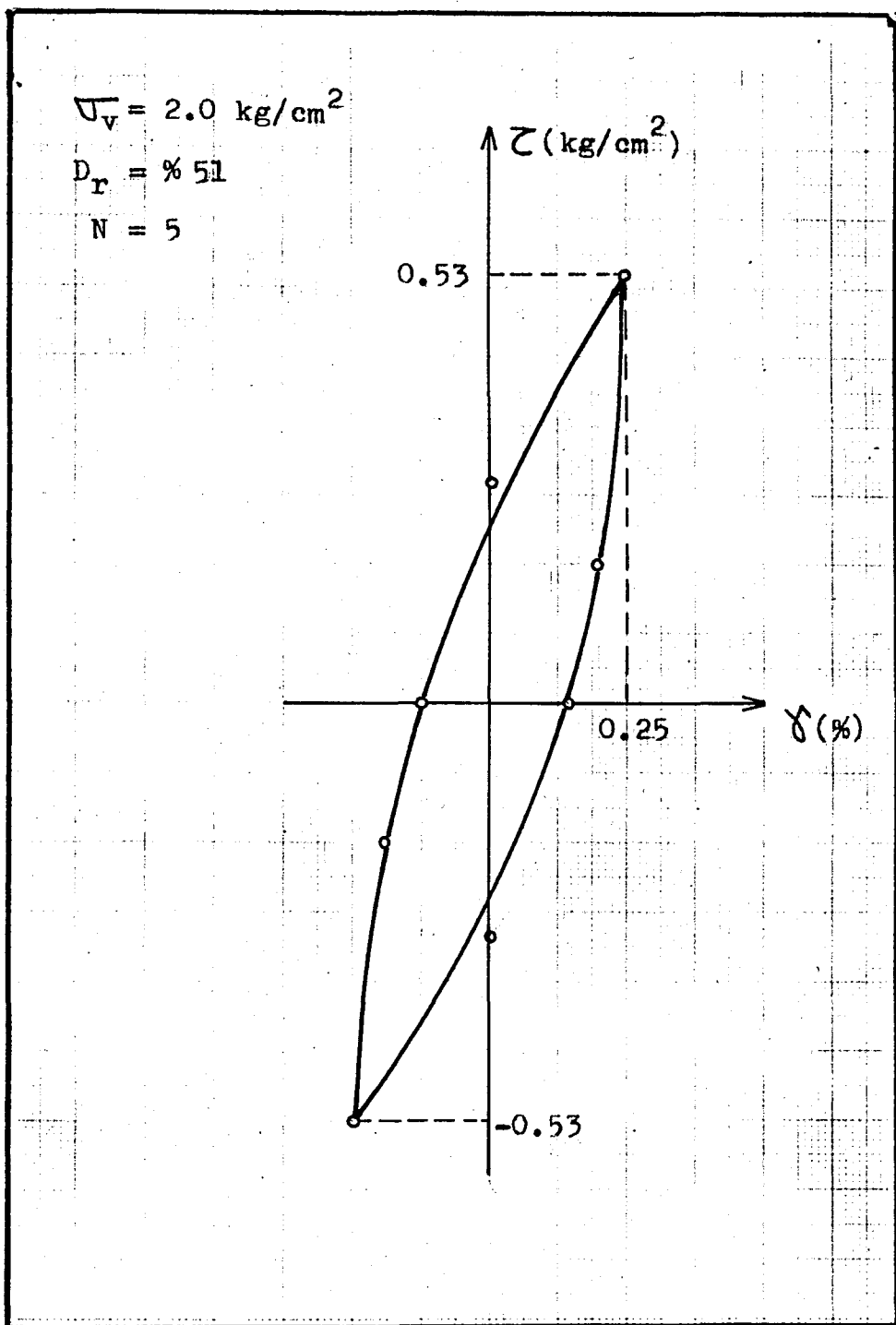


Figure 4.16.- Hysteresis Loop of Test C4

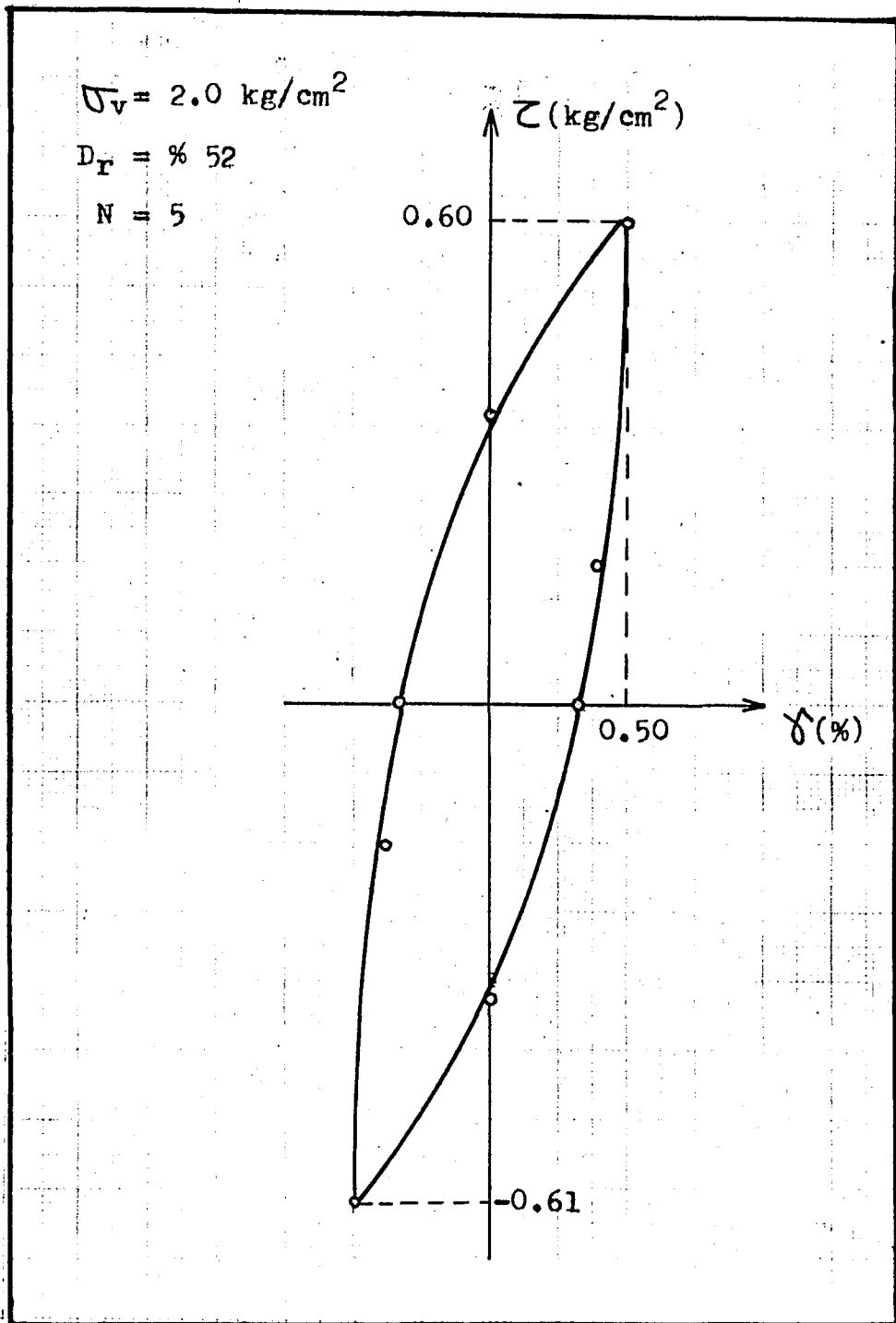


Figure 417- Hysteresis Loop of Test C5

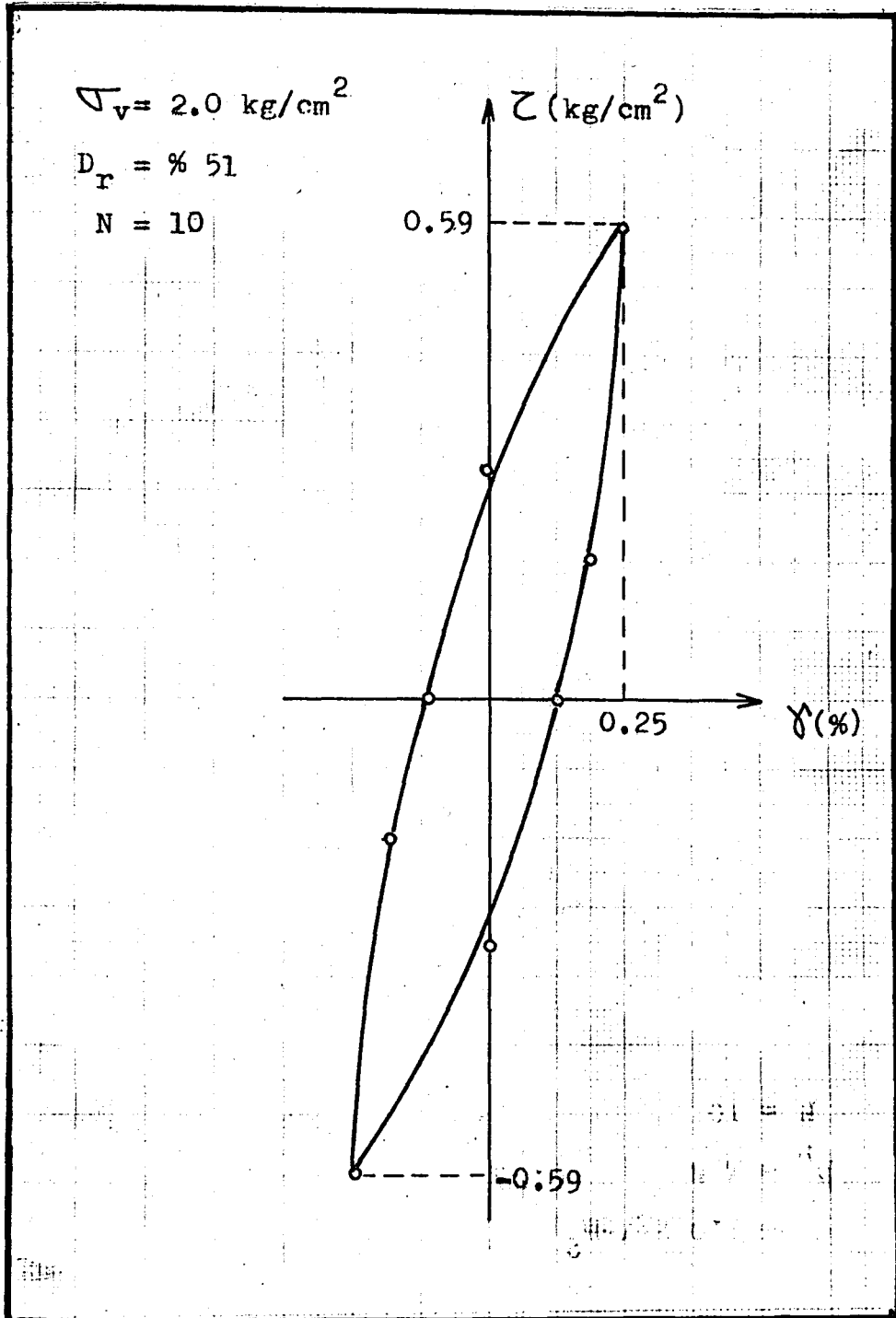


Figure 4.18-Hysteresis Loop of Test C6



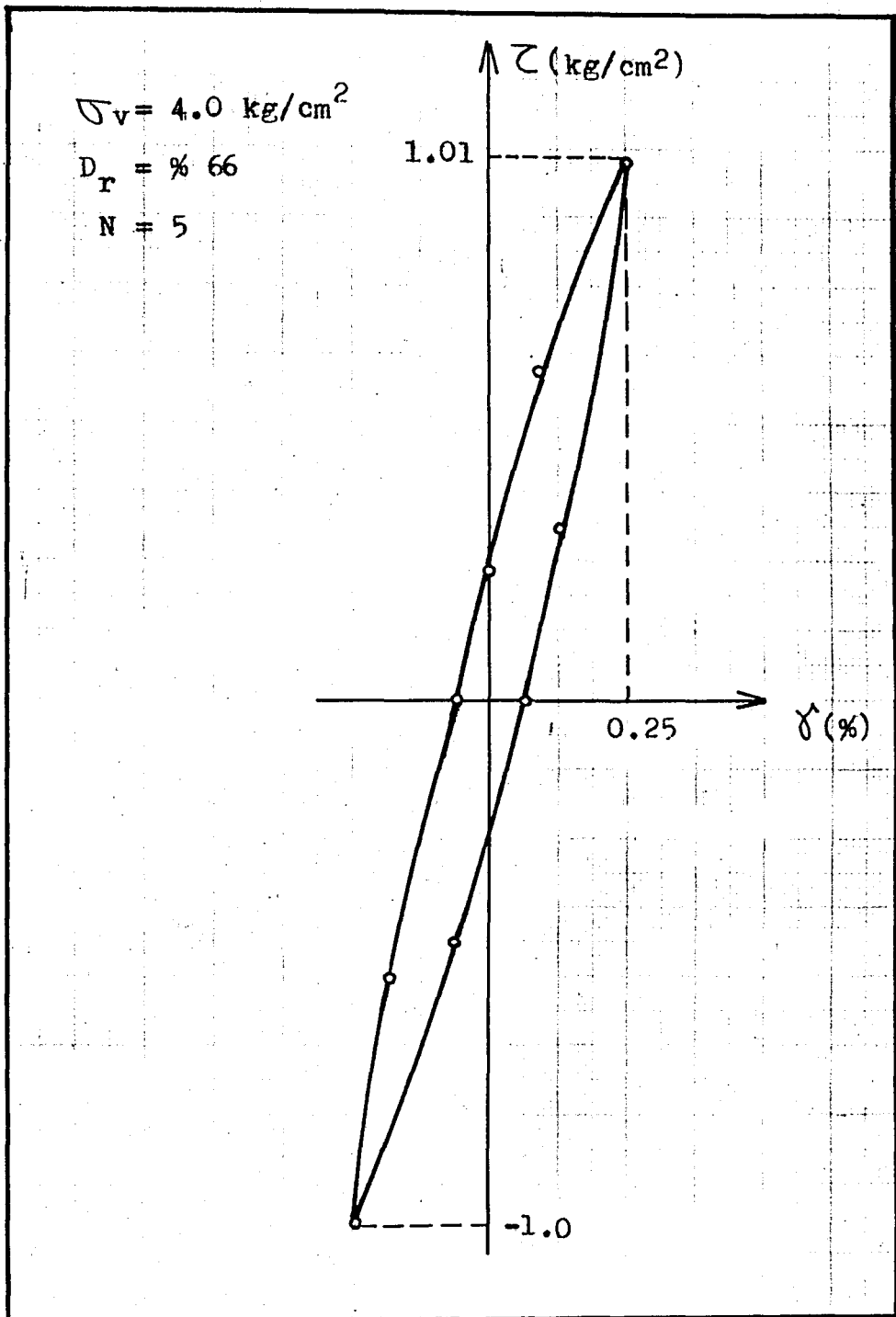


Figure 4.19-Hysteresis Loop of Test D1

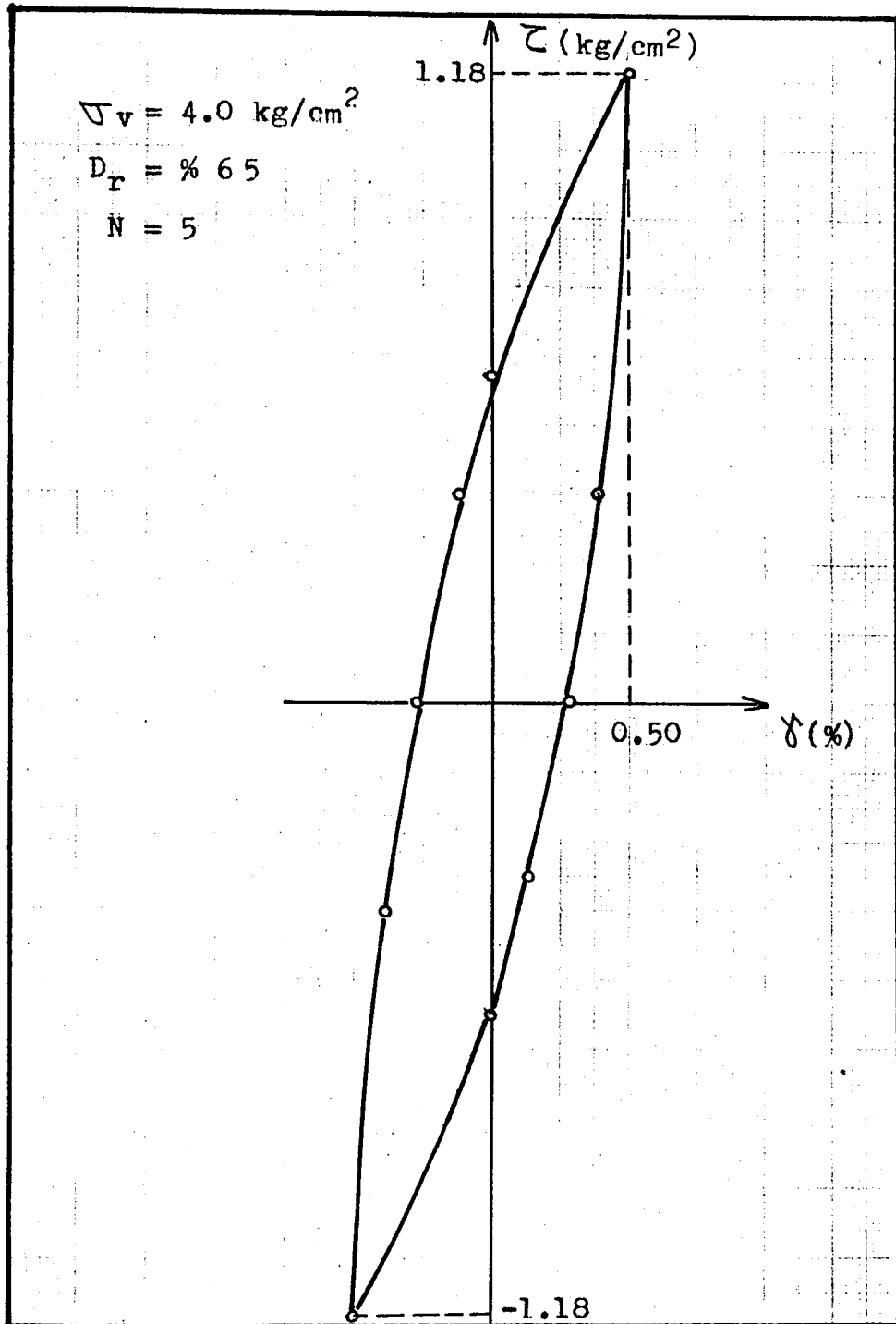


Figure 4.20-Hysteresis Loop of Test D2

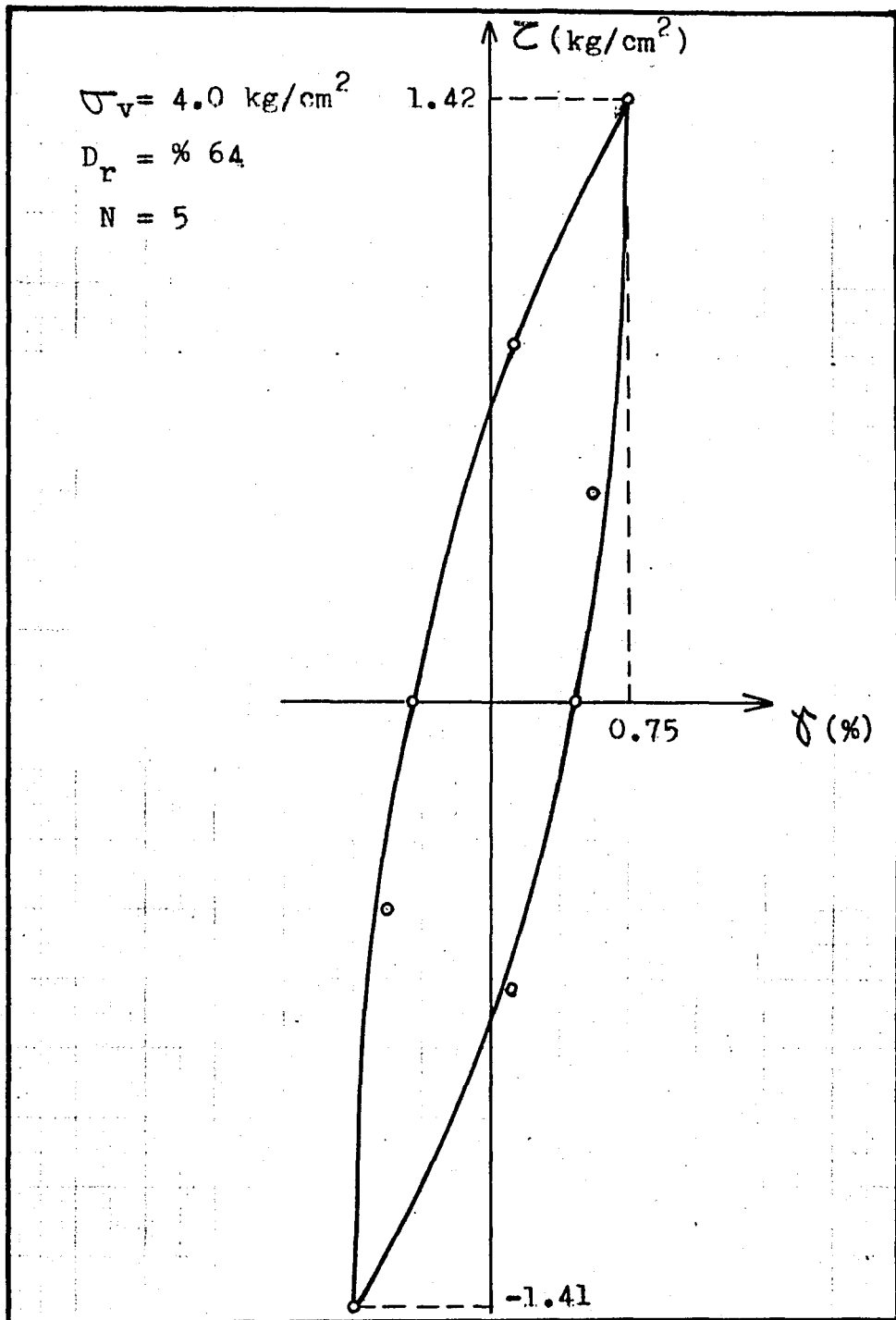


Figure 4.21-Hysteresis Loop of Test D3

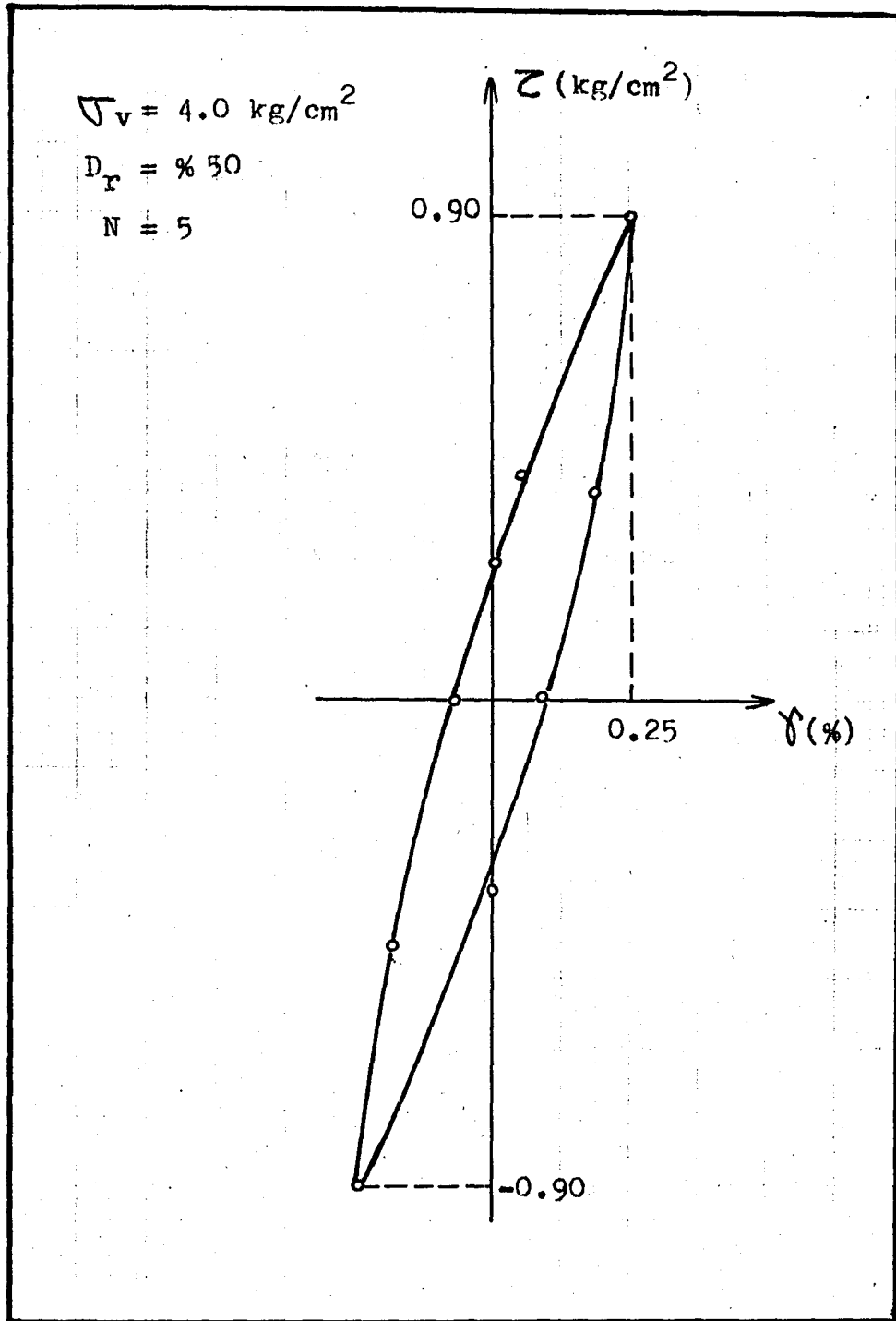


Figure 4.22-Hysteresis Loop of Test D4

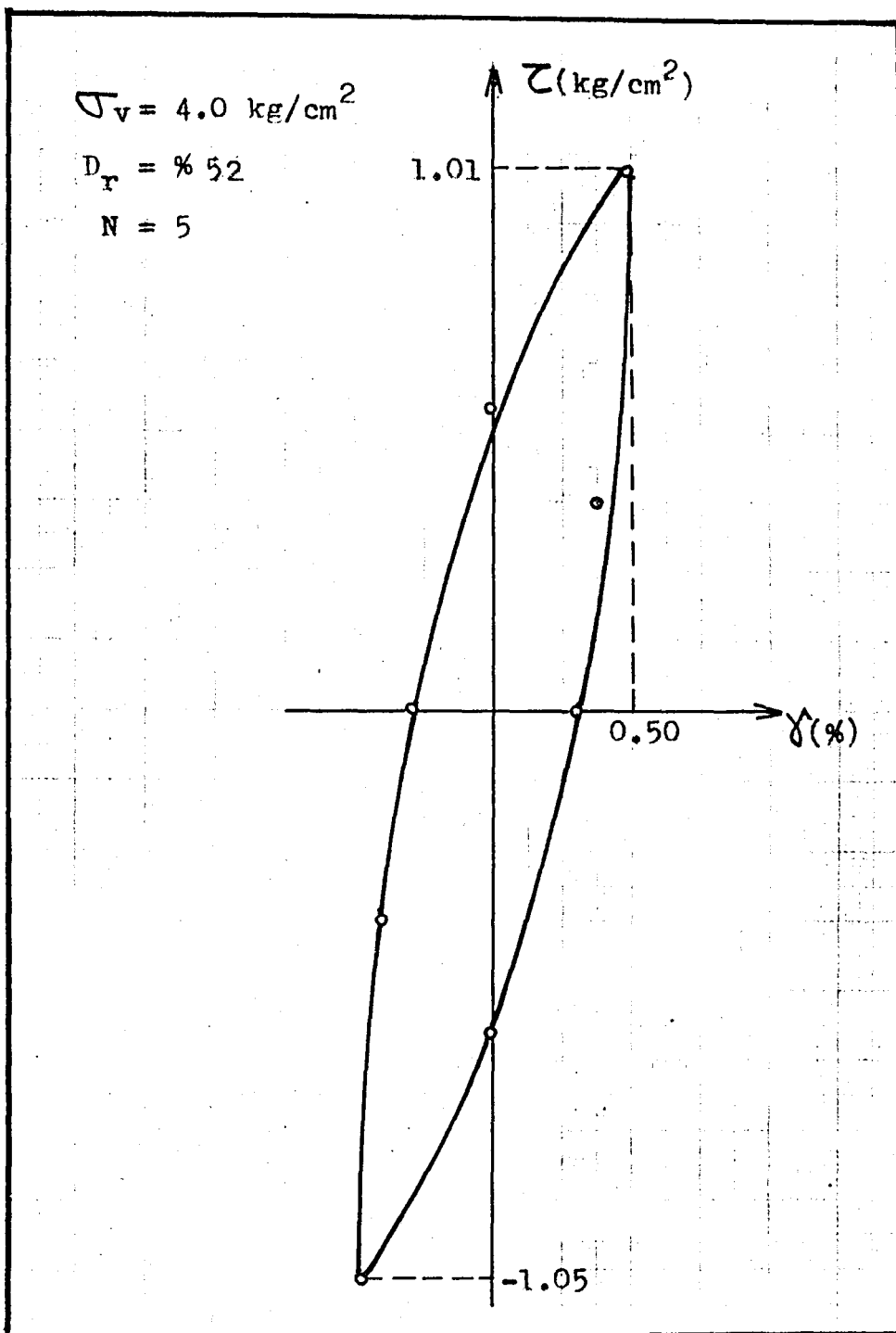


Figure 4.23-Hysteresis Loop of Test D5

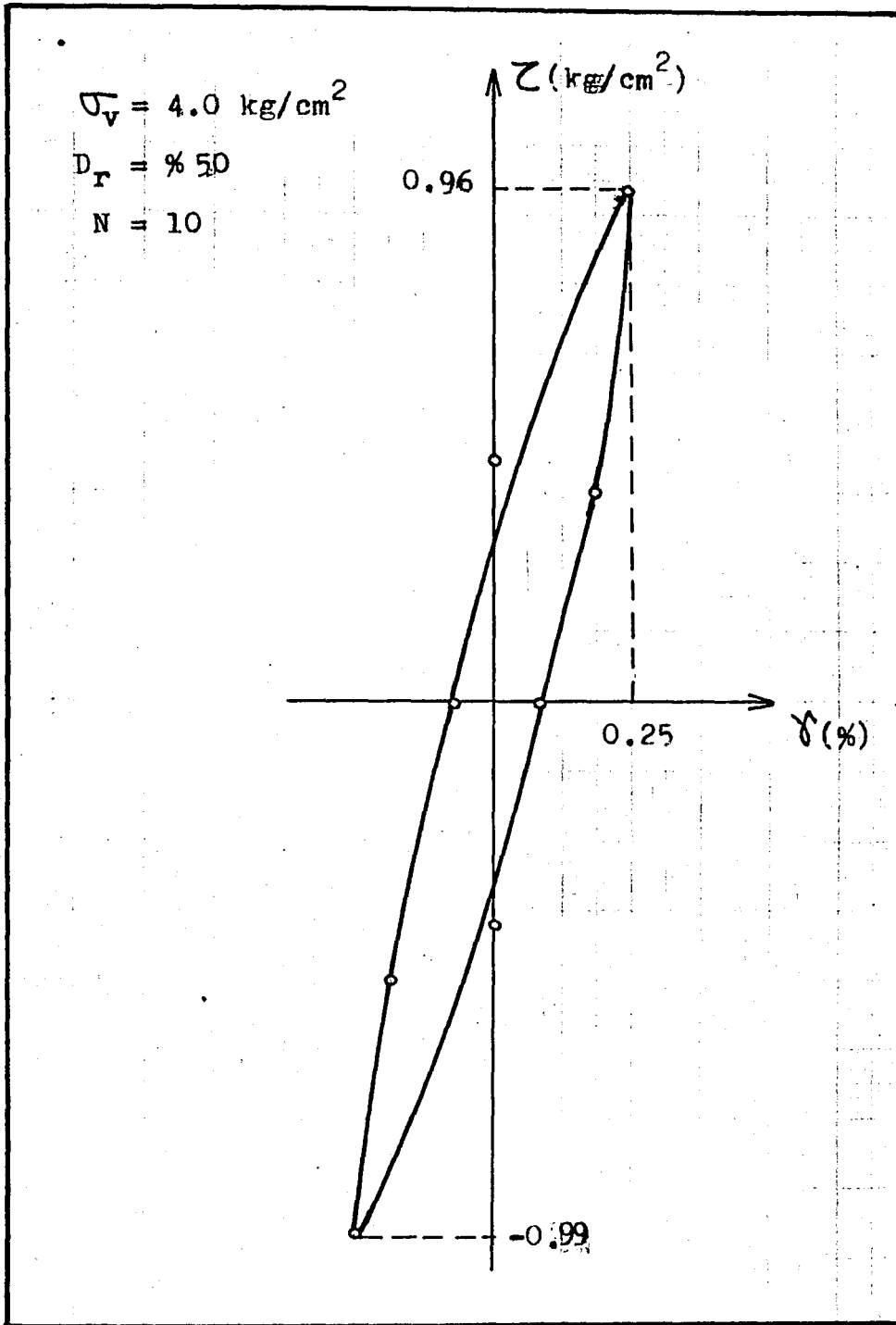


Figure 4.24-Hysteresis Loop of Test D6

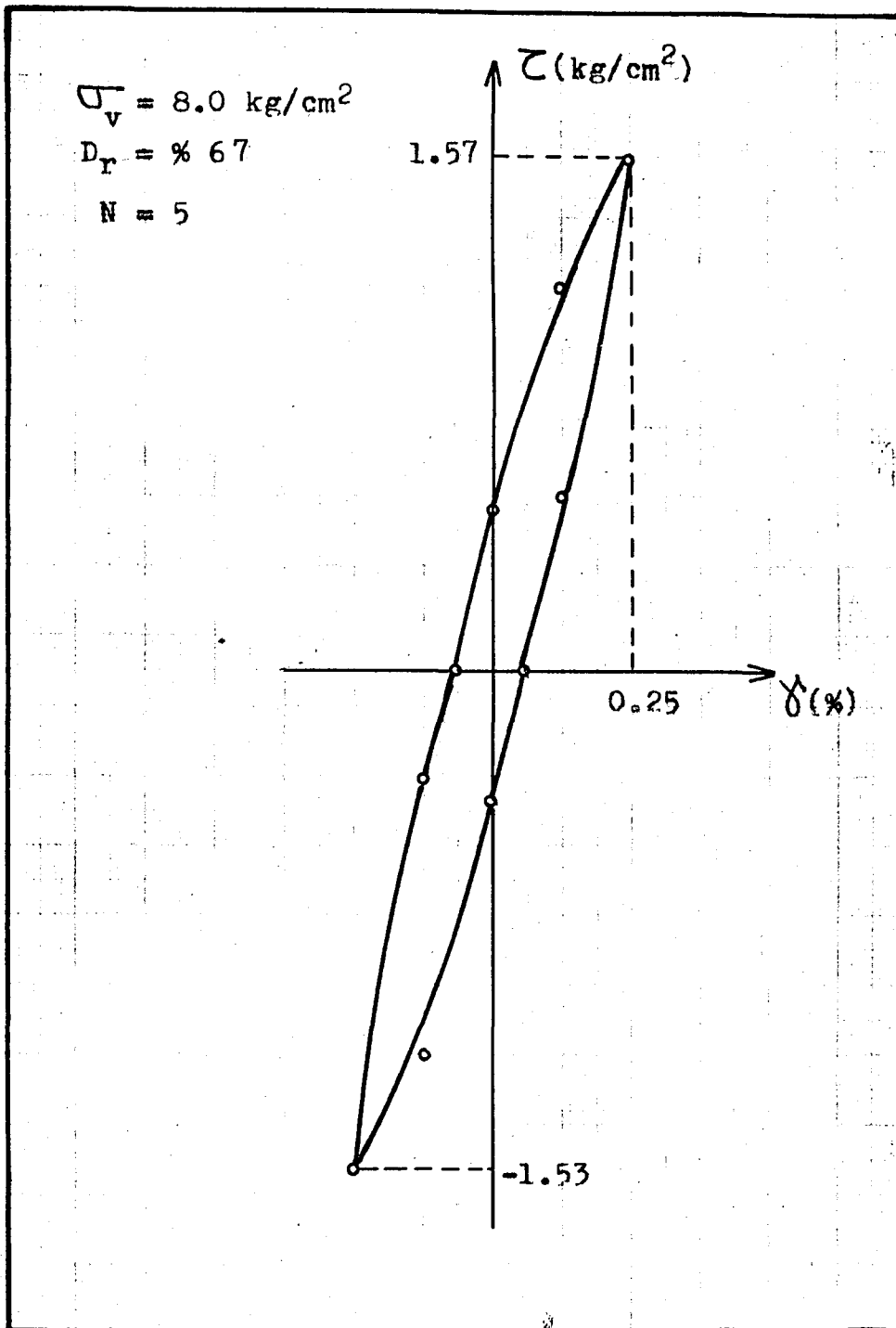


Figure 4.25 - Hysteresis Loop of Test E1

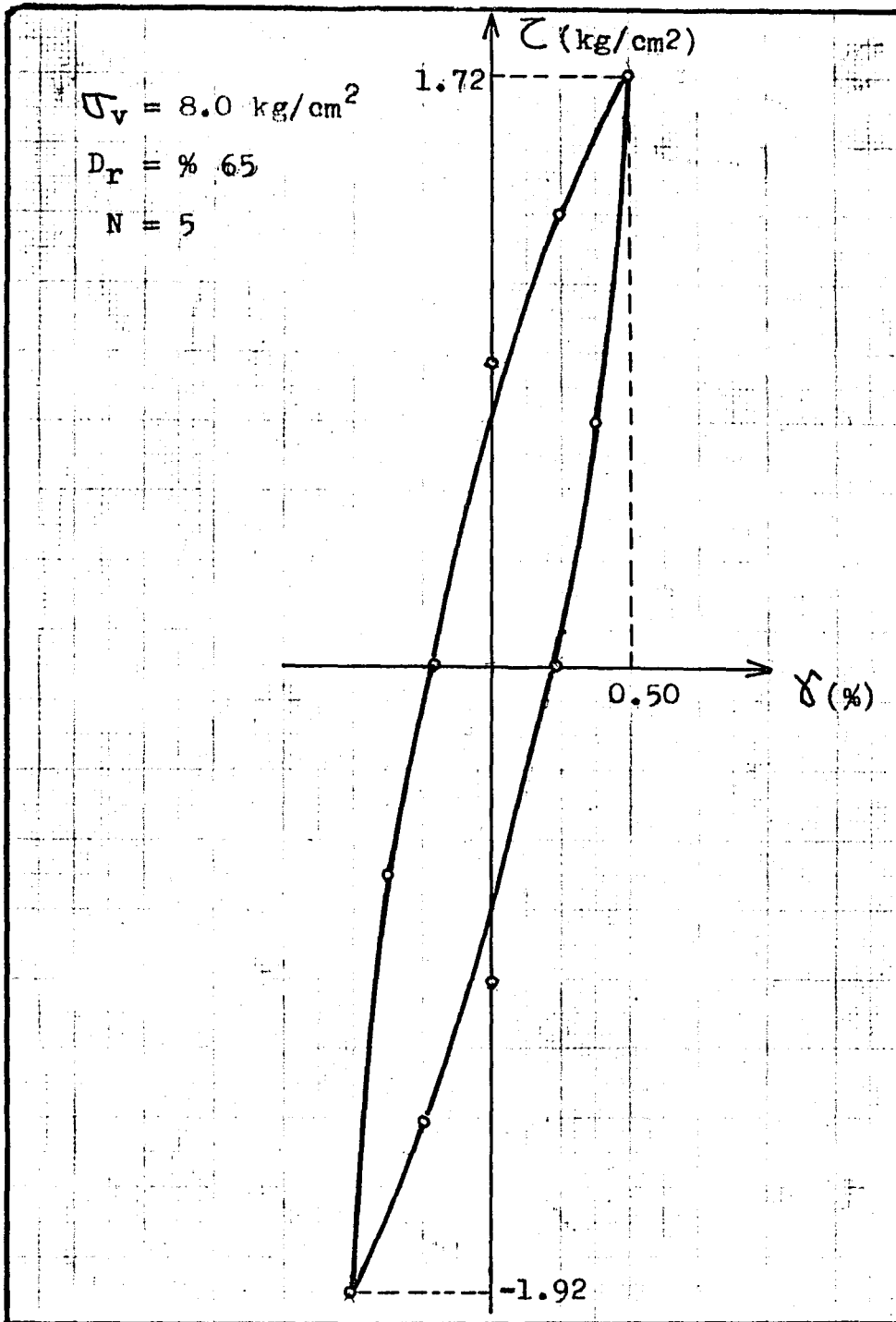


Figure 4.26-Hysteresis Loop of Test E2



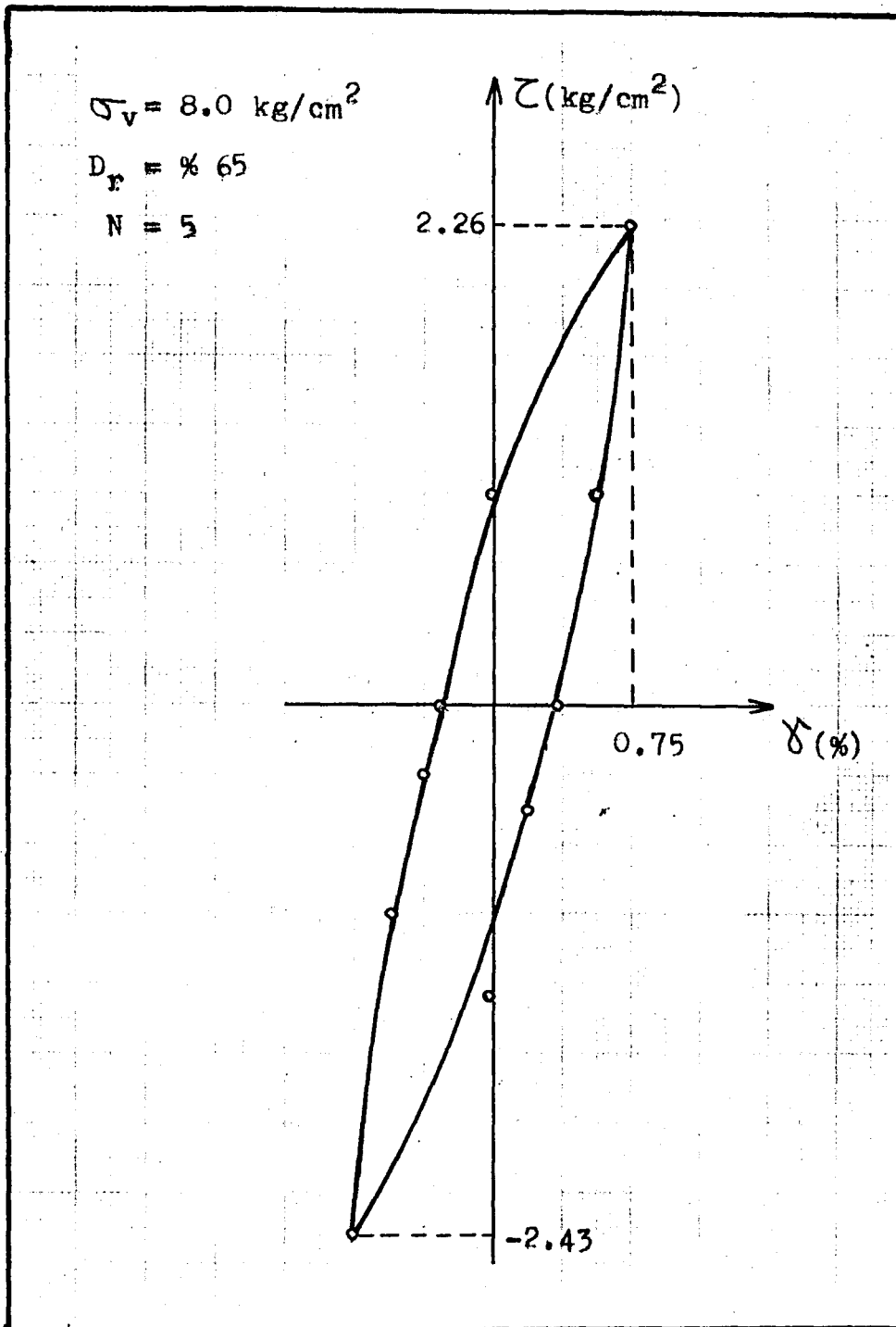


Figure 4.27 - Hysteresis Loop of Test E3

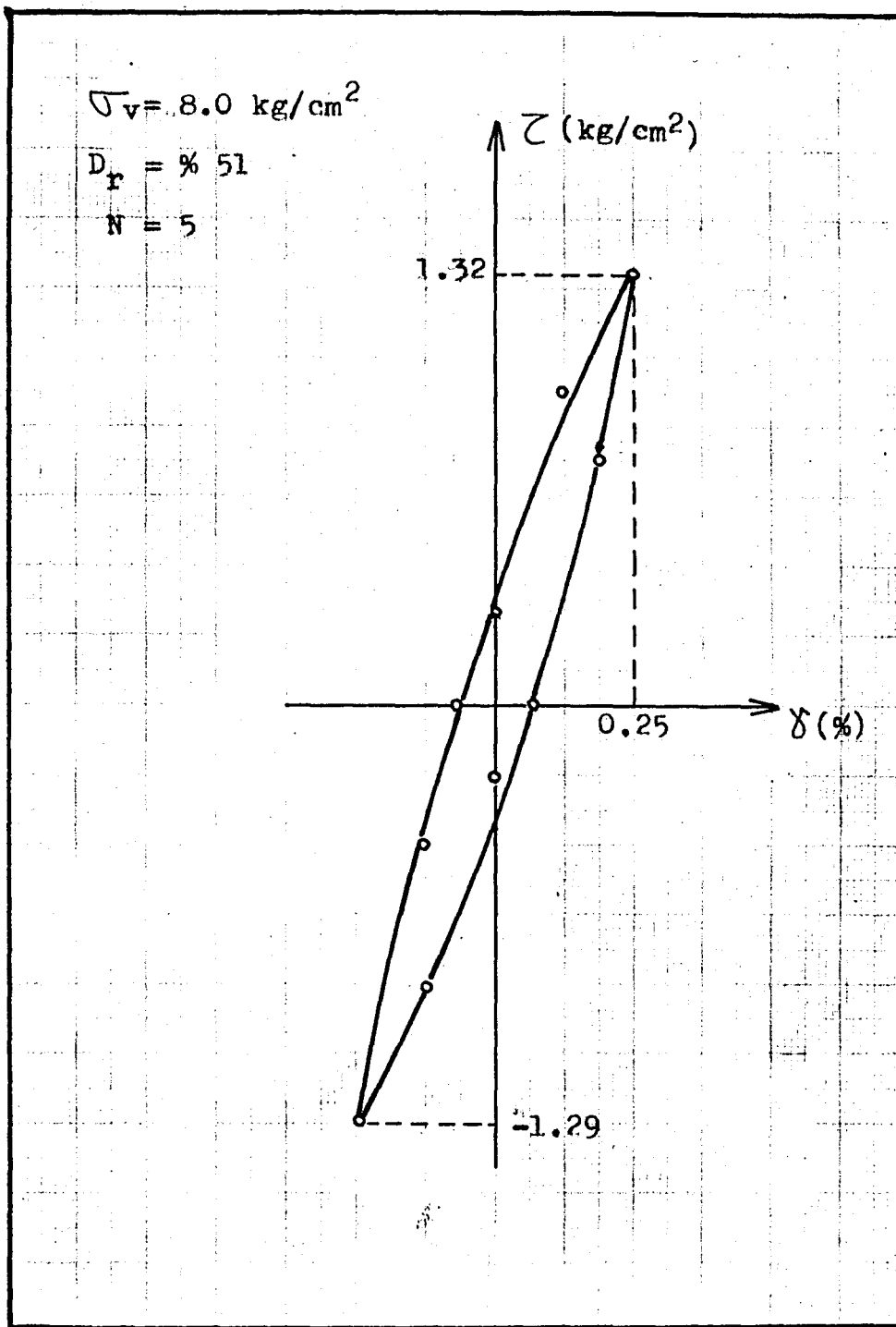


Figure 4.28-Hysteresis Loop of Test E4

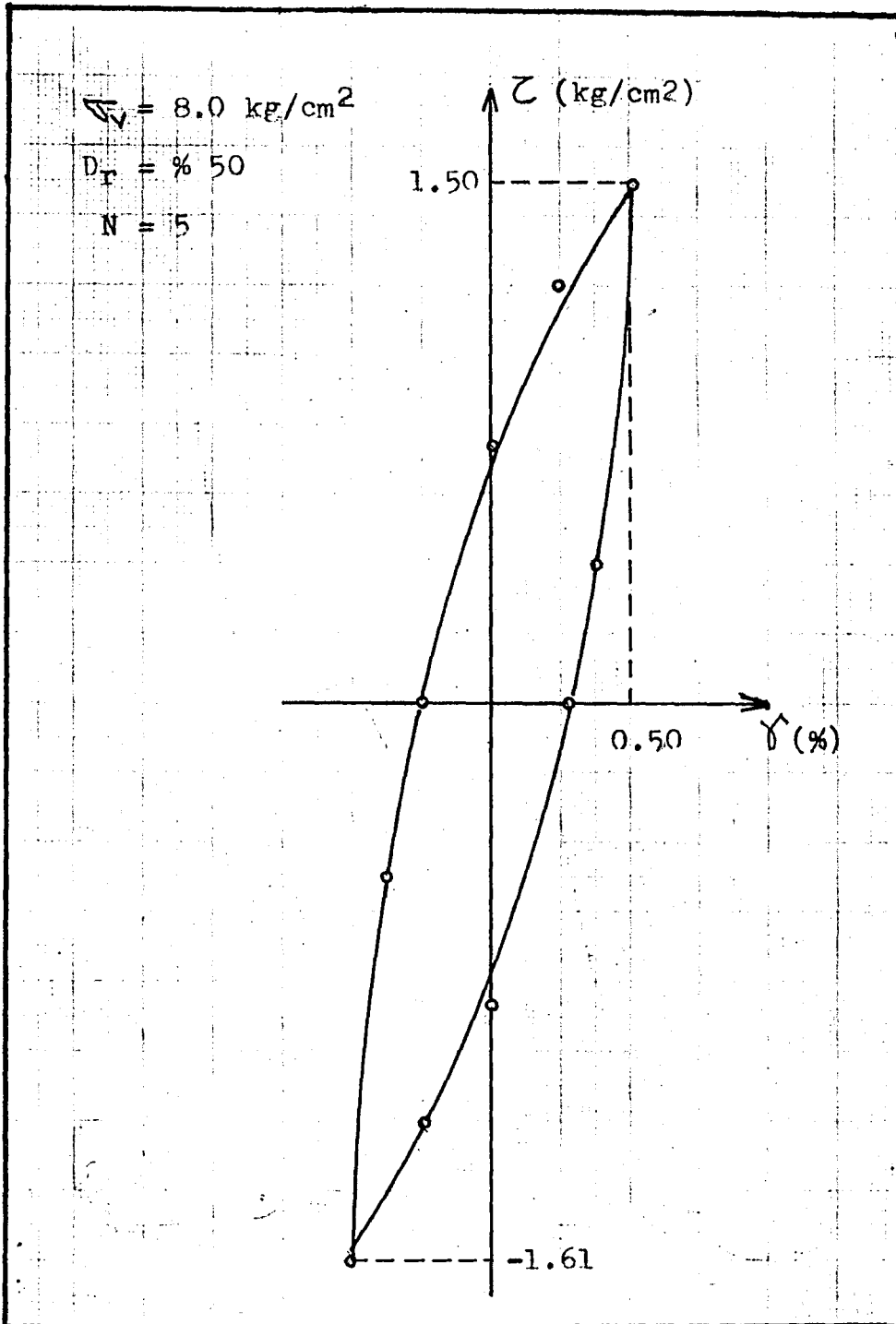


Figure 4.29- Hysteresis Loop of Test E5

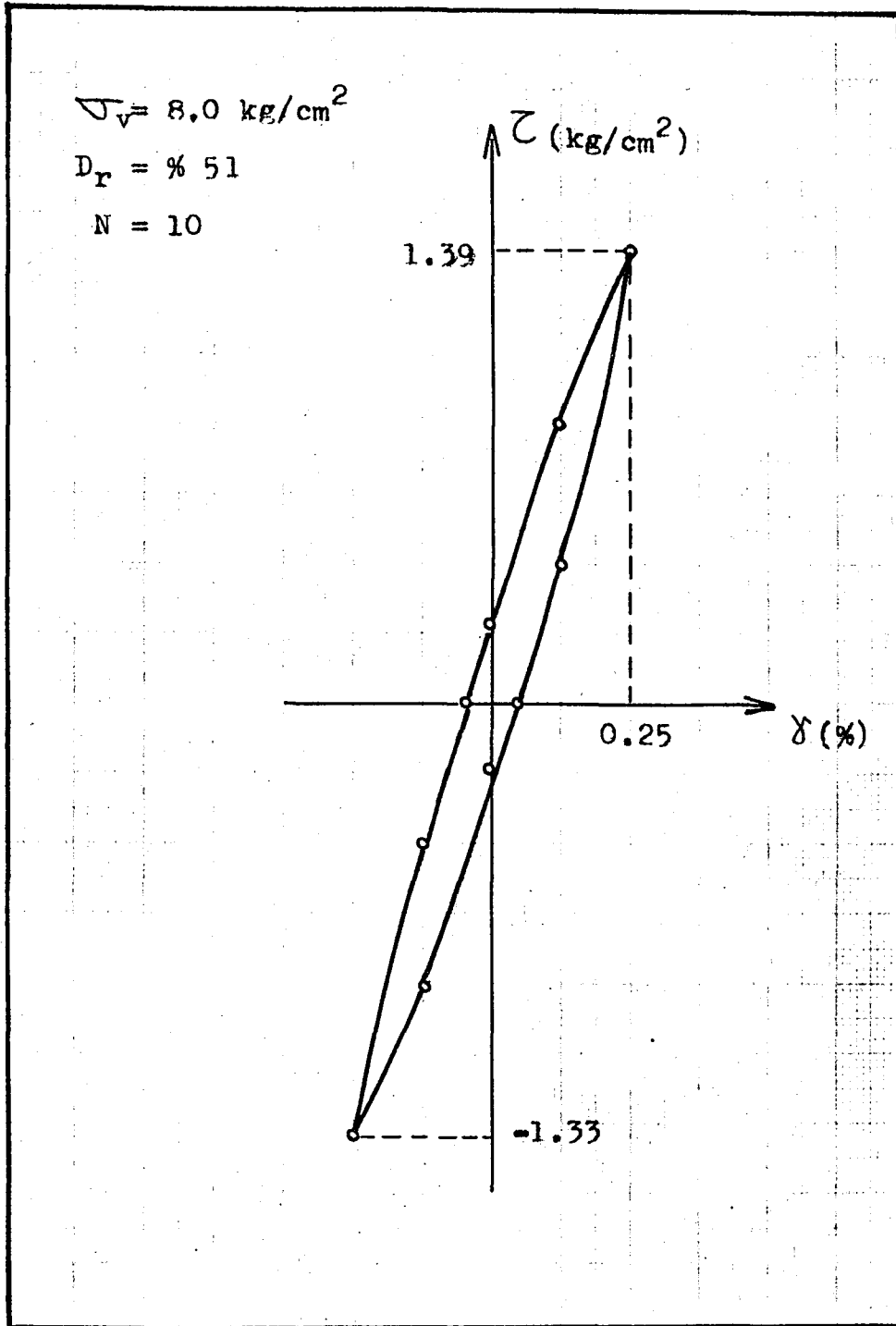


Figure 4.30-Hysteresis Loop of Test E6

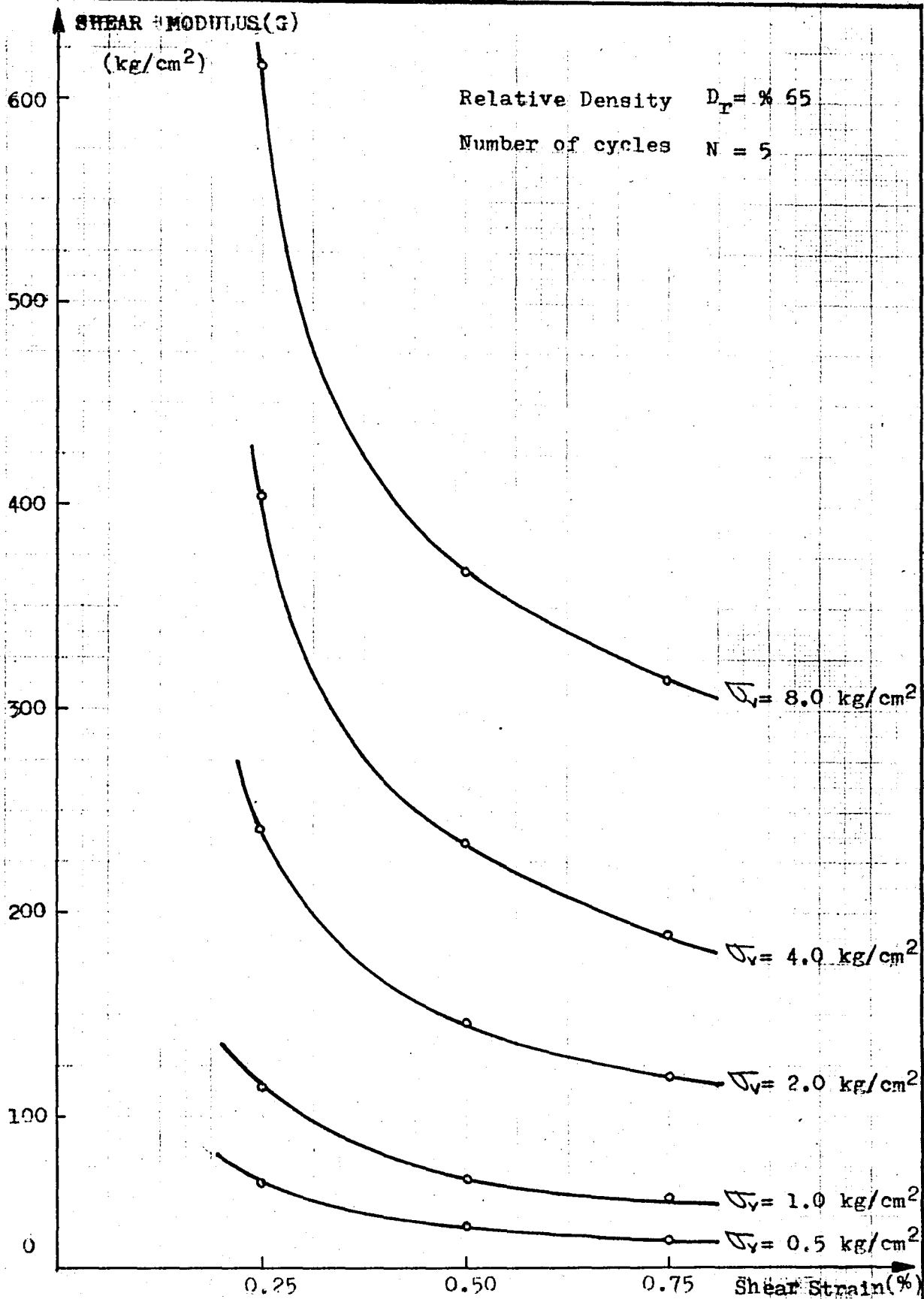


Figure 4.31- Effect of Shear Strain Amplitude and Vertical Stress on Shear Modulus in Fifth Loading Cycle.

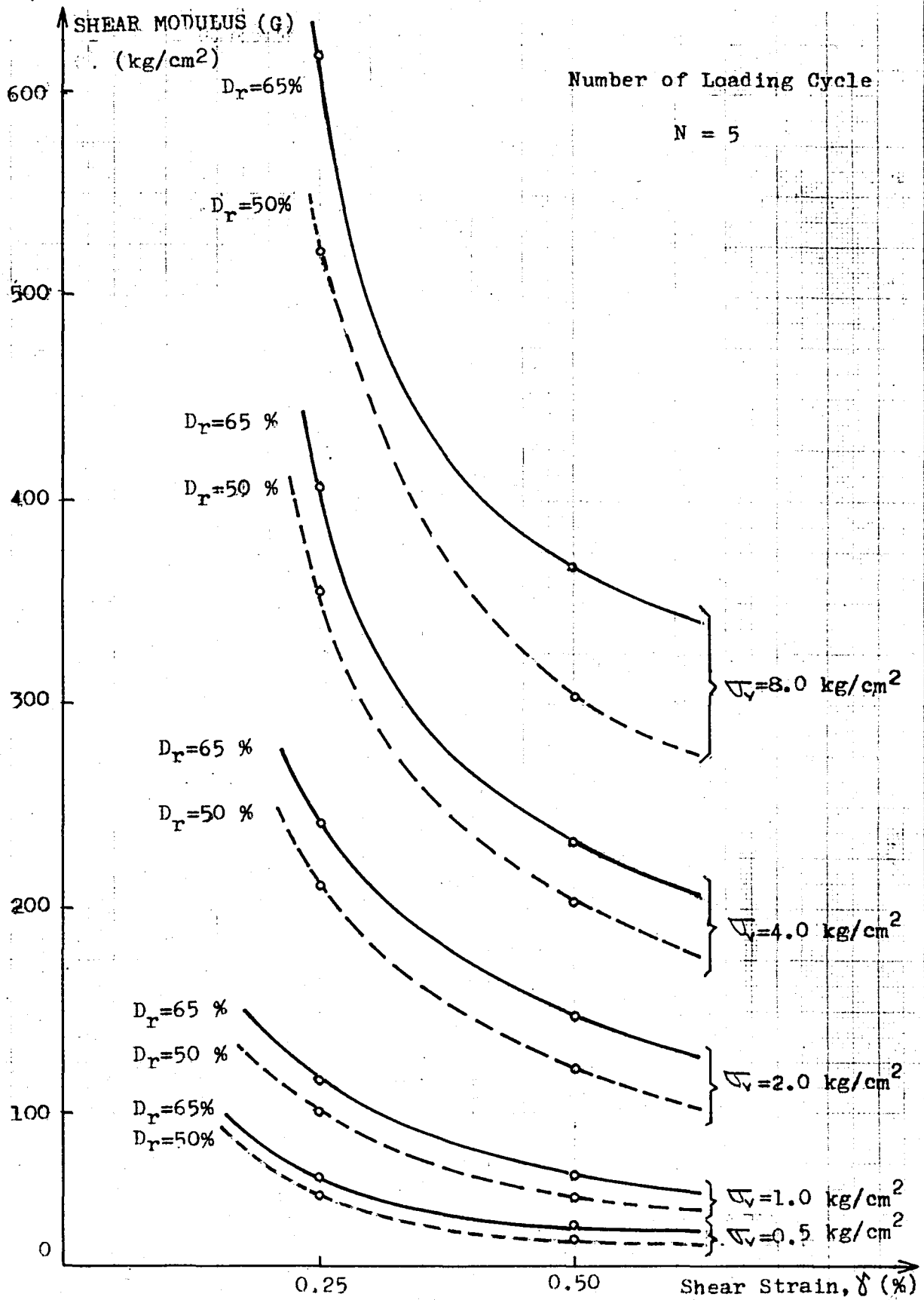


Figure 4.32 - Effects of Vertical Pressure and Relative Density on Shear Modulus in Fifth Loading Cycle.

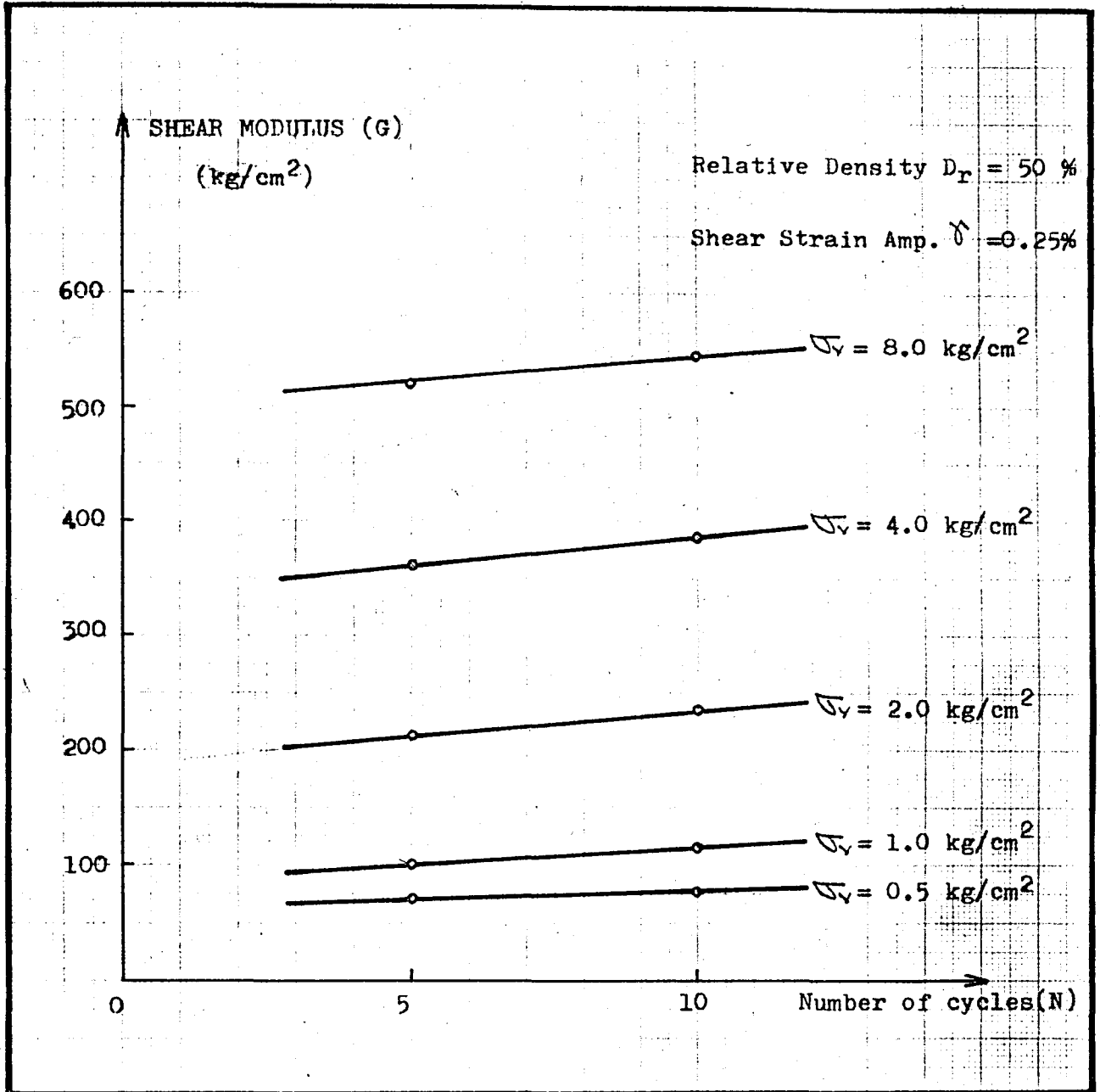


Figure 4.33- Effect of Number of Loading Cycles on Shear Modulus.

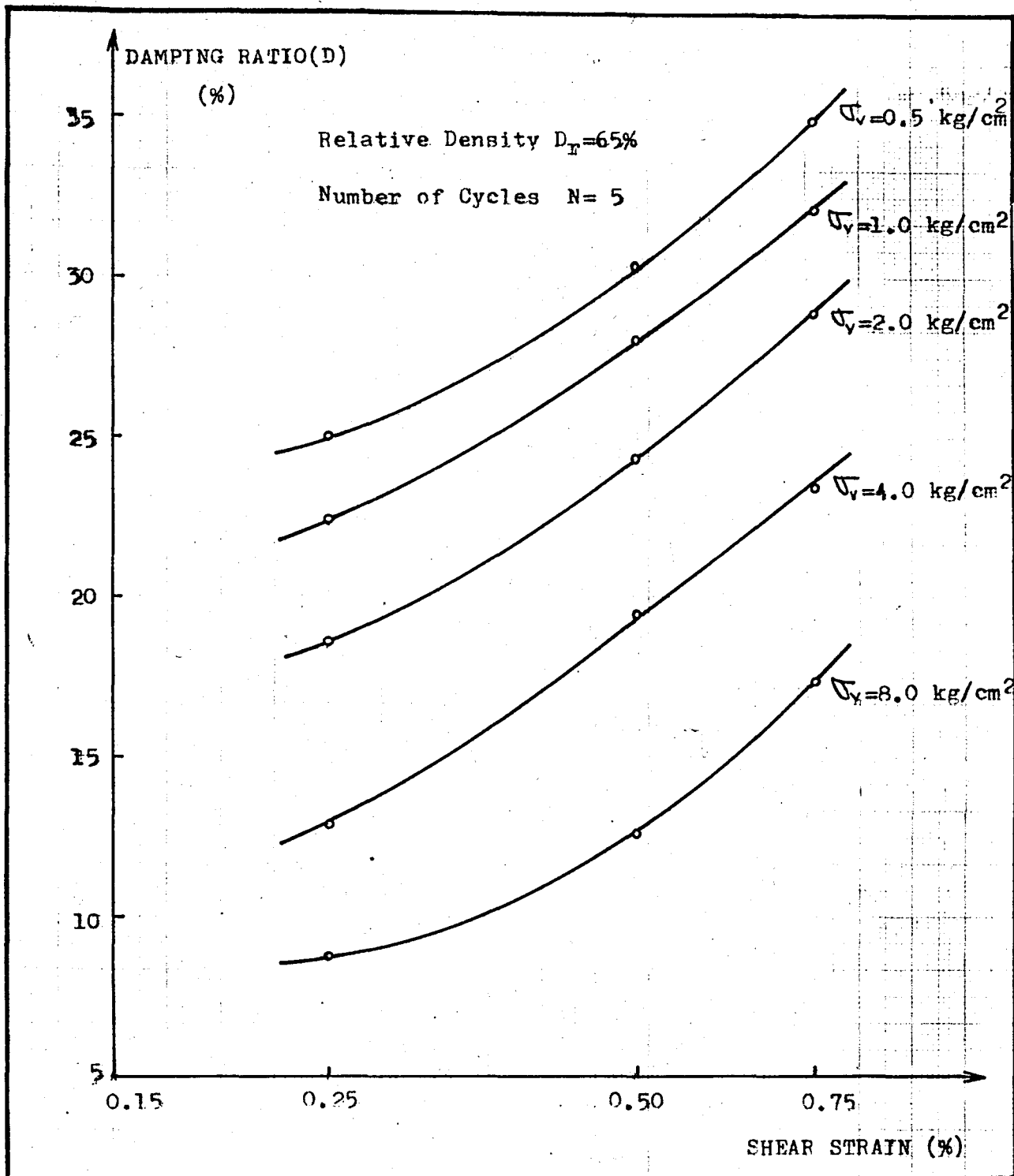


Figure 4.34- Effects of Shear Strain Amplitude and Vertical Pressure on Damping Ratio in Fifth Loading Cycle.



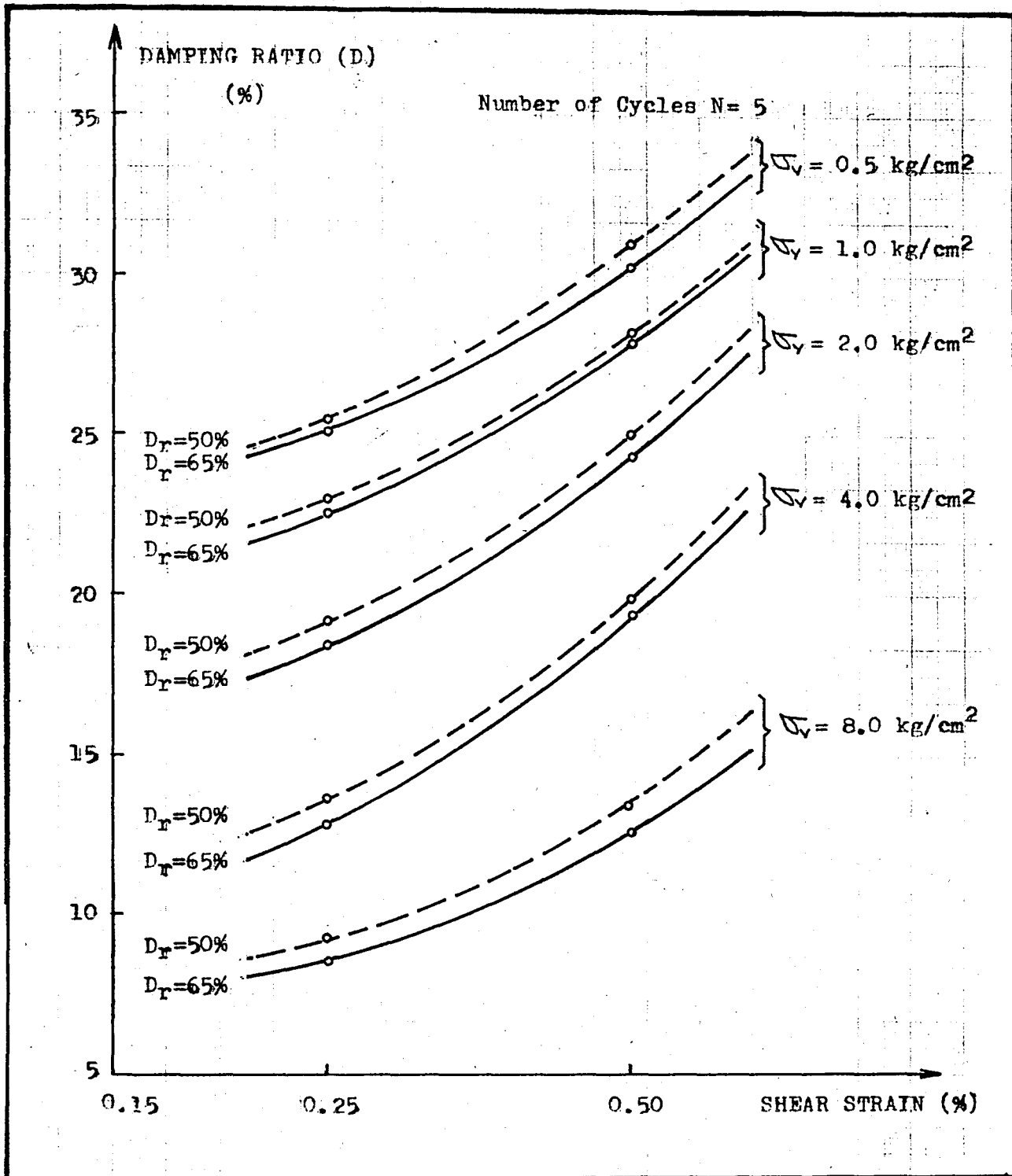


Figure 4.35- Effects of Vertical Pressure and Relative Density On Damping Ratio in Fifth Loading Cycle.

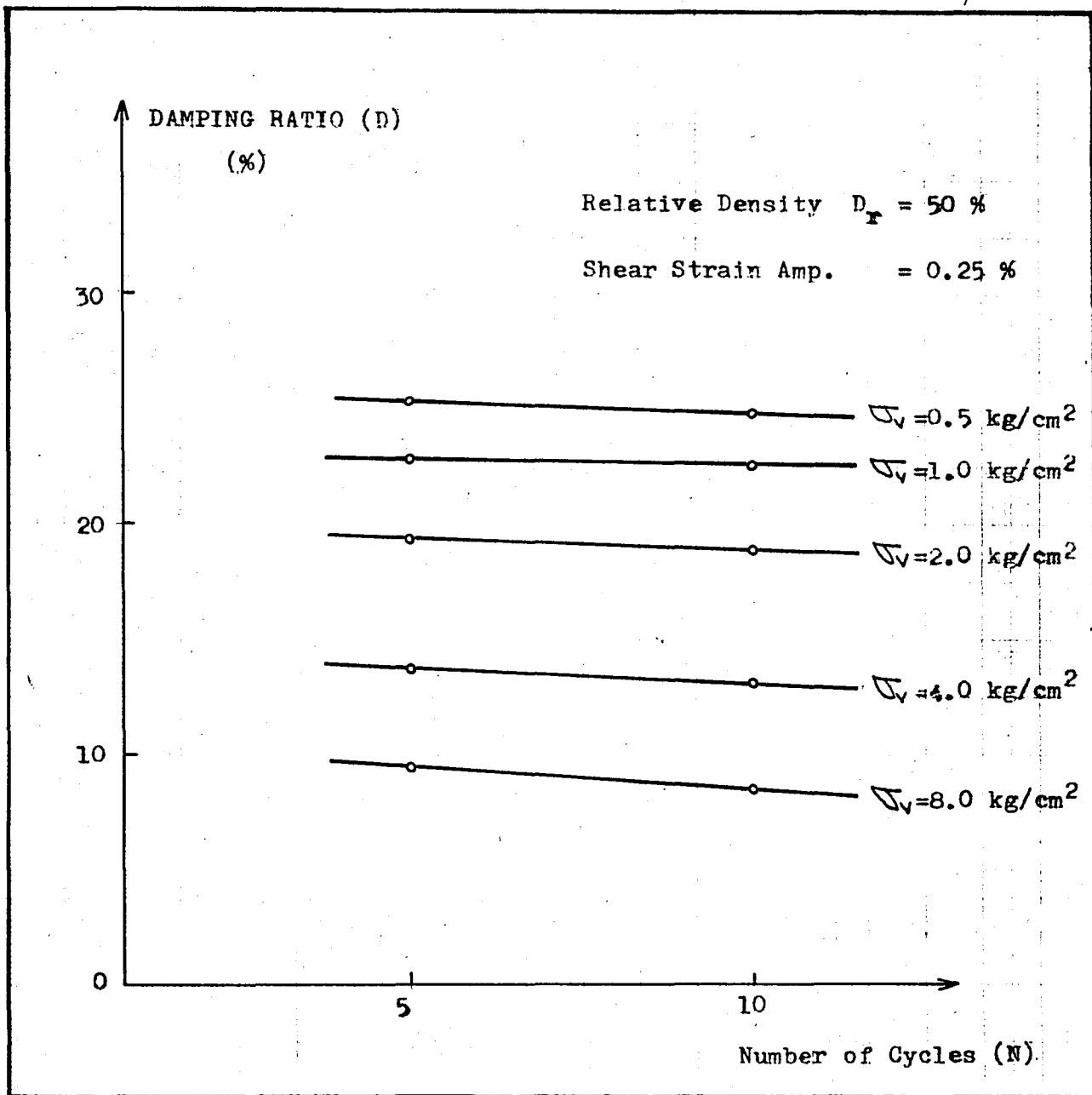


Figure 4.36- Effect of Number of Loading Cycles on Damping Ratio.

## CHAPTER 5

## CONCLUSIONS

In order to better understand the soil behaviour required to predict dynamic behaviour of structures and the propagation of vibrations through soil deposits, the dynamic stress-strain properties of sand represented by values of shear modulus and damping ratio were investigated together with the factors which affect them. The dynamic properties of sand were determined by cyclic loading simple shear tests using the Direct Simple Shear Apparatus developed by the Norwegian Geotechnical Institute.

The following conclusions can be derived from this study:

1) The dynamic shear modulus was found to decrease significantly with increasing values of shear strain amplitude. The damping ratio increases rapidly with increasing shear strain. There is no strain level below which shear modulus and damping ratio are constant in the range studied.

2) Shear modulus increases and damping ratio slightly decreases with the increasing initial relative density. The effect of change in relative density from 50 % to 65 % was rather small compared to the effect of changes in shear strain amplitude. The effect of relative density on damping ratio was even smaller than the effect on shear modulus. Therefore, for any vertical pressure, the relationship between damping ratio and shear strain can be accepted to be independent of the relative density of the sand.

3) Vertical pressure influences shear modulus and damping ratio in a different manner ; shear modulus increases and damping ratio decreases with increasing vertical pressure. The increase of the shear modulus with increasing vertical pressure is not linear. The larger the vertical pressure, the larger the rate of increase in shear modulus.

4) The shear modulus and damping ratio for sand are slightly influenced by the number of loading cycles for the range of vertical pressures included in the test program. The shear modulus increases and damping ratio decreases very slightly with the increasing number of loading cycles. Since the effect of number of loading cycles was not large, average values of damping ratio may appropriately be used for many purposes.

5) In order to evaluate dynamic behaviour of soil represented by shear modulus and damping ratio, many analytical models were developed by a number of investigators such as Seed-Idriss(1970) and Hardin-Drnevich(1972). Shear modulus and damping ratio values obtained in this study were compared with the values obtained by using Seed-Idriss model and Hardin-Drnevich model. It was found that the difference between the values obtained from the two models and the results of tests conducted during this study was between 0.5 % and 40 % in shear modulus values and between 1 % and 14 % in damping ratio values. The main reason of the

difference can be the fact that the both analytical models have been developed for small strain amplitudes (less than 0.10 % ), and give only approximate values for larger strain amplitudes like the ones used in this study (between 0.25 % and 0.75 % ).

## R E F E R E N C E S

1. Barkan, D.D., (1962), "Dynamics of Bases and Foundations ", McGraw-Hill Series in Soils Engineering and Foundation.
2. Bjerrum, L. and Landva, A., (1966), " Direct Simple Shear Tests on a Norwegian Quick Clay ", Geotechnique, Vol. 16, No. 1, pp. 1-20.
3. Bowles, J.E., (1970), " Engineering Properties of Soils and Their Measurement ", McGraw-Hill Book Company, Inc.
4. Castro, G. and Christian, J.T., (1976), " Shear Strength of Soils and Cyclic Loading ", Journal of the Geotechnical Engineering Division, Proceedings of the ASCE, Vol. 102, No. GT9, September, pp. 887-894.
5. Cuellar, V., Bazant, Z.P., Krizek, R.J. and Silver, M.L., (1977), " Densification and Hysteresis of Sand under Cyclic Shear ", Journal of the Geotechnical Engineering Division, Proceedings of the ASCE, Vol. 103, No. GT5, May, pp. 399-416.
6. Drnevich, V.P., Hardin, B.O. and Shippy, D.J., (1977), " Modulus and Damping of Soils by the Resonant Column Method ", Symposium on Dynamic Soil and Rock Testing in the Field and Laboratory for Seismic Studies, June, Denver.
7. Duncan, J.M. and Dunlop, P., (1969), " Behaviour of Soils in

Simple Shear Tests ", Proceedings of the 7<sup>th</sup> International Conference on Soil Mechanics and Foundation Engineering, Mexico, Vol. 1, pp. 101-110.

8. Edil, T.B. and Luh, G., (1978), " Dynamic Modulus and Damping Relationships for Sands ", Proceedings of the ASCE Geotechnical Engineering Division Speciality Conf., Pasadena, CA, Vol. 1, pp. 394-409.
9. Hall, J.R., Jr., and Richart, F.E., Jr., (1963), " Dissipation of Elastic Wave Energy in Granular Soils ", Journal of the Soil Mechanics and Foundations Division, Proceedings of the ASCE, Vol. 89, No. SM6, November, pp. 27-56.
10. Hardin, B.O., (1965), " The Nature of Damping in Sands ", Journal of the Soil Mechanics and Foundations Division, Proceedings of the ASCE, Vol.91, No.SM1, Jan., pp.63-97.
11. Hardin, B.O., (1978), " The Nature of Stress-Strain Behaviour for Soils ", Proceedings of the ASCE, Geotechnical Engineering Division, Speciality Conference Earthquake Engineering and Soil Dynamics, Pasadena, CA, Vol. 1, June, pp. 4-90.
12. Hardin, B.O. and Black, W.L., (1968), " Vibration Modulus of Normally Consolidated Clay ", Journal of the Soil Mechanics and Foundations Division, Proceedings of the ASCE, Vol. 94, No. SM2, pp. 353-369.

13. Hardin, B.O. and Drnevich, V.P., (1972,a), " Shear Modulus and Damping in Soils: Design Equations and Curves ", Journal of the Soil Mechanics and Foundations Division, Proceedings of the ASCE, Vol.98, No.SM7, July, pp.667-692.
14. Hardin, B.O. and Drnevich, V.P., (1972,b), " Shear Modulus and Damping in Soils: Measurement and Parameter Effects", Journal of the Soil Mechanics and Foundations Division, Proceedings of the ASCE, Vol.98, No.SM6, June, pp.603-624.
15. Hardin, B.O. and Music, J., (1965), " Apparatus for Vibration of Soil Specimens During the Triaxial Test ", Instruments and Apparatus for Soil and Rock Mechanics, ASTM STP 392, Am. Soc. Testing Mats., pp. 55-74.
16. Hardin, B.O. and Richart, F.E., Jr., (1963), " Elastic Wave Velocities in Granular Soils ", Journal of the Soil Mechanics and Foundations Division, Proceedings of the ASCE, Vol. 89, No. S11, pp. 36-65.
17. Lawrence, F.V., Jr., (1963), " Propagation Velocity of Ultrasonic Waves Through Sand ", MIT Research Report R63-8 March.
18. Lawrence, F.V., Jr., (1965), " Ultrasonic Shear Wave Velocities in Sand and Clay ", Rep. R64-05, Dept. Civil Eng. , Mass. Inst. Tech., Cambridge, Mass., to WES, Vicksburg, Miss.



19. Matsui, T., Ohara, H. and Ito, T., (1980), " Cyclic Stress-Strain History and Shear Characteristics of Clay ", Journal of the Geotechnical Engineering Division, Proceedings of the ASCE, Vol.106, No. GT10, pp. 1101-1120.
20. Nacci, V.A. and Taylor, R.J., (1967), " Influence of Clay Structure on Elastic Wave Propagation and Dynamic Properties of Earth Materials, Albuquerque, N.M., Aug. 23-25, pp. 491-502.
21. Park, T. K., and Silver, M.L., (1975), " Dynamic Triaxial and Simple Shear Behaviour of Sand ", Journal of the Geotechnical Engineering Division, Proceedings of the ASCE, Vol. 101, No. GT6, June, pp. 513-528.
22. Prange, B., (1977), " Dynamic Response and Wave Propagation in Soils ", Dynamical Methods in Soil and Rock Mechanics 1, Proceedings / Karlsruhe / 5-16 September.
23. Richart, F.E., Jr., (1975), " Some Effects of Dynamic Soil Properties on Soil-Structure Interaction ", Proceedings of the Geotechnical Engineering Division, ASCE, Vol. 101, No. GT12, Dec., pp. 1193-1240.
24. Richart, F.E., Jr., Hall, J.R., Jr. and Woods, R.D., (1970), " Vibrations of Soils and Foundations ", Prentice-Hall, International Series in Theoretical and Applied Mechanics, Englewood Cliffs, N.J., 414 pp.

25. Seed, H.B. and Idriss, I.M., (1970), " Soil Moduli and Damping Factors for Dynamic Response Analysis ", Earthquake Engineering Research Center, College of Engineering, University of California, Berkeley, Calif., Report No. EERC 70-10, Dec.
26. Seed, H.B. and Lee, K.L., (1966), " Liquefaction of Saturated Sands During Cyclic Loading ", Journal of the Soil Mechanics and Foundations Division, Proceedings of the ASCE, Vol. 92, No. SM6, Nov., pp. 105-134.
27. Sherif, M.A., Ishibashi, I. and Gaddah, A.H., (1977), " Damping Ratio for Dry Sands ", Journal of the Geotechnical Engineering Division, Proceedings of the ASCE, Vol.103, No. GT7, July, pp. 743-755.
28. Silver, M.L. and Seed, H.B., (1971), " Deformation Characteristics of Sands Under Cyclic Loading ", Journal of the Soil Mechanics and Foundations Division, Proceedings of the ASCE, Vol. 97, No. SM8, August, pp. 1081-1098.
29. Thiers, G.R. and Seed, H. B., (1968), " Cyclic Stress-Strain Characteristics of Clay ", Journal of the Soil Mechanics and Foundations Division, Proceedings of the ASCE, Vol. 94, No. SM2, March, pp. 555-569.
30. Timmerman, D.H. and Wu, T.H., (1969), " Behaviour of Dry Sand Under Cyclic Loading ", Journal of the Soil Mechanics

and Foundations Division, Proceedings of the ASCE,  
Vol. 95, No. SM4, July, pp. 1097-1111.

31. Woods, R.D., (1978), " Measurement of Dynamic Soil Properties ",  
Proceedings of the ASCE, Geotechnical Engineering  
Division Speciality Conference, Earthquake Engineering  
and Soil Dynamics, Vol. 1, June, Pasadena, CA, pp.91-178.